

# **Analysis of the SII0783 Function in PHB Synthesis in *Synechocystis* PCC 6803: a Crucial Role of NADPH in N-Starvation**

## **Dissertation**

der Mathematisch-Naturwissenschaftlichen Fakultät  
der Eberhard Karls Universität Tübingen  
zur Erlangung des Grades eines  
Doktors der Naturwissenschaften  
(Dr. rer. nat.)

vorgelegt von  
Maximilian Schlebusch  
aus Engelskirchen

Tübingen  
2012

Tag der mündlichen Qualifikation:

03.02.2012

Dekan:

Prof. Dr. Wolfgang Rosenstiel

1. Berichterstatter:

Prof. Dr. Karl Forchhammer

2. Berichterstatter:

Prof. Dr. Wolfgang Wohlleben

## Abstract

Nitrogen frequently is a limiting nutrient in natural habitats. Therefore, cyanobacteria as well as other autotrophic organisms have developed multiple strategies to adapt to nitrogen deficiency. Transcriptomic analyses of the strain *Synechocystis* PCC 6803 under nitrogen-deficient conditions revealed a highly induced gene (*sll0783*), which is annotated as conserved protein with unknown function. This gene is part of a cluster with seven genes and in the upstream region lies a predicted NtcA-binding site. Homologues of this cluster occur in some unicellular, non-diazotrophic cyanobacteria, in several  $\alpha$ -,  $\beta$ - and  $\gamma$ -proteobacteria as well as in some gram-positives. The common link between the heterotrophic bacteria seems to be the ability of nitrogen fixation and production of polyhydroxybutyrate (PHB), whereas among the cyanobacteria only *Synechocystis* PCC 6803 can accumulate PHB.

In this work, a knockout mutant of this gene in *Synechocystis* PCC 6803 was characterised. This mutant was unable to accumulate PHB, a carbon and energy storage compound. The levels of precursor metabolites such as glycogen and acetyl-CoA were not reduced. The impairment in PHB accumulation correlated with a loss of PHB synthase activity during prolonged nitrogen starvation. We could show that the PHB synthase activity appeared to be a target of activity regulation, which was influenced by the NADPH/NADP<sup>+</sup> ratio. The loss of PHB synthase activity in the Sll0783 mutant was caused by decreased NADPH/NADP<sup>+</sup> ratio, which plays a crucial role in PHB synthesis.

## Zusammenfassung

Stickstoff ist häufig ein limitierender Nährstoff in natürlichen Lebensräumen. Aus diesem Grund haben Cyanobakterien und andere autotrophe Organismen verschiedene Strategien entwickelt, um sich an diese Mangelbedingung anzupassen. Transkriptomanalysen des Cyanobakteriums *Synechocystis* PCC 6803 zeigten, dass das Gen *sll0783* unter Stickstoffmangelbedingungen besonders stark induziert wird. *sll0783* codiert für ein konserviertes Protein mit unbekannter Funktion und ist Teil eines Clusters mit sieben Genen. Im Promotorbereich befindet sich ein NtcA-Bindemotiv. Homologe dieses Clusters sind in einigen einzelligen, nicht-diazotrophen Cyanobakterien, in mehreren  $\alpha$ -,  $\beta$ - und  $\gamma$ -Proteobakterien, sowie in einigen grampositiven Bakterien nachgewiesen worden. Das gemeinsame Bindeglied zwischen den heterotrophen Bakterien ist die Fähigkeit Stickstoff zu fixieren und Polyhydroxybutyrat (PHB), ein Kohlenstoff- und Energiespeicher, einzulagern. Unter den Cyanobakterien ist nur *Synechocystis* PCC 6803 in der Lage PHB zu bilden.

In dieser Arbeit wurde eine Knockout-Mutante des Gens *sll0783* in *Synechocystis* PCC 6803 charakterisiert. Diese Mutante konnte nach Stickstoffentzug kein PHB mehr bilden. Während die Glykogen- und Acetyl-CoA-Konzentrationen in der Mutante nicht verringert waren, korrelierte die verminderte PHB-Bildung mit dem Verlust der PHB-Synthase-Aktivität. Es konnte gezeigt werden, dass die PHB-Synthase einer Aktivitätsregulierung unterliegt, welche durch das NADPH/NADP<sup>+</sup>-Verhältnis beeinflusst wird. Der Verlust der PHB-Synthase-Aktivität in der *Sll0783*-Mutante wurde durch ein reduziertes NADPH/NADP<sup>+</sup>-Verhältnis verursacht. Dies spielt eine entscheidende Rolle in der PHB-Synthese.



Für meine Mutter...



# Contents

<b>List of Figures</b>	<b>vii</b>
<b>List of Tables</b>	<b>ix</b>
<b>List of Abbreviations</b>	<b>xi</b>
<b>1 Introduction</b>	<b>1</b>
1.1 Cyanobacteria as photosynthetic prokaryotes . . . . .	1
1.2 Photosynthesis . . . . .	1
1.3 Respiration . . . . .	3
1.4 Carbon metabolism of cyanobacteria . . . . .	3
1.5 Polyhydroxyalkanoates . . . . .	5
1.5.1 Occurrence and diversity of biopolyesters . . . . .	5
1.5.2 PHA synthesis and genes involved . . . . .	6
1.5.3 PHA granules and biogenesis . . . . .	6
1.5.4 <i>In vivo</i> Assembly . . . . .	7
1.5.5 PHA synthase . . . . .	8
1.5.6 PHA depolymerase . . . . .	9
1.5.7 Phasin proteins and PHA-specific regulatory proteins . . . . .	9
1.5.8 Regulation of PHA metabolism . . . . .	9
1.5.9 PHA in cyanobacteria . . . . .	10
1.6 Nitrogen metabolism of Cyanobacteria . . . . .	12
1.6.1 Regulation of nitrogen metabolism . . . . .	13
1.6.1.1 Highly induced genes under nitrogen starvation: the Nit1C cluster . . . . .	14
1.6.1.2 Sequence similarities of the Nit1C operon . . . . .	14
<b>2 Aims of the project</b>	<b>17</b>
<b>3 Results</b>	<b>19</b>
3.1 Analysis of the gene <i>sll0783</i> : phylogeny, promoter and expression . . . . .	19
3.1.1 Phylogenetic analysis of the gene <i>sll0783</i> and its homologues . . . . .	19



## CONTENTS

---

3.1.2	Characterisation of the promoter of <i>sll0783</i> . . . . .	19
3.1.3	Expression of <i>sll0783</i> and surrounding genes . . . . .	20
3.2	Physiological characterisation of the Sll0783 mutant . . . . .	23
3.2.1	Physiological characteristics under nitrogen starvation . . . . .	23
3.2.2	Recovery process after nitrogen starvation . . . . .	26
3.2.3	Influence of light conditions . . . . .	27
3.3	PHB accumulation in wild type and the Sll0783 mutant . . . . .	27
3.3.1	Quantification of PHB accumulation . . . . .	27
3.3.2	Analysis of carbon metabolism and precursor metabolites . . . . .	29
3.3.3	Influence of potassium and phosphate starvation on PHB accumulation . . . . .	31
3.4	Expression of PHB synthesis genes . . . . .	31
3.5	Biochemical analysis of PHB synthase activity . . . . .	32
3.5.1	PHB synthase activity in different fractions . . . . .	32
3.5.2	Reactivation of the Sll0783 mutant PHB synthase . . . . .	34
3.5.3	Influence of acetyl phosphate and other metabolites . . . . .	35
3.5.4	The role of Sll0783 in the Nit1C cluster . . . . .	37
3.5.5	Phenotype of a PII mutant concerning PHB accumulation . . . . .	37
3.6	Purification of PHB granules in Percoll gradients . . . . .	38
3.6.1	Identification of PHB granule associated proteins . . . . .	40
3.6.2	Identification of outer membrane particles as contamination of PHB granule purification process . . . . .	42
3.7	Subcellular localisation of the PHB synthase . . . . .	44
3.8	Metabolomic profiling . . . . .	44
3.9	The role of the NADPH pool . . . . .	46
3.9.1	Quantification of NADPH and NADP <sup>+</sup> upon nitrogen starvation . . . . .	50
<b>4</b>	<b>Discussion</b> . . . . .	<b>53</b>
4.1	Analysis of the gene <i>sll0783</i> . . . . .	53
4.2	Physiological analysis of the Sll0783 mutant . . . . .	54
4.3	PHB accumulation in the Sll0783 mutant . . . . .	55
4.4	Purification of PHB granules . . . . .	57
4.4.1	Subcellular localisation of the PHB granules . . . . .	59
4.5	Evaluation of the metabolic profiling . . . . .	59
4.6	PHB synthase activity is influenced by NADPH . . . . .	60
4.6.1	NADPH/NADP <sup>+</sup> ratio is crucial for PHB accumulation . . . . .	60

---

<b>5</b>	<b>Materials &amp; methods</b>	<b>65</b>
5.1	Organisms and culture conditions . . . . .	65
5.1.1	Strains and organisms used in this work . . . . .	65
5.1.2	Culture conditions for cyanobacteria . . . . .	66
5.1.3	Culture conditions of <i>E.coli</i> . . . . .	66
5.2	Bioinformatic data analyses . . . . .	66
5.3	Analytical methods and fluorescence microscopy . . . . .	67
5.3.1	Growth and pigmentation . . . . .	67
5.3.2	Modulated chlorophyll fluorescence . . . . .	67
5.3.3	Fluorescence microscopy of PHB granules . . . . .	67
5.3.4	Outer membrane stain . . . . .	68
5.3.5	Fluorescence quantification . . . . .	68
5.3.6	Acetyl-CoA determination . . . . .	68
5.3.7	Glycogen determination . . . . .	69
5.3.8	NADP <sup>+</sup> /NADPH assay . . . . .	69
5.3.9	GC-EI-TOF-MS compound identification and data processing . . . . .	69
5.4	Molecular genetic methods . . . . .	70
5.4.1	Standard methods . . . . .	70
5.4.2	Long flanking homology polymerase chain reaction (LFH-PCR) . . . . .	70
5.4.3	Analysis of 5' end of <i>sll0783</i> transcript . . . . .	70
5.4.4	RNA isolation and cDNA synthesis . . . . .	71
5.4.5	quantitative RT-PCR . . . . .	71
5.4.6	Construction of C-terminal eGfp fusion proteins . . . . .	72
5.5	Protein techniques . . . . .	73
5.5.1	Protein quantification . . . . .	73
5.5.2	Preparation of cell extracts . . . . .	73
5.5.3	PHB synthase assay . . . . .	74
5.5.4	Reactivation of PHB synthase by swapping supernatants . . . . .	74
5.5.5	<i>In vitro</i> activation of PHB synthase . . . . .	74
5.5.6	Granula preparation . . . . .	74
5.5.7	Overexpression and purification of Slr1829 . . . . .	75
5.5.8	Overexpression and purification of Sll0783 . . . . .	75
5.5.9	Generation of antiserum . . . . .	76
5.5.10	Immunoblot analysis . . . . .	76
	<b>References</b>	<b>77</b>

## CONTENTS

---

# List of Figures

1.1	Schematic representation of the photosynthetic apparatus . . . . .	2
1.2	Schematic overview of PHA synthesis and the involved enzymes . . . . .	6
1.3	Schematic presentation of PHA granule biogenesis . . . . .	7
1.4	The four different PHA synthase classes . . . . .	8
1.5	Schematic representation of the genetic organization of PHB synthesis genes in cyanobacteria. . . . .	11
1.6	Schematic representation of the Nit1C-cluster of <i>Synechocystis</i> PCC 6803. . .	15
3.1	Comparison of 16S and Sll0783-homologues phylogeny. . . . .	20
3.2	Protein neighbour-joining tree for Sll0783 homologues . . . . .	21
3.3	Promoter analysis of <i>sll0783</i> homologues in cyanobacteria . . . . .	22
3.4	Expression of <i>slr0801</i> (black bars), <i>sll0783</i> (dotted bars) and <i>sll0784</i> (dashed bars) . . . . .	23
3.5	Physiological characteristics of <i>Synechocystis</i> PCC 6803 wild type (filled squares)and Sll0783 mutant (open squares). . . . .	24
3.6	Recovery of <i>Synechocystis</i> PCC 6803 wild type (filled squares) and Sll0783 mutant (open squares) from previous nitrogen starvation. . . . .	25
3.7	Analysis of the storage polymers glycogen and PHB . . . . .	26
3.8	Recovery of <i>Synechocystis</i> wild type (filled symbols) and Sll0783 mutant (open symbols) with 5 mM ammonium. . . . .	27
3.9	Recovery of <i>Synechocystis</i> PCC 6803 wild type (filled squares) and Sll0783 mutant (open squares) from previous nitrogen starvation under different light intensities. . . . .	28
3.10	Fluorescence microscopy of <i>Synechocystis</i> PCC 6803 wild type and Sll0783 mutant cells under nitrogen limiting conditions at indicated time points. . .	29
3.11	Quantification of PHB accumulation. . . . .	30
3.12	Influence of different carbon sources on PHB accumulation . . . . .	30
3.13	Quantification of the acetyl-CoA and glycogen during nitrogen starvation. . .	31
3.14	Fluorescence microscopy of wild type and Sll0783 mutant under different nu- trient starvation conditions. . . . .	32

## LIST OF FIGURES

---

3.15	Transcript abundance of PHB synthesis genes in wild type (black bars) and the Sll0783 mutant (spotted bars). . . . .	33
3.16	PHB synthase activity assays from <i>Synechocystis</i> PCC 6803 wild type (filled squares) and Sll0783 mutant (open squares) upon nitrogen starvation. . . . .	34
3.17	The role of Sll0783 in the Nit1C cluster . . . . .	37
3.18	Phenotype of a PII mutant regarding PHB accumulation upon nitrogen and phosphate starvation. . . . .	38
3.19	PHB granule purification by Percoll gradient. . . . .	39
3.20	SDS-PAGE analysis of native PHB granule . . . . .	40
3.21	Fluorescence microscopy of PHB granules and labelled outer membranes during the Percoll purification procedure. . . . .	43
3.22	Subcellular localisation of PHB synthase fusion proteins (PhaE-Gfp and PhaC-Gfp) under nitrogen starvation . . . . .	45
3.23	Schematic model of the C-terminal Gfp fusion proteins (PhaE-Gfp and PhaC-Gfp) . . . . .	46
3.24	Relative contents of TCA cycle metabolites. . . . .	47
3.25	Relative contents of selected amino acids. . . . .	48
3.26	Relative contents of glycolysis metabolites and sorbitol. . . . .	49
3.27	Influence of specific inhibitors on the PHB synthase activity. . . . .	50
3.28	NADPH/NADP <sup>+</sup> ratio of different strains under nitrogen starvation. . . . .	51
4.1	Schematic representation of the Nit1C cluster of <i>Synechocystis</i> PCC 6803. . . . .	54
4.2	Analysis of the impaired PHB accumulation of the Sll0783 mutant . . . . .	56
4.3	Proposed model of PHB granules considering function of porins . . . . .	59
4.4	Comparison of predicted models of the monooxygenase Slr0801 and the Sll0783 protein with the structure of phenylacetone monooxygenase (PdB:1w4x) (Malito <i>et al.</i> , 2004) . . . . .	62
4.5	Model of the impaired PHB accumulation in the Sll0783 mutant . . . . .	63

# List of Tables

3.1	Reactivation of PHB synthase by swapping different fractions . . . . .	35
3.2	Influence of different metabolites on PHB synthase activitiy . . . . .	36
3.3	Influence of different metabolites on PHB synthase activitiy after 96h of nitrogen starvation . . . . .	36
3.4	Assignment of single bands of the SDS-PAGE (Figure 3.20) to ORFs of the <i>Synechocystis</i> PCC 6803 genome identified by MALDI-TOF. . . . .	41
3.5	Table contains reciprocal best hit paris by blast2 between different proteins and different cyanobacterial species. . . . .	42
4.1	PHB accumulation upon different nutrient starvation conditions . . . . .	57
5.1	Strains and organisms relevant for this work. . . . .	65
5.2	Plasmids used in this study . . . . .	66
5.3	List of oligonucleotides for LFH-PCR . . . . .	71
5.4	List of oligonucleotides used for 5' RACE . . . . .	71
5.5	List of oligonucleotides used for qPCR . . . . .	72
5.6	List of oligonucleotides for the construction C-terminal eGfp fusion proteins. . . . .	73
5.7	List of oligonucleotides for Slr1829 overexpression. . . . .	75
5.8	List of oligonucleotides for Sll0783 overexpression. . . . .	75

## LIST OF ABBREVIATIONS

---

# List of Abbreviations

<b>A</b>	Absorbance	<b>GOGAT</b>	Glutamine 2-oxoglutarate amido-transferase
<b>ADP</b>	Adenosine diphosphate	<b>GS</b>	Glutamine synthetase
<b>Amp</b>	Ampicillin	<b>h</b>	hours
<b>ATP</b>	Adenosine triphosphate	<b>kDa</b>	Kilodalton (Atomic mass unit)
<b>bp</b>	base pair	<b>Kan</b>	Kanamycin
<b>C<sub>i</sub></b>	inorganic carbon	<b>LFH-PCR</b>	Long flanking homology - polymerase chain reaction
<b>°C</b>	degree Celsius	<b>LB</b>	Lysogeny broth
<b>CCM</b>	Carbon concentrating mechanism	<b>min</b>	minute
<b>CoA</b>	Coenzyme A	<b>MALDI-TOF</b>	Matrix-assisted laser desorption/ionization-time-of-flight mass
<b>chl <i>a</i></b>	Chlorophyll <i>a</i>	<b>NAD</b>	Nicotinamide adenine dinucleotide
<b>CCCP</b>	Carbonyl cyanide <i>m</i> -chlorophenyl hydrazine	<b>NADP</b>	Nicotinamide adenine dinucleotide phosphate
<b>Cyt b6/f</b>	cytochrome b6/f complex	<b>od</b>	optical density
<b>Da</b>	Dalton	<b>2-OG</b>	2-oxoglutarate
<b>DCCD</b>	N,N-dicyclohexylcarbodiimide	<b>OPP</b>	oxidative pentose-phosphate pathway
<b>DCMU</b>	(3-(3,4-dichlorophenyl)-1,1-dimethylurea)	<b>PCR</b>	Polymerase chain reaction
<b>DTNB</b>	5,5-dithiobis(2-nitrobenzoic acid)	<b>PEP</b>	Phosphoenolpyruvate
<b>EDTA</b>	Ethylene-diamine-tetraacetic acid;	<b>3-PGA</b>	3-phosphoglyceric acid
<b>et al.</b>	and others	<b>PHA</b>	Polyhydroxyalkanoates
<b>FNR</b>	ferredoxin-NADP <sup>+</sup> reductase	<b>PHB</b>	poly-(R)-3-hydroxybutyrate
<b><i>g</i></b>	gravitational acceleration	<b>PHMO</b>	phenylacetone monooxygenase
<b>GAP</b>	PHB granule associated protein	<b>PS I</b>	Photosystem I
<b>GC-MS</b>	Gas chromatography-mass spectrometry	<b>PS II</b>	Photosystem II
		<b>rpm</b>	rounds per minute
		<b>SDS-PAGE</b>	sodium dodecyl sulfate polyacrylamide gel electrophoresis
		<b>Tris</b>	tris(hydroxymethyl)aminomethane
		<b>TCA</b>	tricarboxylic acid
		<b>w/w</b>	weight by weight



## LIST OF ABBREVIATIONS

---

# 1

## Introduction

### 1.1 Cyanobacteria as photosynthetic prokaryotes

Cyanobacteria are prokaryotes that belong to the bacteria domain and are characterised by the ability of oxygenic photosynthesis (Carr & Whitton, 1982) and chlorophyll *a* synthesis (Whitton & Potts, 2000). They are Gram-negative bacteria and possess a cell wall with peptidoglycan. With regard to evolution, they are the link between bacteria and plants. Photosynthesis is operated by two photosystems containing chlorophyll *a* and phycobilisomes as the characteristic light-harvesting systems. The development of oxygenic photosynthesis caused the switch from an ancient anoxygenic to present day oxygenic atmosphere. Cyanobacteria possess a considerable morphological diversity from unicellular coccoid or rod-shaped strains, to complex true multicellular filamentous strains (Meeks & Elhai, 2002). Many strains are capable of cell differentiation, where heterocysts play the most significant role, due to their trait of nitrogen (N) fixation (Fay *et al.*, 1968). Also, some unicellular cyanobacteria are able to fix molecular nitrogen (Mitsui *et al.*, 1986). Cyanobacteria evolved about 2.4 billion years before present and due to their morphological diversity and metabolic flexibility they colonise nearly all habitats from the arctic tundra to the desert, in warm springs and all marine and freshwater habitats. They are important primary producers and contribute up to 4% on global biomass production (Pearl, 2000). Particularly, the marine nitrogen-fixing cyanobacteria play a key role in oceanic N-cycle. Apart from the free living cyanobacteria, several symbioses with fungi (lichens and *Geosiphon pyriformis*), plants (e.g. cycads), ferns (*Azolla*), mosses (*Anthoceros*) or animals (e.g. corals) are known (Rai *et al.*, 2002).

### 1.2 Photosynthesis

Photosynthesis can be defined as the synthesis of organic compounds through fixation of carbon dioxide (CO<sub>2</sub>) using light as energy source. The photosynthetic process is separated in the light reaction and in CO<sub>2</sub> fixation. The light reaction leads to the production of NADPH and ATP, utilising water as electron donor, and O<sub>2</sub> is released as a by-product (Ke, 2001).

# 1. INTRODUCTION

The products NADPH and ATP are subsequently used in the CO<sub>2</sub> fixation reactions via the Calvin cycle (Heineke, 2001; Tabita, 1994) and other assimilatory reactions, in particular, N-assimilation.

The light reactions in cyanobacterial photosynthetic electron transport from water to NADP<sup>+</sup> are catalysed by different membrane-bound protein complexes, embedded in the thylakoid membranes and are connected by different soluble electron carriers (Vermaas, 2001). Cyanobacteria as oxygenic photosynthetic organism use two coupled photosystems, which are connected by the cytochrome b<sub>6</sub>/f complex (cyt b<sub>6</sub>/f) and the mobile electron carriers, plastoquinone (PQ) and cytochrome c553 (or plastocyanin(PC)) (Figure 1.1). The light reactions also lead to the formation of an electrochemical proton gradient across the thylakoid membrane, which is the driving force for ATP synthesis (Frasch, 1994). Photosystem II (PS II) is a multimeric complex consisting of a light-harvesting system (phycobilisomes), the reaction centre and the oxygen-evolving complex. PS II catalyses the light-driven oxidation of water and the reduction of bound quinones. When light energy is absorbed by the phycobili-

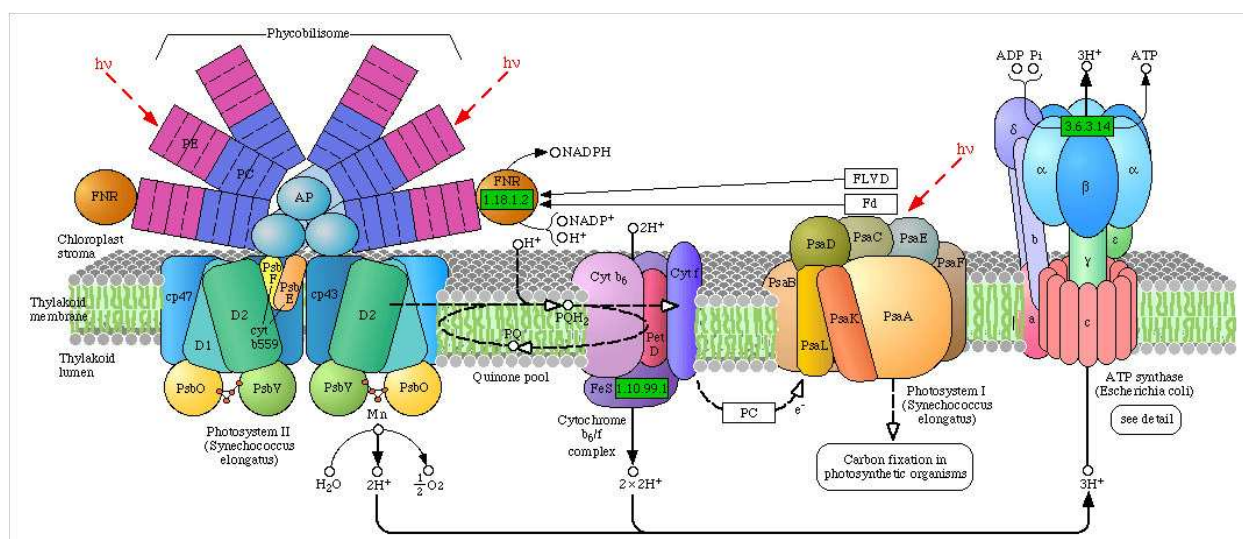


**Figure 1.1: Schematic representation of the photosynthetic apparatus** - This picture illustrates the phycobilisomes, the components of the photosynthetic electron transport and the ATP synthase complex. Source: [www.genome.jp/kegg-bin/show\\_pathway?map00195](http://www.genome.jp/kegg-bin/show_pathway?map00195).

somes, energy is transferred to the reaction centre of PS II, where an electron is transferred from an excited state of reaction centre chlorophyll *a* P<sub>680</sub> to a phaeophytin. Via a bound quinone (Q<sub>A</sub>) the electron is transferred to a loosely bound quinone (Q<sub>B</sub>). After a second electron is transferred to the semiquinone, fully reduced quinone is released and replaced by an oxidised quinone. The oxidised P<sub>680</sub><sup>+</sup> is reduced via a tyrosine residue in position 161 on the D1 protein. Tyrosine<sup>+</sup> is neutralised by the oxygen-evolving complex, which catalyses the oxidation of two molecules H<sub>2</sub>O and releases O<sub>2</sub>. The plastoquinone pool mediates the transport of the electrons from PS II to the cyt b<sub>6</sub>/f complex. The cyt b<sub>6</sub>/f complex catalyses the quinol reduction and transfers the electron to plastocyanin, which is the electron

donor to PS I. PS I is defined as light-driven plastocyanin:ferredoxin oxidoreductase. After illumination, an electron is transferred from an excited state of the reaction centre P<sub>700</sub> to the stromal side of PS I via a chlorophyll, phylloquinone and three iron sulphur clusters. The terminal electron acceptor of PS I is the water-soluble protein ferredoxin, which transfers the electrons from PS I to ferredoxin-NADP<sup>+</sup> reductase (FNR). In addition, ferredoxins provide the reductive power for different reactions in cyanobacterial nitrogen assimilation. FNR catalyses the electron transfer from reduced ferredoxin to NADP<sup>+</sup>.

## 1.3 Respiration

In general, respiration is a bioenergetic process, which oxidises organic carbon compounds to generate membrane potential coupled to the synthesis of ATP. This generation of ATP is mainly achieved via a process called oxidative phosphorylation (Hill, 2001).

In cyanobacteria respiration is unique in many ways, since photosynthesis and respiration do not take place in different compartments, and the corresponding electron transport chains share identical protein components and mobile electron carriers (Vermaas, 2001). Glycolysis, the oxidative pentose-phosphate pathway (OPP), and the reactions of the incomplete TCC lead to production of CO<sub>2</sub>, reductive equivalents (mainly NADH) and carbon skeletons that are used in biosynthesis as well as in continued oxidation. Respiration is often defined as a mostly membrane-bound electron transport process leading to the formation of ATP in the dark (Schmetterer, 1994).

Cyanobacteria possess two distinct and complete respiratory chains, one being located in the cytoplasmic membrane and the other located in the thylakoid membranes. Both pathways contain an equivalent of the mitochondrial and bacterial-type NAD(P)H dehydrogenase (NDH-1 or complex I), a succinate dehydrogenase (equivalent to complex II of mitochondrial respiratory chain (Cooley & Vermaas, 2001; Cooley *et al.*, 2000)), cytochrome b<sub>6</sub>/f complex (equivalent to complex III of mitochondrial respiratory chain), and terminal oxidases of the cytochrome c aa<sub>3</sub>-type (Cta; equivalent to complex IV of mitochondrial respiratory chain), the cytochrome bd-type (Cyd), and the cytochrome bo-type (CtaII). Moreover, the respiratory chains comprise the plastoquinone pool (PQ/PQH<sub>2</sub>) mediating electron transport to the cytochrome b<sub>6</sub>/f complex. Plastocyanin, cytochrome c<sub>553</sub> or cytochrome cM transfers electrons from the cytochrome b<sub>6</sub>/f complex to the terminal oxidases. Although recent genetic approaches provided new insights, many open questions concerning the location and the functionality of some constituents of the respiratory chain remain unsolved.

## 1.4 Carbon metabolism of cyanobacteria

As an environmental adaptation, cyanobacteria evolved a CO<sub>2</sub>-concentrating-mechanism (CCM) that enables an effective CO<sub>2</sub> fixation. The CCM comprises the active transport and

## 1. INTRODUCTION

---

accumulation of inorganic carbon ( $C_i$ ,  $\text{HCO}_3^-$ , and  $\text{CO}_2$ ). Cyanobacteria can possess up to five distinct transport systems for  $C_i$  uptake:

- BCT1 is an inducible, high-affinity  $\text{HCO}_3^-$ -transporter which is encoded by the *cm-pABCD* operon. This transport system belongs to the traffic ATPase family (Omata *et al.*, 1999).
- SbtA is an inducible, high-affinity  $\text{Na}^+$ -dependent  $\text{HCO}_3^-$ -transporter (Shibata *et al.*, 2002). This transporter probably acts as a  $\text{Na}^+/\text{HCO}_3^-$ -symporter.
- BicA, a low-affinity, high-flux  $\text{Na}^+$ -dependent  $\text{HCO}_3^-$ -transporter belongs to the widespread SulP/SLC26 family (Price *et al.*, 2004) and also acts as a probable  $\text{Na}^+/\text{HCO}_3^-$ -symporter.
- NDH-I4 is a constitutive, low affinity  $\text{CO}_2$  uptake system based on a specialised NADPH dehydrogenase (NDH-I) complex (Maeda *et al.*, 2002; Shibata *et al.*, 2001).
- NDH-I3, a second  $\text{CO}_2$  uptake system based on a modified NDH-1 complex that is inducible under  $C_i$  limitation and is of higher uptake affinity than NDHI4 (Klughammer *et al.*, 1999; Maeda *et al.*, 2002; Shibata *et al.*, 2001) and has been confirmed to be located on the thylakoid membrane in *Synechocystis* PCC 6803 (Prommeenate *et al.*, 2004; Zhang *et al.*, 2004)

Since cyanobacteria thrive in nearly all habitats, the presence of the different  $C_i$  uptake systems in cyanobacteria highly correlates with the nature of the aquatic habitat. Open ocean marine species show a restricted suite of transporters with the extreme represented by *Prochlorococcus* species, which have no  $\text{CO}_2$  uptake systems and only a limited range of  $\text{HCO}_3^-$  transporters. Symbiotic species with constant environments also show a reduced set of transporters. Freshwater species, which occupy lakes possess the widest range on  $C_i$  transport systems.

The cellular  $C_i$  pool is utilised to provide elevated  $\text{CO}_2$  concentrations around the primary  $\text{CO}_2$ -fixing enzyme ribulose biphosphate carboxylase/oxygenase (RubisCO). In cyanobacteria, RubisCO is located in unique micro-compartments known as carboxysomes. Carboxysomes also contain a specific carbon anhydrase (CA), which catalyses the conversion of  $\text{HCO}_3^-$  to  $\text{CO}_2$ . The proteinaceous shell of the carboxysomes builds a leak barrier for  $\text{CO}_2$  to gain optimal  $\text{CO}_2$  concentrations for the RubisCO. RubisCO is a bifunctional enzyme, which uses both  $\text{CO}_2$  and  $\text{O}_2$  as substrates. A raise in the  $\text{CO}_2$  concentration favours the carboxylase reaction with 3-phosphoglycerate (3-PGA) as product. Through the action of the Calvin cycle, 3-PGA is converted into triosephosphates, which serve as the initial C-skeleton for the formation of many cellular intermediates and glycogen. Moreover, the Calvin cycle regenerates 3-PGA, consuming ATP and NADPH, to ribulose-1,5-phosphate.

Since the CO<sub>2</sub> fixation process is very energy intensive, consuming about 30% of the produced energy, cyanobacteria as well as most phototrophic (micro-) organisms have developed mechanisms for the storage of carbon as well as energy. The major C-storage compound in cyanobacteria is glycogen. The synthesis involves four enzymes (Kromkamp, 1987):

- ADP-glucose pyrophosphorylase, which synthesises the monosaccharide donor.
- glycogen synthetase, which polymerises the monosaccharides into  $\alpha$ -(1-4)-glucose-polymers.
- a branching enzyme, which rearranges the polymers to give (1-6)-branches in the chain.
- mobilisation of glycogen is catalysed by glycogen phosphorylase.

In most species, glycogen accumulated during the day serves as the predominant metabolic fuel at night. Glucose residues derived from glycogen are catabolised via the oxidative pentose-phosphate pathway (OPP), glycolysis, and an incomplete tricarboxylic acid cycle (Cooley *et al.*, 2000), leading to the production of ATP and C-skeletons needed as anabolic precursors (Stal & Moezelaar, 1997). In cyanobacteria, the primary function of the oxidative branch of the TCA cycle is the synthesis of 2-oxoglutarate which serves as the C-skeleton for the assimilation of ammonia through the GS-GOGAT cycle (Zhang *et al.*, 2006).

## 1.5 Polyhydroxyalkanoates

Since the supply of most nutrients can fluctuate considerably, most organisms evolved mechanism to store excess of nutrients and/or energy under favourable growth conditions. The preferred kind of storage materials are polymers, because polymers can be stored in insoluble inclusions without affecting osmolarity. Microorganisms store various types of polymers. Cyanophycin, a polymer of arginine and aspartate, serves as nitrogen reserve. The nutrients phosphate and sulphur are stored as polyphosphate and sulphur globules. Lipids are stored as triacylglycerols or wax esters. Reduced carbon can be stored in several ways: lipids, glycogen and polyhydroxyalkanoates (PHA). The most widely distributed C-storage compound of bacteria is glycogen, a polysaccharide. A major focus of this work is on PHA accumulation, which has been poorly investigated in cyanobacteria.

### 1.5.1 Occurrence and diversity of biopolyesters

PHAs are the most complex class of water-insoluble biopolyesters. They occur in a variety of diverse taxonomic and physiological groups of the domain bacteria (both Gram-negative and Gram-positive, aerobic and anaerobic). PHA is also described in one Archaea (*Halobacteriaceae*). The most abundant PHA is polyhydroxybutyrate (PHB) consisting of hydroxybutyric acid. However, many other hydroxyalkanoate monomers are known. Therefore, PHAs are classified according to the number of carbon atoms in the monomer. Short

## 1. INTRODUCTION

chain length PHAs like PHB are composed of (R)-3-hydroxy-fatty acids with 3-5 C-atoms. Medium chain length PHAs (PHA<sub>MCL</sub>) monomers consists of 6-14 carbon atoms and long chain length PHAs (PHA<sub>LCL</sub>) are composed of monomers with more than 14 C-atoms. Most microorganisms synthesise either PHB or PHA<sub>MCL</sub>.

### 1.5.2 PHA synthesis and genes involved

The key enzyme of PHA synthesis is the PHA synthase, which catalyses the polymerisation of (R)-3-hydroxyacyl-CoA thioester monomers to the polyester. PHA synthase is encoded by the genes *phaC* and *phaE* or *phaR* (see section 1.5.5). For PHB synthesis the  $\beta$ -ketothiolase (*phaA*) condenses two molecules of acetyl-CoA to acetoacetyl-CoA. Subsequently, the NADPH-dependent acetoacetyl-CoA reductase (*phaB*) reduces acetoacetyl-CoA to (R)-3-hydroxybutyryl-CoA. Other PHAs like PHA<sub>MCL</sub> are produced from intermediates of fatty acid  $\beta$ -oxidation and/or fatty acid *de novo* biosynthesis. Gluconate, glucose or glycerol are metabolised to acetyl-CoA and enter the fatty acid *de novo* biosynthesis pathway, where the intermediate hydroxyacyl-ACP is converted into hydroxyacyl-CoA. The PHA genes are often clustered in operons. In *Ralstonia eutropha* (in the following *R. eutropha*) the three PHB biosynthesis genes are clustered in the *phaCAB* operon.

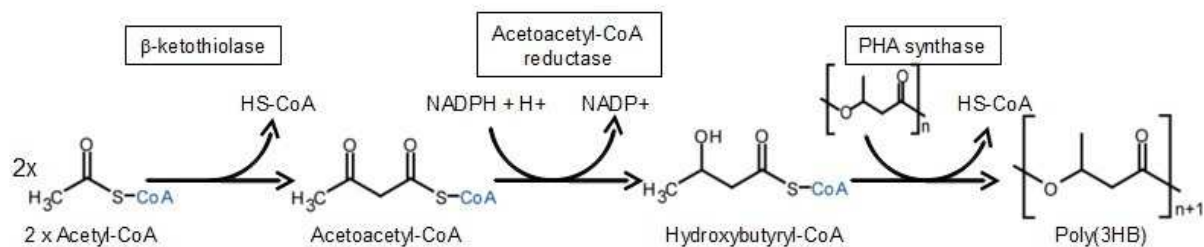


**Figure 1.2:** Schematic overview of PHA synthesis and the involved enzymes - adapted from Rehm (2006)

### 1.5.3 PHA granules and biogenesis

PHA granules appear as water-insoluble spherical inclusions. The major constituents are PHB in addition to a minor fraction of proteins and lipids (Griebel *et al.*, 1968). PHB granules are not homogeneous: they are divided in an inner solid core and a coat, which is predominantly in a mobile state (Barnard & Sanders, 1989; Dunlop & Robards, 1973). The mobile state is achieved by the presence of water, which acts as plasticiser. Since the PHB polymer has a melting point of 180 °C, it is necessary to decrease the melting point. Only the hydrated amorphous elastomeric form of PHB is a substrate for the PHB depolymerase (Barnard & Sanders, 1989). The amorphous PHA granule is surrounded by a phospholipid monolayer with embedded or attached proteins. Atomic force microscopy (AFM) studies

support a complex surface structure with globular, porin-like structures at the granule surface (Dennis *et al.*, 2008). It is suggested that at these structures the PHA metabolism takes place. The known granule-associated proteins (GAP) are the PHA synthase, the intracellular PHA depolymerase, phasin proteins and regulatory proteins.

#### 1.5.4 *In vivo* Assembly

The PHA synthase possesses all properties for self-assembling of spherical inclusion. Biosynthesis of PHA starts as soon as the substrate hydroxyacyl-CoA is available. Although the process of *in vivo* granule formation is still unclear, there are currently two models discussed in literature.

In the micelle model, the PHA synthase is distributed randomly in the cytoplasm. When substrate is present and the PHA synthase synthesises the polyester chain, which is covalently attached to the PHA synthase. The growing polyester chain converts the PHA synthase into an amphipathic molecule. Hydrophobic interactions lead to a self-assembly process. When the PHA inclusion increases in size, phospholipids and GAPs become incorporated.

According to the budding model, PHA synthase locates at the cytoplasmic membrane and PHA synthesis is directed into the phospholipid bilayer. The growing PHA molecules cause an inflation of the cytoplasmic membrane. The PHA inclusion is surrounded by a phospholipid monolayer with embedded GAPs.

Results from different experiments support both models. In *R. eutropha* PHA granules

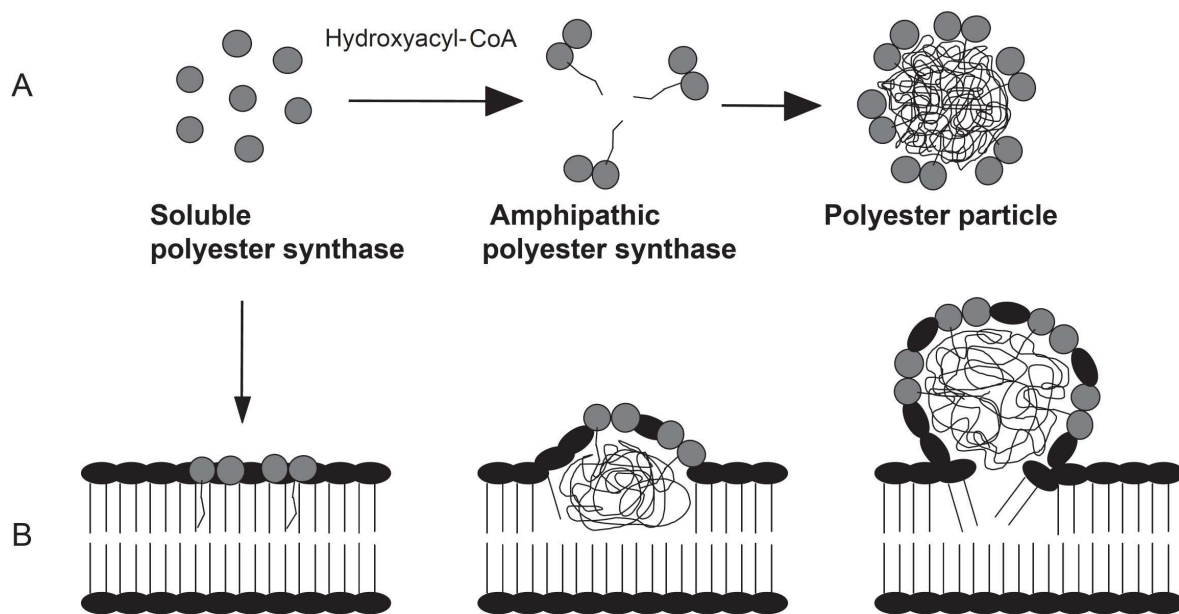


**Figure 1.3: Schematic presentation of PHA granule biogenesis - (A) Micelle model and (B) budding model (adapted from Rehm (2006)).**

emerge from nucleation site in the centre of the cell (Tian *et al.*, 2005). In contrast, emerg-







## 1. INTRODUCTION

---

ing PHA granules are frequently located close to the cell poles as well as to the cytoplasmic membrane (Jendrossek, 2005). In support of the budding model, PHA synthase eGfp fusions revealed PHA granules at the cell poles and located to mid-cell representing the future cell poles dependent on proper chromosome condensation (Peters & Rehm, 2005). In other organisms, localisation of the early stage PHA granules were shown to be near the cytoplasmic membrane or to the cell pole (Jendrossek, 2007). After assembly of the surface of the polyester granule and attachment of proteins, the PHA synthase continues to incorporate polymer. The PHA granules increase in size depending on physiological conditions like carbon or energy supply.

### 1.5.5 PHA synthase

PHA synthase is the key enzyme in PHA synthesis and catalyses the polymerisation reaction of (R)-3-hydroxybutyrate to the polyoxoester. PHA synthases are classified according to their number of subunits and the size of their substrates. PHA synthases belonging to Class I are homodimeric proteins. The subunit (PhaC) is about 60-73 kDa in size and hydroxyacyl-CoA is composed of 3-5 carbon atoms (PHA<sub>SCL</sub>). Class I PHA synthases are present in *R. eutropha*. Class II PHA synthases are, similar to class I, homodimeric but differ in substrate specificity. Substrates are hydroxyacyl-CoA monomers composed of 6-14 carbon atoms (PHA<sub>MCL</sub>). This class is represented by *Pseudomonas aeruginosa*. Class III PHA synthases are composed of two different subunits (PhaC and PhaE) forming a heterodimer, both about 40 kDa and use short-chain monomers as substrate. This class is represented by *Allochromatium vinosum*. Cyanobacteria also have class III PHA synthases. The class IV enzymes, represented by *Bacillus megaterium*, consists of two subunits (PhaC and PhaR), with PhaC being about 40 kDa and PhaR about 20 kDa in size. Substrates of class IV PHA synthases are short-chain monomers.

Class	Subunits	Species	Substrate
I	 ~60–73 kDa	<i>Cupriavidus necator</i>	3HA <sub>SCL</sub> -CoA (~C3–C5) 4HA <sub>SCL</sub> -CoA, 5HA <sub>SCL</sub> -CoA, 3MA <sub>SCL</sub> -CoA
II	 ~60–65 kDa	<i>Pseudomonas aeruginosa</i>	3HA <sub>MCL</sub> -CoA (~≥C5)
III	 ~40 kDa ~40 kD	<i>Allochromatium vinosum</i>	3HA <sub>MCL</sub> -CoA (3HA <sub>MCL</sub> -CoA [~C6–C8], 4HA-CoA, 5HA-CoA)
IV	 ~40 kDa ~22 kDa	<i>Bacillus megaterium</i>	3HA <sub>SCL</sub> -CoA

**Figure 1.4: The four different PHA synthase classes** - adapted from (Rehm, 2006)

### 1.5.6 PHA depolymerase

In general, two types of PHA depolymerases exist (Jendrossek & Handrick, 2002). Extracellular PHA depolymerases are secreted to the environment and catalyse the degradation of PHA, which becomes available from dead cells. Intracellular PHA depolymerases are specific for native, amorphous PHA (Handrick *et al.*, 2000). The PHA depolymerase is located at the surface of the PHA granules. In *R. eutropha* PHB depolymerase catalyses the degradation of PHB into 3-hydroxybutyrate (3HB). Further, 3HB is converted via acetoacetate and acetoacetyl-CoA into acetyl-CoA, catalysed by 3HB dehydrogenase, acetoacetate:succinyl-CoA transferase and ketothiolase (Doi *et al.*, 1990).

### 1.5.7 Phasin proteins and PHA-specific regulatory proteins

Phasin proteins are non-catalytic proteins bound to the PHA granules. They establish the boundary between hydrophilic cytoplasm and the hydrophobic polyester core and prevent fusion of PHA granules (Jurasek & Marchessault, 2004). The phasin proteins are very abundant and constitute up to 5 % of total cell protein (Wieczorek *et al.*, 1995), suggesting that most of the PHA granule surface is covered by phasins. Phasin proteins are important for the structure and morphology of the PHA granules (Dennis *et al.*, 2008). PHA-specific regulatory proteins have the feature to bind non-covalently PHA granules and DNA regions. These proteins can act as transcription regulators (Maehara *et al.*, 2001; Potter *et al.*, 2002) or bind unspecific DNA to assure equal separation of PHA granules (Pfeiffer *et al.*, 2011).

### 1.5.8 Regulation of PHA metabolism

Knowledge on the regulation of PHA metabolism is relatively limited. PHA metabolism is regulated at different levels.

- Expression of PHA synthesis genes is activated due to specific environmental signals (e.g. nutrient starvation).
- Enzymatic activity of the PHA synthesis proteins is activated by metabolic intermediates or specific signal molecules.
- Competing pathways are inhibited with simultaneous enrichment of PHA synthesis intermediates.

Most regulatory mechanisms on transcriptional level have been characterised in *Pseudomonas* species. The transcriptional regulator, PhbRPS, was found in *Pseudomonas* sp61-3 and is required to produce PHB homopolymers. *Pseudomonas* species are able to produce PHB copolymers consisting of monomers with different side chain length. The PhaRPS regulator is only involved in PHB homopolymer production. In *Pseudomonas putida* KT2442 a two-component system controls PHA synthesis. The LemA/GacA two component system senses

## 1. INTRODUCTION

---

environmental conditions and integrates these signals to the level of gene expression. Since many *Pseudomonas* species synthesise PHAs from fatty acid biosynthesis (e.g. growth on gluconate) or through fatty acid degradation (e.g. growth on fatty acids) (Huijberts *et al.*, 1992), the different PHA synthases are differentially controlled. The PHA synthase for PHA synthesis from gluconate is controlled by RpoN, which is an alternative sigma factor of the RNA polymerase. RpoN is involved in activation of non-house-keeping promoters. In contrast, the PHA synthesis pathway from fatty acid degradation is RpoN-independent (Timm & Steinbuchel, 1992).

In *Actinobacter sp.* the PHA synthesis genes are under the control of the Pho regulon (Schembri *et al.*, 1995). In *Vibrio* the transcriptional activator LuxR activates not only the *luxCDABE* genes for bioluminescence but also the genes for PHB synthesis (Miyamoto *et al.*, 1998). In *Azospirillum brasilense* SP7 the two-component system NtrB-NtrC, normally involved in nitrogen regulation, is somehow involved in the regulation of PHB synthesis.

The  $\beta$ -ketothiolase is competitively inhibited by the product of its reaction, Coenzyme A. In addition, PHA synthesis is stimulated by both high intracellular concentrations of NADPH and high ratios of NADPH/NADP<sup>+</sup> (Lee *et al.*, 1994). Since high NADPH concentrations inhibit citrate synthase of the TCA pathway, acetyl-CoA mainly enters the PHA synthesis pathway under high energy conditions. The activity of the depolymerase is controlled by phosphorylation by the phosphoenolpyruvate-dependent phosphotransferase system enzyme IIA<sup>Ntr</sup> (Pries *et al.*, 1991). PHB synthase from *R. eutropha* expressed in *E. coli* is affected by the Pta-AckA system, indicating regulatory influence of acetyl phosphate (Miyake *et al.*, 2000).

### 1.5.9 PHA in cyanobacteria

Many cyanobacteria have the ability to accumulate PHA. The trait of PHA accumulation is scattered through the phylum of the cyanobacteria. The most common PHA is PHB and only one strain is known to produce polyhydroxyvalerate (PHV). Many studies are based on ultra-morphological evidences of PHB granules, whereas the biochemical proof is lacking.

Since genomes of several cyanobacterial strains are available, similarity search of known PHB synthases reveals six cyanobacterial strains containing genes for PHA synthase (*Synechocystis* PCC 6803, *Microcystis aeruginosa* NIES-843, *Arthrospira maxima* CS-328, *Cyanothece sp.* PCC 7424, *Cyanothece sp.* PCC 7425 and *Cyanothece sp.* PCC 7822 (received by a reciprocal best hit paris by blast2 between *slr1829* and the genomes present in cyanobase <http://genome.kazusa.or.jp/cyanobase>)). All identified cyanobacterial PHA synthases are similar to the Class III PHA synthases with a characteristic conserved cyanobacterial box (Hai *et al.*, 2001). The genetic organization of the PHB synthesis genes is slightly different in cyanobacteria compared to *Allochromatium vinosum*, where PHB synthesis genes form a cluster including a regulatory protein PhaR and a protein of the phasin family. In *Microcystis aeruginosa* NIES-843, *Cyanothece* PCC 7424 and *Cyanothece* PCC 7425 PHB

synthesis genes occur in one *phaABEC* operon, whereas in *Synechocystis* PCC 6803 and *Arthrospira maxima* CS-328 the operon structure is split in a *phaEC* and a *phaAB* operon (Figure 1.5). The regulator PhaR and the phasin PhaP are missing in cyanobacteria.

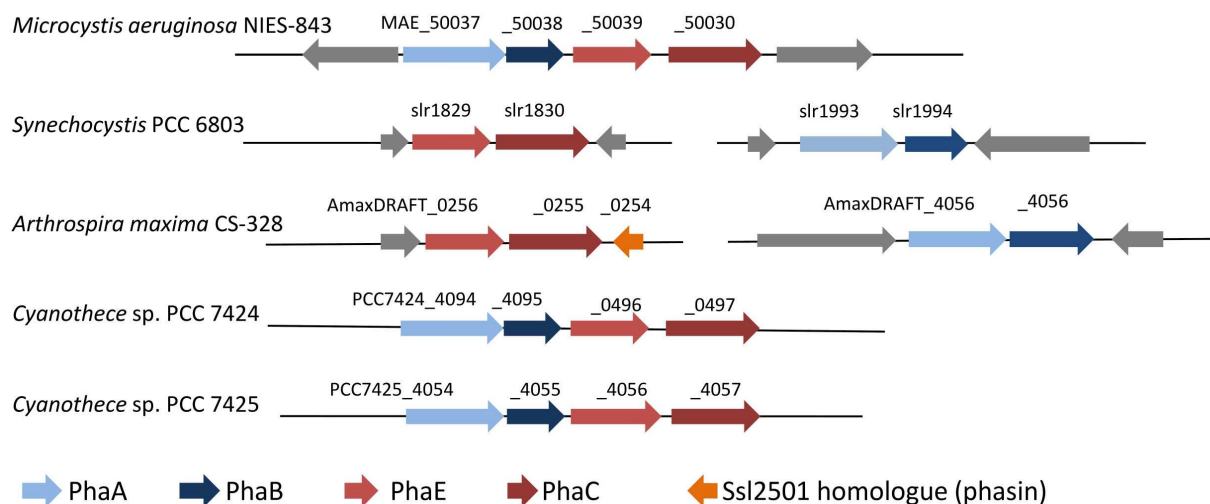


**Figure 1.5: Schematic representation of the genetic organization of PHB synthesis genes in cyanobacteria. -**

During the past decade, several publications on the physiology and function of PHB in cyanobacteria have been published. In the thermophilic strain *Synechococcus* MA 19 regulation of the PHB synthase was characterised (Miyake *et al.*, 1997). Activity of the PHB synthase was exclusively found in the membrane fraction. Thus, it was suggested that the PHB synthase is attached to the thylakoid membrane. Upon nitrogen starvation an increase of activity was observed, which was not affected by addition of chloramphenicol. This implied a posttranslational modification. This hypothesis was supported by the fact that addition of acetyl phosphate increases the activity. Acetyl phosphate is synthesised by the enzyme phosphotransacetylase, which catalyses the reversible transfer of the acetyl group from acetyl phosphate to CoA forming acetyl-CoA and inorganic phosphate. In the literature, acetyl phosphate often is described as sensor metabolite (Juntarajumnong *et al.*, 2007; Morrison *et al.*, 2005), but it is ambiguous whether acetyl phosphate is a sensor metabolite or acts as unspecific phosphor-donor for response regulators. However, Miyake *et al.* (1997) showed that the activity of the phosphotransacetylase also increased during nitrogen starvation. This led to the assumption that during nitrogen starvation first the acetylCoA pool increases due to a blocked anabolism. Subsequently, phosphotransacetylase activity increases followed by an increase of the acetyl phosphate concentration. Finally, PHB synthase is activated by acetyl phosphate to synthesise PHB.

Another strain of interest is the diazotrophic cyanobacterium *Nostoc muscorum*, which accumulates PHB to levels sufficient for potential industrial applications (Sharma & Mallick,

## 1. INTRODUCTION

---

2005). Under optimal conditions, *Nostoc muscorum* accumulates up to 40% PHB of cell dry weight. PHB accumulation depends on several factors. It is induced by an alkaline pH, which is in agreement with a study with *Rhodobacter sphaeroides* (Khatipov *et al.*, 1998). *Nostoc muscorum* accumulates higher levels of PHB under N<sub>2</sub>-fixing conditions than under growth with combined nitrogen. Additionally, light-dark cycles promote PHB accumulation. Cell cultures supplemented with an excess of different carbon sources (acetate, glucose, fructose, maltose and ethanol) show an increased PHB accumulation. Acetate is directly utilised for the synthesis of PHB, whereas glucose is utilised via the pentose phosphate pathway accompanied with an increase of the NADPH pool, which is required for the acetoacetyl-CoA reductase reaction. Maximum PHB accumulation is reported in case of glucose and acetate supplementation, because precursor availability is ensured and an adequate amount of the reduction equivalent NADPH is present. PHB accumulation is also induced by phosphate starvation. ATP production is known to decrease markedly with the onset of phosphate limitation, while the reduction of NADP<sup>+</sup> through non-cyclic photosynthetic electron flow is not inhibited (Bottomley & Stewart, 1976; Konopka & Schnur, 1981).

In *Synechocystis* PCC 6803, genetics and physiology of PHB accumulation have been explored. *Synechocystis* PCC 6803 possesses a class III PHA synthase (Hein *et al.*, 1998), which is encoded by the genes *slr1829* (PhaE) and *slr1830* (PhaC). In addition, the  $\beta$ -ketothiolase and the acetoacetyl-CoA reductase were identified and characterised (Taroncher-Oldenburg *et al.*, 2000). In *Synechocystis* PCC 6803, PHB accumulation is induced by limitation of the phosphate and nitrate supply and by high light conditions (Panda *et al.*, 2006). Furthermore, reduced dissolved oxygen concentration induces PHB accumulation, which is explained by a surplus of NADPH, caused by a reduced respiration rate (Panda *et al.*, 2006). Fructose also stimulates PHB production by increasing the NADPH pool due to utilisation via oxidative pentose phosphate pathway (Panda *et al.*, 2005).

### 1.6 Nitrogen metabolism of Cyanobacteria

Since nitrogen is an essential building block of amino acids and nucleic acids, it is an essential nutrient for all living organism. Nitrogen frequently is a limiting nutrient in natural habitats. Therefore, cyanobacteria as well as other autotrophic organisms have developed multiple strategies to adapt to nitrogen deficiency (Merrick & Edwards, 1995). Cyanobacteria are able to use a range of nitrogen compounds like nitrate, nitrite, ammonia, cyanate, urea or even some amino acids as nitrogen source (Luque & Forchhammer, 2007). Many strains fix atmospheric nitrogen, they separate either spatially or temporarily the process of oxygenic photosynthesis and oxygen-sensitive nitrogen fixation. Filamentous cyanobacteria (e.g. *Anabaena* and *Nostoc*) differentiate some cells to heterocysts with an anoxygenic environment, whereas some unicellular diazotrophic species (e.g. *Cyanothece*) fix nitrogen only in the dark periods of a day cycle (Gallon, 2001).

Ammonium is the preferred N-source, because further reduction is not necessary. Most cyanobacteria possess ammonia permeases, which are necessary for ammonium uptake at low concentrations (Montesinos *et al.*, 1998). Under high concentrations of ammonium in the medium, it can permeate the cell membrane. In many environments nitrate is the most abundant N-species, although concentrations of available nitrate and nitrite may be low (in  $\mu\text{M}$  range). Therefore, specific nitrate uptake systems are required to concentrate nitrate inside the cells (Luque *et al.*, 1994). Intracellular nitrate needs a two-step reduction to ammonia, which is catalysed by the ferredoxin-nitrate reductase (NR) and the ferredoxin-nitrite reductase (Nir) (Suzuki *et al.*, 1993). The electron donor for this reaction is ferredoxin, which is reduced by PS I.

Assimilation of ammonium is operated by the glutamine synthetase-glutamate synthase cycle (GS/GOGAT) (Wolk *et al.*, 1976). GS transfers ammonium to the  $\gamma$ -carboxylgroup of glutamate. Initial phosphorylation of the  $\gamma$ -carboxylgroup of glutamate by ATP provides high efficiency of this reaction. The amide group of the formed glutamine is subsequently transferred to 2-oxoglutarate (2-OG) by the glutamine-2-oxoglutarate-amido transferase (GOGAT). The electrons for this reductive amination are provided by PS I-reduced ferredoxin. The products of this reaction are two molecules glutamate, whereof one serves as substrate for the GS. Thus, the GS/GOGAT cycle produces one glutamate from 2-OG and ammonium consuming ATP and two reduction equivalents. Since cyanobacteria lack a 2-oxoglutarate dehydrogenase, 2-OG is mainly used for the biosynthesis of glutamate and glutamine-derived compounds. The role of 2-OG as a carbon skeleton for nitrogen assimilation makes it signalling molecule for the C/N ration (Forchhammer, 2004).

### 1.6.1 Regulation of nitrogen metabolism

In order to adapt to changes in type and availability of N-sources, cyanobacteria evolved adequate mechanisms for sensing and response. Since ammonium is the preferred nitrogen source, it represses the assimilation of other nitrogen compounds (Flores & Herrero, 2005; Muro-Pastor *et al.*, 2003). The regulation of nitrogen metabolism is mainly operated by the transcription factor NtcA and the regulatory protein PII.

PII signalling proteins are homotrimeric proteins of 12-13 kDa subunits. Under nitrogen-limiting conditions, a high intracellular 2-OG level leads to phosphorylation of residue Ser49 on each subunit of the PII protein, resulting in four different modification states of PII (Forchhammer & Tandeau de Marsac, 1994). In addition to the C/N ratio, PII senses the energy level by the binding of ATP and ADP (Forchhammer, 2008). Thus, PII integrates the different signals from carbon, nitrogen and energy status into different conformation and modification states, which results in different activity of the target proteins. In *Synechococcus elongatus* PCC 7942 (in the following *S. elongatus* 7942), the PII targets are N-acetyl-L-glutamate kinase (NAGK) (Maheswaran *et al.*, 2004), the key enzyme of arginine biosynthesis and PipX (PII interacting protein X) (Espinosa *et al.*, 2006). Additionally, *Synechocystis*

## 1. INTRODUCTION

---

PCC 6803 PII interacts with PamA (PII associated membrane protein A) (Osanai *et al.*, 2005). Physiological studies indicate that PII signalling is involved in the regulation of nitrate utilisation (Kloft & Forchhammer, 2005; Takatani *et al.*, 2006), in bicarbonate uptake and in gene expression via the global nitrogen control factor NtcA.

The transcription factor NtcA belongs to the CRP-FNR-family with an N-terminal sensor domain and a C-terminal helix-turn-helix DNA-binding domain (Vega-Palás *et al.*, 1992). The perfect DNA binding signature of NtcA is the palindrome GTA N<sub>8</sub> TAC (Luque *et al.*, 1994). NtcA is also able to bind imperfect NtcA-binding sites. NtcA expression is positively autoregulated and its upregulation is followed by a transcriptional change of a number of genes, the NtcA regulon (Su *et al.*, 2005). In *S. elongatus* 7942, NtcA activates the expression of nitrate assimilatory genes (*nirA*, *nrtABCD*, *narB*), genes for ammonium uptake (*amt1*), glutamine synthetase (*glnA*) and the gene for the PII protein (*glnB*) (Herrero *et al.*, 2001). The expression of the *cynABDS* operon, involved in cyanate uptake and degradation is also induced by NtcA. Recently, some new NtcA-regulated genes have been discovered (Rasch, 2009). This microarray studies of *S. elongatus* 7942 wild type strain and a NtcA knockout mutant revealed that *pilT3* (twitching mobility protein), *rpoD4-codA* (sigma factor group 2, cytosin deaminase), and *mocD* (hydrocarbon oxygenase) have imperfect NtcA binding sites and that the expression of these genes are controlled by NtcA. In addition, a new gene cluster of seven genes was identified. The gene cluster has been termed Nit1C, because the second gene has homologies to a nitrilase of the Nit1C subfamily (Podar *et al.*, 2005).

### 1.6.1.1 Highly induced genes under nitrogen starvation: the Nit1C cluster

The Nsi5 protein was firstly described in a proteome analysis of nitrogen deprived *S. elongatus* 7942 cells (Aldehni *et al.*, 2003). This study identified several proteins, which were highly induced upon nitrogen starvation. One of these proteins, termed Nsi5 (Nitrogen starvation induced no. 5) was identified as the hypothetical protein Synpcc7942.0840. Further analyses revealed that this gene is part of the Nit1C cluster, which is highly conserved in amino acid composition and gene arrangement. The gene cluster is sparsely but broadly distributed in bacteria, including *Actinobacteria*, *Proteobacteria*, and *Cyanobacteria*. The seven genes of the predicted operon occur in the order (1) hypothetical protein, (2) nitrilase, (3) radical S-adenosyl methionine (SAM) superfamily member, (4) acetyltransferase, (5) AIR synthase, and (6) hypothetical protein. The seventh gene encodes a predicted flavoprotein, putatively involved in K<sup>+</sup> transport. This gene is located either at the beginning of the cluster but on the opposite strand (cyanobacteria) or as the last gene of the cluster, in the same orientation as the others (proteobacteria).

### 1.6.1.2 Sequence similarities of the Nit1C operon

The first protein, Sll0783 of the gene cluster shows similarity to the DsrE proteins. In *Allochrocatium vinosum* DsrE is essential for the oxidation of stored sulphur via the Dsr

system (Pott & Dahl, 1998). In detail, DsrE forms a complex with DsrF and DsrH, where DsrE is probably the acceptor for persulfide sulphur originated from sulphur stored in the periplasm. The DsrEFH complex is similar to the TusBCD complex from *E. coli*, which is involved in 2-thiouridine biosynthesis. TusBCD mediates sulphur transfer from TusA to TusBCD binding partner TusE (Dahl *et al.*, 2008).

The second gene, Sll0784, is a nitrilase, which hydrolyses organic nitriles to carboxylic acids

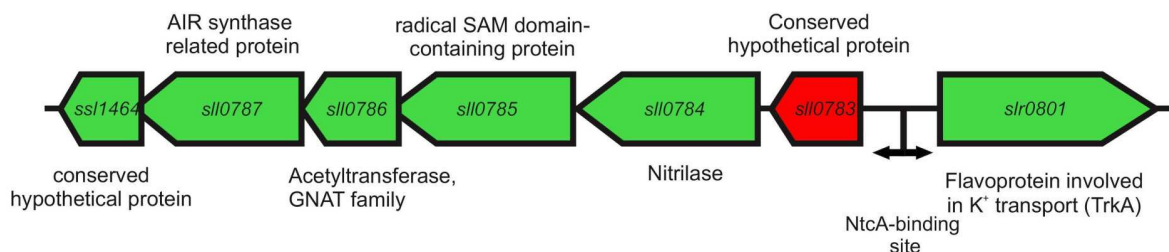


**Figure 1.6: Schematic representation of the Nit1C-cluster of *Synechocystis* PCC 6803.** - General function predictions are indicated.

and ammonium via a covalently bound acyl residue. Most bacterial nitrilases are inducible by the presence of nitriles, which indicates a role in detoxification or utilisation (Banerjee *et al.*, 2006). The nitrilase PinA from plant-associated *Pseudomonas fluorescens* SBW25 enables this organism to utilise  $\beta$ -cyanoalanine, which is common in the plant environment as nitrogen source (Howden *et al.*, 2009).  $\beta$ -cyanoalanine is also produced by the marine organism *Vibrio* sp. as anticyanobacterial substance (Yoshikawa *et al.*, 2000). The nitrilase Sll0784 of *Synechocystis* PCC 6803 is similar to the group of aliphatic nitrilases and was characterised previously (Heinemann *et al.*, 2003). It shows a clear preference for fumaro-dinitrile and also to larger benzene derivatives. Dinitriles with fewer than six carbon atoms were converted to mononitriles. Since this study had a biotechnology background, no suggestion about the possible physiological role was proposed.

The next gene, Sll0785, is a member of the radical SAM superfamily, which catalyses diverse reactions like unusual methylations, isomerisation, sulphur insertion, ring formation, anaerobic oxidation or protein radical formation (Sofia *et al.*, 2001). Members of the radical SAM superfamily are characterized by a conserved CxxxCxxC motif, which coordinates the iron sulphur cluster. The common mechanism is the cleavage of the  $[4\text{Fe-4S}]^{1+}$ -SAM complex to  $[4\text{Fe-4S}]^{2+}$ -Met and the 5-deoxyadenosyl radical, which abstracts a hydrogen atom from the substrate to initiate a radical mechanism.

The gene product of *sll0786* is a predicted acetyltransferase and shows similarities with the Gcn5-related N-acetyltransferases (GNAT). This group includes eukaryotic histone acetyltransferases like Gcn5, Hat1, Hpa2 and Elp3 (Sterner & Berger, 2000). Some Elp3-related proteins are two-domain acetyltransferases, where the N-terminal domain is similar to the



## 1. INTRODUCTION

---

radical SAM superfamily. While the Elp3 proteins are part of the RNA polymerase II holoenzyme, the putative function of the two domain enzyme is histone demethylation (Chinenov, 2002). In the described gene cluster the GNAT is in direct neighbourhood of a radical SAM enzyme, which could be a hint to a conserved catalytic mechanism.

The gene product of *sll0787* is a predicted AIR synthetase-related protein. This family includes hydrogenase expression/formation protein, HypE, which may be involved in the maturation of NifE hydrogenase, 5-aminoimidazole ribonucleotide (AIR) synthase, which is involved in *de novo* purine biosynthesis; and selenide water dikinase, an enzyme which synthesises selenophosphate from selenide and ATP.

Homologues of the gene *slr0801* are annotated as TrkA of the Trk potassium transport system and harbour a FAD and a NADPH binding site. The Trk potassium transporter is a constitutive K<sup>+</sup> transporter in *E. coli* (Rhoads *et al.*, 1976). TrkA is a peripheral membrane protein located on the cytoplasmic side of the membrane (Bossemeyer *et al.*, 1989). Furthermore, it shows significant homologies with a monooxygenase.

In *S. elongatus* 7942 knockout mutants of the Nit1C cluster were constructed (Rasch, 2009). Physiological investigations of this mutants revealed that knockout of the first gene exhibits no severe phenotype (Rasch, 2009). In contrast to that, a knockout mutant of the *sll0783* gene in *Synechocystis* PCC 6803 was probably impaired in PHB accumulation under nitrogen starvation and was unable to completely phosphorylate the PII protein (Sauer, 2001). Therefore, analysis of the phenotype of the Sll0783 deficient *Synechocystis* strain could provide insights in the function of this highly nitrogen-starvation induced gene.

## 2

# Aims of the project

In previous work, a gene cluster of seven genes, which is highly induced upon nitrogen starvation, was identified. The function of this gene cluster was completely unclear. Initial investigations of Sll0783 knock-out mutant indicated that PHB accumulation is impaired. It was not known whether the PHB synthesis genes were impaired or the activity of the corresponding enzymes was reduced or other requirements of PHB synthase were afflicted. Therefore, the first part of this thesis was the characterisation of the impaired PHB accumulation in the Sll0783 mutant. This included detailed fluorescence microscopy of nitrogen starved cells together with quantification by HPLC and fluorescence spectroscopy. Subsequently, the requirements of the impaired PHB accumulation should be analysed to reveal the cause of the phenotype. Furthermore, the link between the missing Sll0783 protein and the impaired PHB synthesis was completely unclear. Therefore, a basic characterisation of PHB-formation of *Synechocystis* was necessary.

The second part of this work was the investigation of the function of the Nit1C gene cluster. Analysis of gene expression, promoter structure and comparison of homologous genes should provide information about the physiological function of this gene cluster.

## 2. AIMS OF THE PROJECT

---

# 3

## Results

### 3.1 Analysis of the gene *sll0783*: phylogeny, promoter and expression

#### 3.1.1 Phylogenetic analysis of the gene *sll0783* and its homologues

Bioinformatic analyses of the *sll0783* gene predict a product of 160 amino acids with a mass of 17.64 kDa and a conserved DsrE domain (pfam02635). It is a putative cytoplasmic soluble protein without any signal sequences. A PSI-Blast search showed that homologous sequences occur in several cyanobacteria, in a variety of  $\alpha$ -,  $\beta$ - and  $\gamma$ - proteobacteria as well as in some Gram-positives (Figure 3.2). The gene occurs broadly but sparsely among the bacteria. Almost all heterotrophic strains accumulate PHAs and many of them can fix nitrogen. By contrast, the cyanobacteria containing the *sll0783* homologue do not accumulate PHA, except of *Synechocystis* PCC 6803. All cyanobacteria with *sll0783* homologues are unicellular, non-diazotrophic and are known to grow in oligotrophic habitats. The strain *Prochlorococcus marinus* MIT 9301 possesses the smallest cyanobacterial genome and is known for a reductive evolution imposed by a static and extremely nutrient-poor environment, which causes a loss of dispensable genes (Scanlan *et al.*, 2009). To gain further insights in the phylogeny of the *sll0783* gene, a phylogenetic tree of the cyanobacterial *sll0783* homologues was compared with the 16S phylogeny of these organisms (Figure 3.1). This comparison reveals a remarkably similar phylogeny, suggesting early acquisition of this gene during cyanobacterial evolution.

#### 3.1.2 Characterisation of the promoter of *sll0783*

In *S. elongatus* 7942, the *sll0783* homologue gene is under control of the NtcA promoter (Rasch, 2009). Since in cyanobacteria many regulatory mechanisms are conserved, we analysed the DNA sequences upstream of the cyanobacterial *sll0783* homologues. The upstream regions often contains the perfect NtcA-recognition site GTA-N<sub>8</sub>-TAC, indicating

### 3. RESULTS

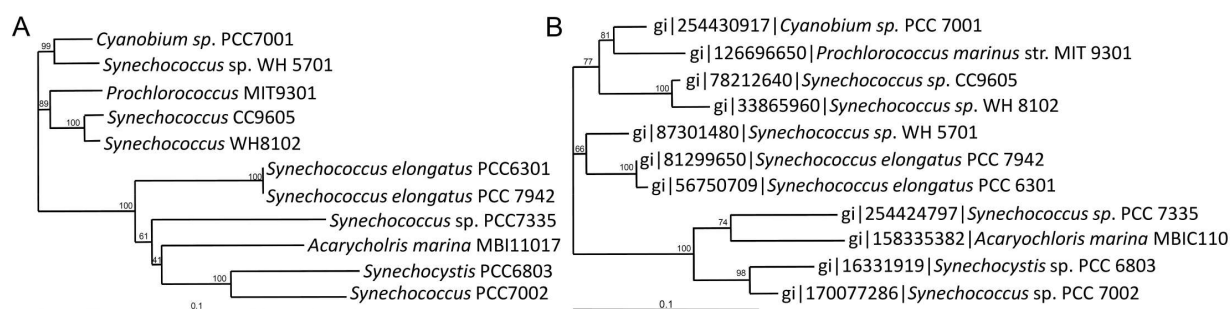


**Figure 3.1: Comparison of 16S and Sll0783-homologues phylogeny.** - (A) 16S rRNA neighbour-joining tree from known cyanobacteria containing the Nit1C cluster. (B) Protein neighbour-joining tree for Sll0783-homologues from known cyanobacteria containing the Nit1C cluster. Trees were constructed from alignments using ClustalX v2.0.11. Bootstrap values are given at nodes if at least 50. (Schlebusch & Forchhammer, 2010)

that the NtcA-dependent expression and maybe the function of *sll0783* might be conserved in cyanobacteria (Figure 3.3A). In *Synechocystis* PCC 6803, the upstream region of *sll0783* displays an imperfect NtcA recognition site (Aldehni & Forchhammer, 2006; Herrero *et al.*, 2001). Furthermore, in *Synechocystis* PCC 6803 the intergenic region between *sll0783* and the potential flavoprotein *slr0801* has a size of 465 bp, which is substantially larger than the corresponding intergenic region in other cyanobacteria containing this gene cluster. Therefore, we experimentally determined the location of the transcriptional start point of *sll0783* to reveal whether it matches the potential NtcA binding site. The 5' end of the *sll0783* transcript was determined by the 5'RACE method (see Materials and Methods). The putative transcriptional start point (tsp), as deduced from this experiment, is located 48 bp upstream of the predicted ATG start codon (Figure 3.3B). According to this result, the promoter seems to be a non-canonical class I promoter with a -35 site and a putative NtcA binding site 107 bp upstream of the tsp (Herrero *et al.*, 2004).

#### 3.1.3 Expression of *sll0783* and surrounding genes

The expression of *sll0783* and its surrounding genes *sll0784* and *slr0801* was determined by qRT-PCR in *Synechocystis* PCC 6803 wild type and a Sll0783 knockout mutant with cells grown under nitrate-repleted conditions and shifted to nitrate-depleted conditions. Under nitrate-repleted conditions, the genes *sll0783*, *sll0784* and *slr0801* of the wild type were only slightly expressed, whereas under nitrogen-starvation conditions, all three genes were highly induced after 6 hours. Transcripts of *sll0783* and *sll0784* increased about 250-fold and 200-fold, respectively, whereas *slr0801* transcripts increased 30-fold. During the course of nitrogen starvation, the expression of these genes was regressing again (Figure 3.4A)(Schlebusch & Forchhammer, 2010). In the *sll0783* mutant, expression of *slr0801* was not impaired in comparison to the wild type. The *sll0784* gene, downstream of *sll0783*, was constitutively

### 3.1 Analysis of the gene *slI0783*: phylogeny, promoter and expression

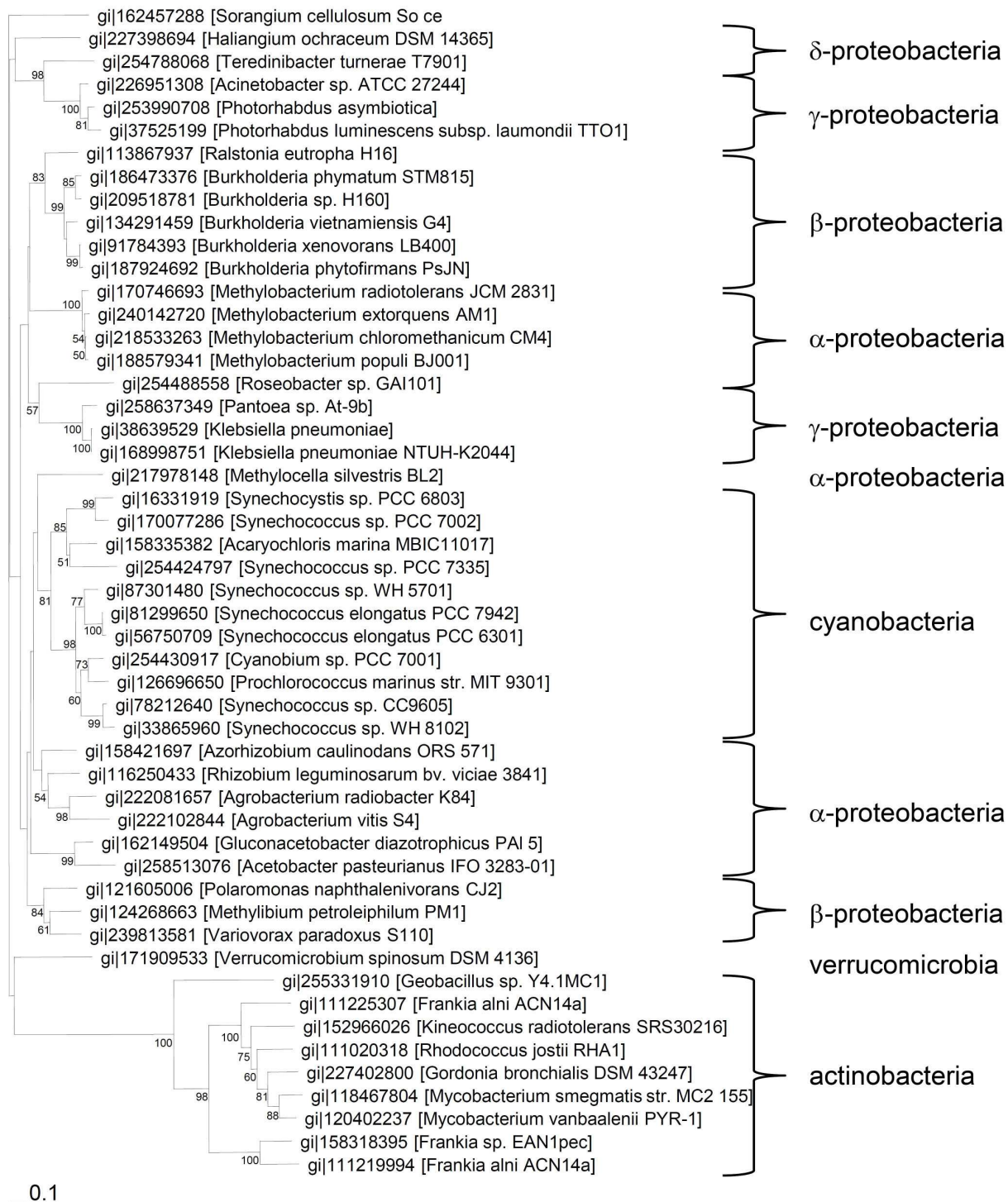


**Figure 3.2: Protein neighbour-joining tree for SII0783 homologues** - SII0783 homologues are indicated with gi numbers, from known bacteria containing the SII0783 homologues (Species name in parentheses). On the right side are shown the major bacterial kingdoms. Trees were constructed from alignments using ClustalX v2.0.11. Bootstrap values are given at nodes if at least 50. (Schlebusch & Forchhammer, 2010)

### 3. RESULTS

**A**

Synechococcus PCC7002	TTAACT <b>GTA</b> AGACCCGCT <b>TCA</b> ...N <sub>23</sub> ... <b>TAC</b> CGATCC N <sub>226</sub> <b>ATG</b>
Prochlorococcus marinus MIT 9301	AATTT <b>GGT</b> GATATCGGT <b>TAC</b> ...N <sub>20</sub> ... <b>CAG</b> AGAATGTTCTAAGTTTTTTTAAATTTTCATG
Synechococcus elongatus PCC7942	TATTT <b>AGT</b> AGTCACCGT <b>TAC</b> ...N <sub>20</sub> ... <b>TAG</b> TTAATTG...N46... <b>ATG</b>
Synechococcus WH8102	TGTGTT <b>GTA</b> GCCAAGGC <b>CAC</b> ...N <sub>23</sub> ... <b>TC</b> ATCCAGTTT...N71... <b>ATG</b>
Acaryochloris marina MBIL11017	GGCTGC <b>GTA</b> CCCTTA <b>TAC</b> ...N <sub>24</sub> ... <b>TA</b> AGAAGCCTCA...N <sub>273</sub> ... <b>ATG</b>

**B**

			-35		-10		+1
<i>slI0783</i>	<b>AGAT</b> AATCTTCA	<b>TACA</b> ...	N <sub>39</sub> ...	TGATACA	N <sub>21</sub>	TA N <sub>3</sub> T	GATACAT <b><u>GA</u></b>
<i>glnA</i>	<b>TGTA</b> TCAGCTGT	<b>TACA</b> ...	N <sub>22</sub> .....	.....	TA N <sub>3</sub> T	GGATAGT <b><u>CG</u></b>	
	<b>GTA</b> N <sub>8</sub>	<b>TAC</b> N <sub>22</sub>			TA N <sub>3</sub> T	N <sub>4-5</sub>	<b><u>tsp</u></b>

**Figure 3.3: Promoter analysis of *slI0783* homologues in cyanobacteria** - (A) Putative NtcA-binding sites in the upstream region of *slI0783* homologues in cyanobacteria containing this gene cluster. Startcodon is marked red. Nucleotides matching those of the GTA and TAC triplets of the NtcA-binding site are boldface. (B) Sequence of 5'end of *slI0783* transcript. Total RNA from nitrogen-starved *Synechocystis* PCC 6803 wild type cells was isolated and analysed by using the 5'RACE method. Sequencing the cDNA revealed the 5'end of the *slI0783*-transcript (+1), indicating a potential transcription start site (tsp). The potential NtcA binding site upstream of the tsp is aligned to the NtcA binding site in the promoter of the *glnA* gene (*slr1765*). Below, the consensus canonical NtcA binding sequence is shown. The putative NtcA-binding motif is highlighted in bold and the possible tsp is underlined (Schlebusch & Forchhammer, 2010).

expressed in the mutant as a result of the insertion of a terminator-free, promoter-carrying kanamycin resistance cartridge in *sll0783*, driving transcription in direction of the downstream (*sll0784*) genes (Figure 3.4B).

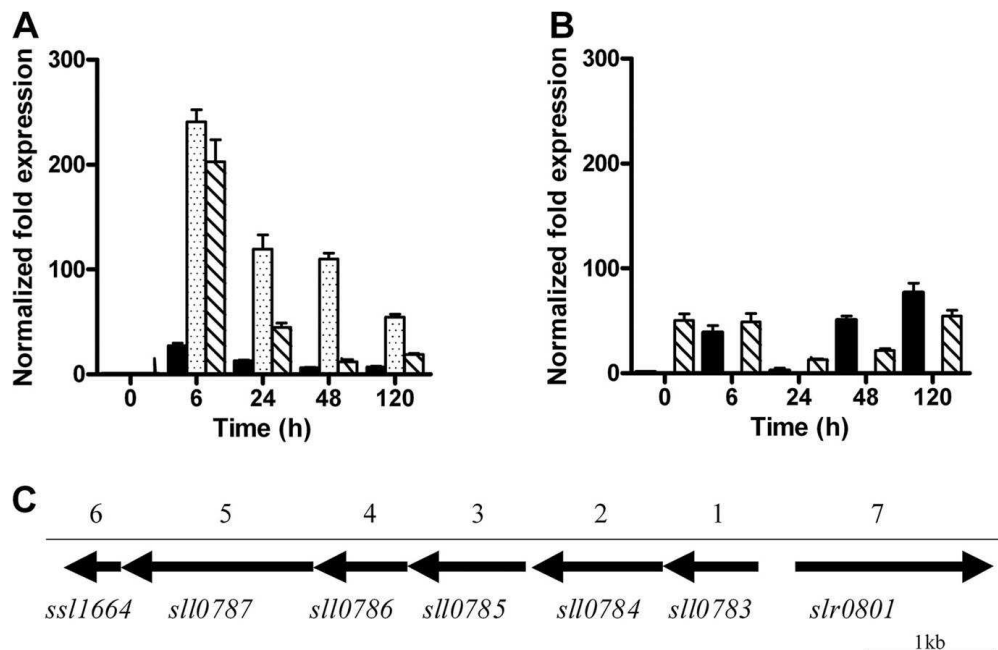


**Figure 3.4:** Expression of *slr0801* (black bars), *sll0783* (dotted bars) and *sll0784* (dashed bars) - (A) *Synechocystis* PCC 6803 wild type and (B) Sll0783 mutant under nitrogen deficient conditions. Levels of mRNA were determined by qRT-PCR and normalised to the mRNA level of *rnpB*. Time point zero of the wild type was set to one. For details see Material and Methods 5.4.5 (p.71). (C) In scale schematic representation of the *sll0783* gene cluster. Standard deviations from triplicate experiments are indicated by error bars. (Schlebusch & Forchhammer, 2010).

## 3.2 Physiological characterisation of the Sll0783 mutant

### 3.2.1 Physiological characteristics under nitrogen starvation

Since the highest expression of *sll0783* occurred upon nitrogen starvation, the physiological characteristics of chlorosis were investigated. Therefore, the growth rate, photosynthetic activity and pigment content of *Synechocystis* PCC 6803 wild type and Sll0783 mutant were analysed. Figure 3.5 shows that wild type and Sll0783 mutant performed the chlorosis in a similar manner. The loss of *sll0783* did not change the global cellular response upon nitrogen starvation.



### 3. RESULTS

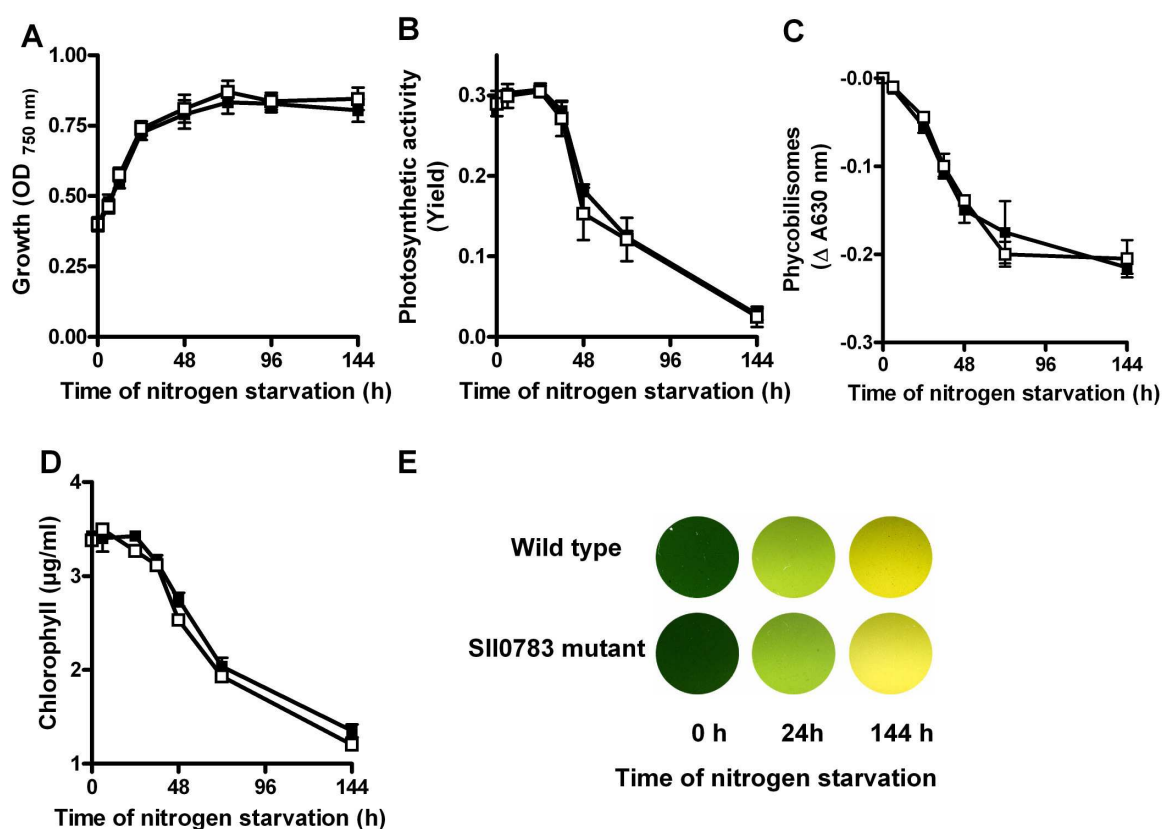


**Figure 3.5: Physiological characteristics of *Synechocystis* PCC 6803 wild type (filled squares) and Sll0783 mutant (open squares).** - (A) Growth of wild type and the Sll0783 mutant upon nitrogen starvation was followed by measuring the optical density of the culture at 750 nm. (B) Photosynthetic activity measured with WALTER-PAM chlorophyll fluorometer. (C) Change in *in vivo* phycobilisome quantity was determined by difference spectra analysis. Absorption change at 630 nm corresponds to phycobiliproteins. (D) Chlorophyll *a* content measured by determined by methanolic chlorophyll extraction. (E) Digital pictures of 3 ml liquid cultures of wild type and Sll0783 mutant in microtiter plates at different time points upon nitrogen starvation. Standard deviations from triplicate experiments are indicated by error bars.

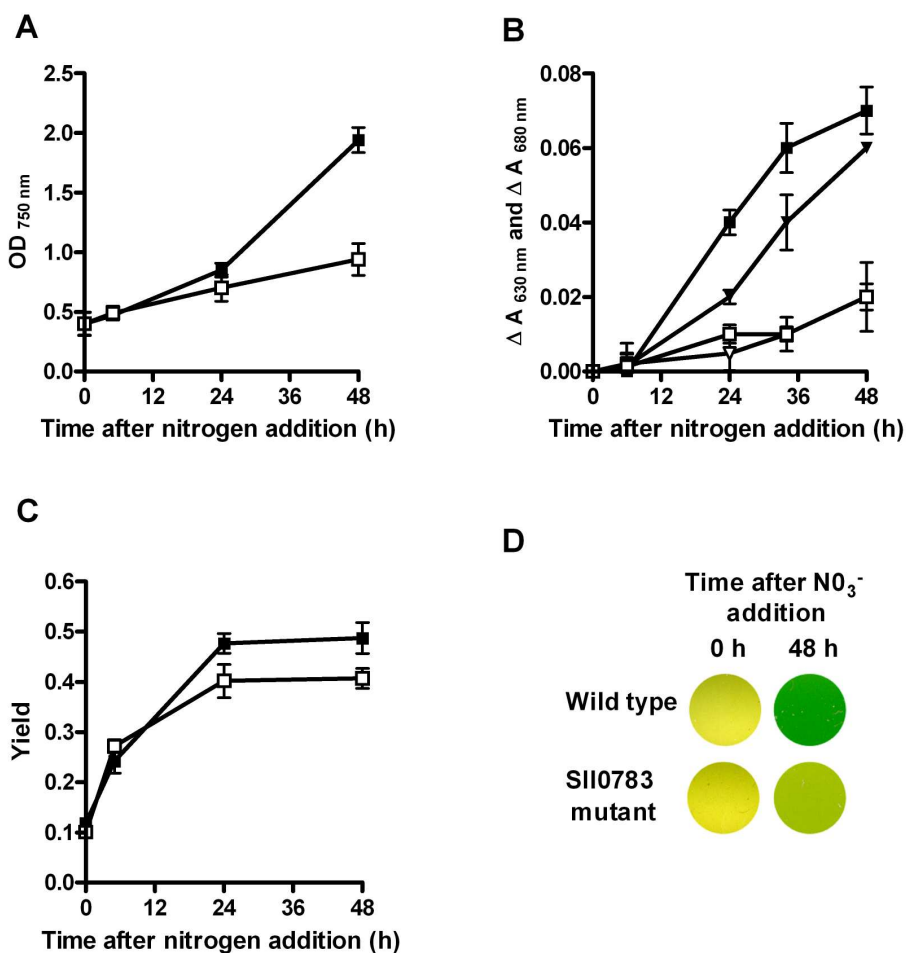


**Figure 3.6:** Recovery of *Synechocystis* PCC 6803 wild type (filled squares) and Sll0783 mutant (open squares) from previous nitrogen starvation. - 5 mM sodium nitrate was added to 72 h nitrogen starved cells. Cell cultures were illuminated with  $50 \mu\text{M}$  photons  $\text{m}^{-2} \text{s}^{-1}$ . In the time course various parameters were determined. (A) Growth of wild type and the Sll0783 mutant was followed by measuring the optical density of the culture at 750 nm. (B) Changes in *in vivo* chlorophyll *a* and phycobilisome quantity as determined by difference spectra analysis. Absorption change at 680 nm corresponds to chlorophyll *a* (triangles), 630 nm corresponds to phycobiliproteins (squares). (C) Photosynthetic activity determined by quantum efficiency (Yield) of PS II. (D) Digital pictures of 3 ml liquid cultures of wild type and Sll0783 mutant in microtiter plates at indicated time points. Standard deviations from triplicate experiments are indicated by error bars.

### 3. RESULTS

#### 3.2.2 Recovery process after nitrogen starvation

Under nitrogen starvation, pigmentation and photosynthetic activity in the *slr0783* mutant decayed as fast as in the wild type. However, after adding 5 mM sodium nitrate to cells, which had been starved for combined nitrogen for three days, the Sll0783 mutant was unable to recover as fast as the wild type (Figure 3.6 A). Following the onset of recovery, the mutant showed a prolonged lag phase compared to the wild type strain. The impairment of recovery was clearly visible in the time course of chlorophyll *a* and phycobilisome content (Figure 3.6B) and photosynthetic activity (Figure 3.6C).

During nitrogen starvation, *Synechocystis* PCC 6803 stores excess carbon in different storage polymers. The common C-storage polymer is glycogen, which is mostly accumulated during the day and degraded by night. For long-term carbon storage, *Synechocystis* PCC 6803 is able to synthesise PHB. In order to investigate the impaired recovery from nitrogen starvation in the Sll0783 mutant, glycogen and PHB level were quantified during the recovery phase. As shown in Figure 3.7A, glycogen turn-over was apparently not impaired in the Sll0783 mutant. Both, wild type and Sll0783 mutant rapidly utilised glycogen in the first 12 h after the addition of nitrogen. Thereafter, the glycogen level slightly increased again (Figure 3.7A). During the same period of time, the wild type degraded the previously accumulated PHB reserves, whereas the mutant did not alter its low PHB content (Figure 3.7B)(Schlebusch & Forchhammer, 2010).

Recovery from chlorosis was also tested with ammonium as nitrogen source. After addition

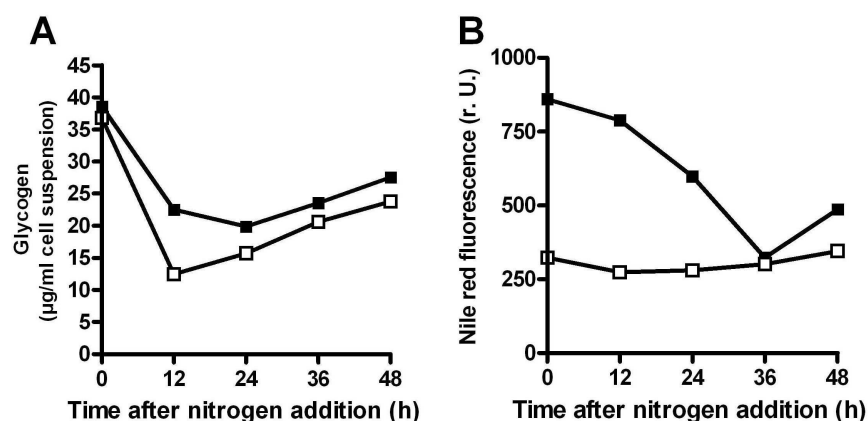


**Figure 3.7: Analysis of the storage polymers glycogen and PHB** - 5 mM sodium nitrate was added to nitrogen starved *Synechocystis* PCC 6803 wild type (filled squares) and Sll0783 mutant (open squares) cells (72 h). (A) Determination of the Glycogen content. (B) Quantification of Nile red fluorescence, indicating the amount of PHB.

of ammonium, growth rate and photosynthetic activity increased in wild type and in the Sll0783 mutant in a similar way, indicating that PHB mobilisation may be advantageous for the utilisation of nitrate (Figure 3.8).

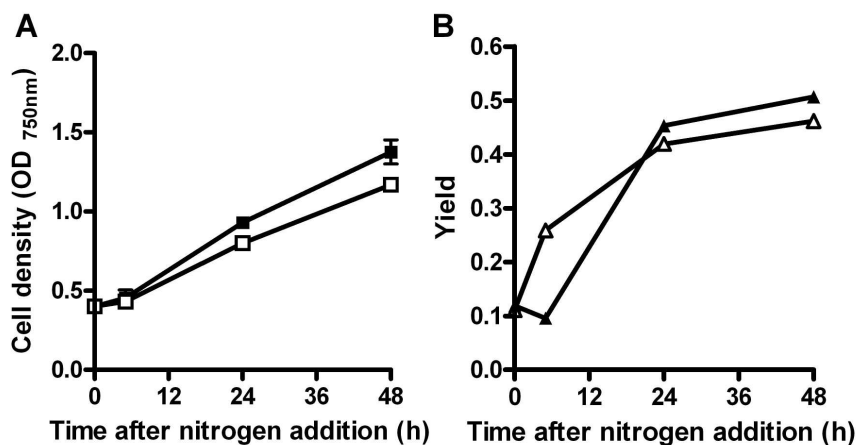


**Figure 3.8:** Recovery of *Synechocystis* wild type (filled symbols) and Sll0783 mutant (open symbols) with 5 mM ammonium. - (A) Cell density followed by OD<sub>750nm</sub> (B) Photosynthetic activity determined by quantum efficiency (Yield) of PS II.

### 3.2.3 Influence of light conditions

The recovery from nitrogen starvation was further tested with nitrate as N-source using different light intensities. Under high light intensities ( $100 \mu\text{M photons m}^{-2} \text{s}^{-1}$ ) both, optical density and pigmentation increased in the wild type faster than in the Sll0783 mutant. Under dark conditions wild type and Sll0783 mutant did not grow. Moreover, the wild type did not synthesise photosynthetic pigments, whereas the Sll0783 mutant synthesised pigments and showed a visible colouration (Figure 3.9).

## 3.3 PHB accumulation in wild type and the Sll0783 mutant

Under nitrogen-limiting conditions, both *Synechocystis* PCC 6803 wild type and Sll0783 mutant started with the formation of PHB granules as revealed by fluorescence microscopy of Nile red-stained cells. Nile red is a hydrophobic fluorescence dye, which is specific for hydrophobic substances like membranes and PHB granules. Over the course of time, size and amount of wild type granules increased. After 4 weeks, the wild type cells were filled with large quantities of PHB granules. In contrast, the Sll0783 mutant PHB granules did neither increase in size nor in number after 36 h. After 4 weeks the visible amount of PHB was similar to the amount after 36 h (Figure 3.10).

### 3.3.1 Quantification of PHB accumulation

To quantify the microscopically visible difference in PHB accumulation, the whole PHB content of the cells was determined by HPLC analyses (Figure 3.11A). After 120 h N-starvation, the wild type reached a PHB content of 5.7% PHB (w/w cell dry weight) whereas the amount

### 3. RESULTS

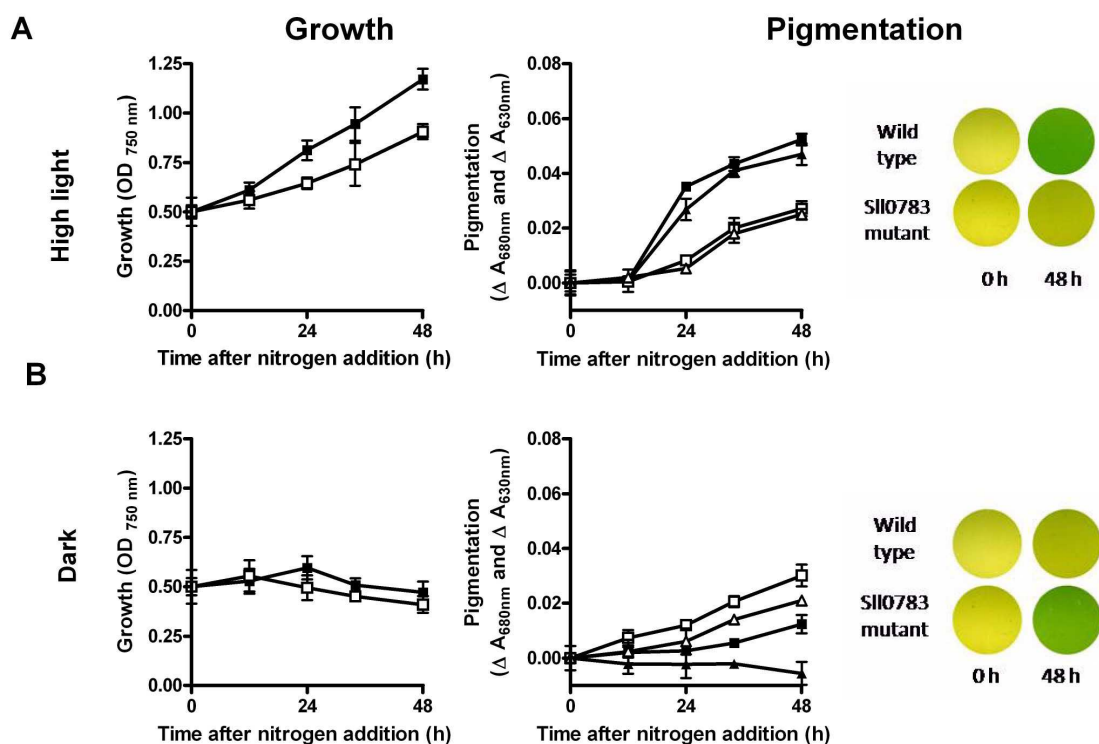


**Figure 3.9: Recovery of *Synechocystis* PCC 6803 wild type (filled squares) and Sll0783 mutant (open squares) from previous nitrogen starvation under different light intensities.** - 5 mM sodium nitrate was added to 72 h nitrogen starved cells and cells were incubated under (A) high light conditions and (B) in the dark. Growth was followed by measuring the optical density at 750 nm. Pigmentation was documented by changes in *in vivo* chlorophyll *a* and phycobilisome quantity as determined by difference spectra analysis. Absorption change at 680 nm corresponds to chlorophyll *a* (triangles), 630 nm corresponds to phycobiliproteins (squares). Digital pictures of 3 ml liquid cultures of wild type and Sll0783 mutant in microtiter plates at indicated time points after addition of nitrogen are shown. Standard deviations from triplicate experiments are indicated by error bars.

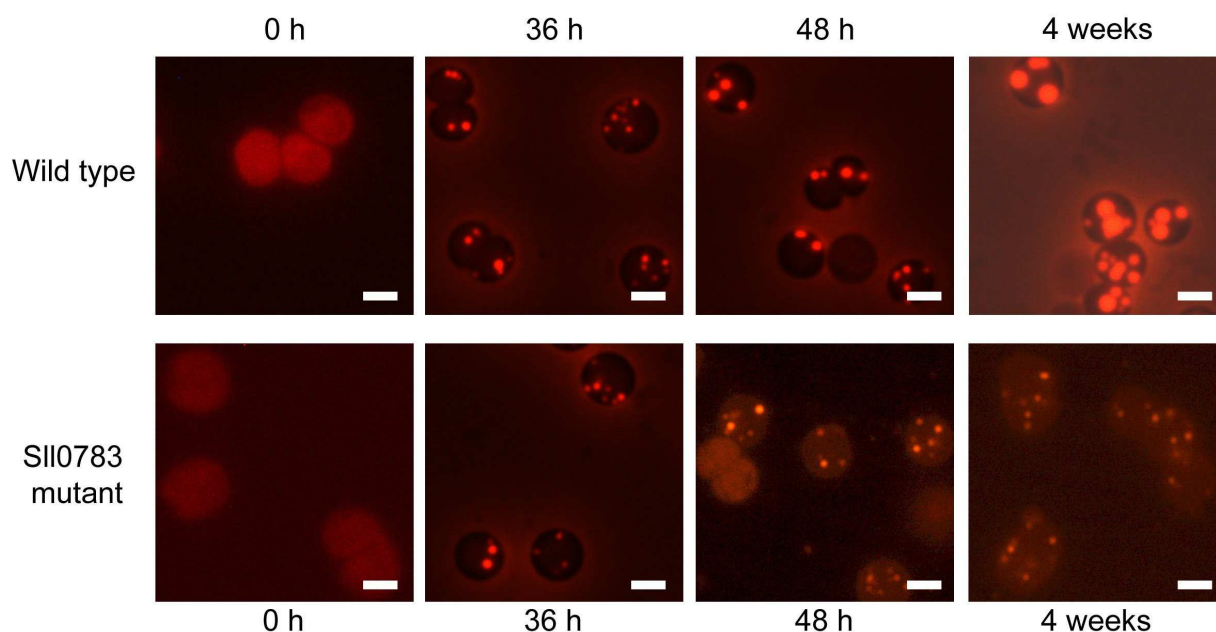


**Figure 3.10: Fluorescence microscopy of *Synechocystis* PCC 6803 wild type and Sll0783 mutant cells under nitrogen limiting conditions at indicated time points. - PHB granules were stained by Nile red and detected with the Cy3 channel. White bar: 1  $\mu$ m.**

of PHB in the mutant is about 10 times lower. Furthermore, the Nile red fluorescence of the PHB granules was measured with a fluorescence spectrophotometer. The amount of fluorescence after 120 h of nitrogen starvation was about 5 times lower in the Sll0783 mutant than in the wild type. (Figure 3.11B). The lower difference to the wild type as compared to HPLC analysis may be accounted for background Nile red fluorescence of membranes.

### 3.3.2 Analysis of carbon metabolism and precursor metabolites

Since PHB is a C-storage compound (Dawes & Senior, 1973), addition of C-sources like acetate and  $\text{CO}_2$  should boost PHB accumulation. In order to restore the impaired PHB accumulation in the Sll0783 mutant, these conditions were tested upon nitrogen starvation. Both, addition of 5 mM acetate and bubbling with 2%  $\text{CO}_2$  resulted in an increased PHB accumulation in wild type cells, whereas PHB accumulation in the Sll0783 mutant was unaffected. The impaired PHB accumulation under nitrogen starvation was not restored by addition of acetate or higher  $\text{CO}_2$  concentration (Figure 3.12).

In order to test whether the reduced accumulation of PHB in the Sll0783 mutant was due to an indirect effect of reduced  $\text{CO}_2$  fixation or precursor limitation, the glycogen and acetyl-CoA content of the cells was determined. For glycogen, there was no difference between wild type and Sll0783 mutant (Figure 3.13B). The level of acetyl-CoA in the wild type increased only slightly during N-starvation, whereas in the mutant, the level almost doubled (Figure 3.13A). Therefore, the impaired PHB accumulation is unlikely a consequence of limitation of the precursor molecule acetyl-CoA or a general carbon limitation.

### 3. RESULTS

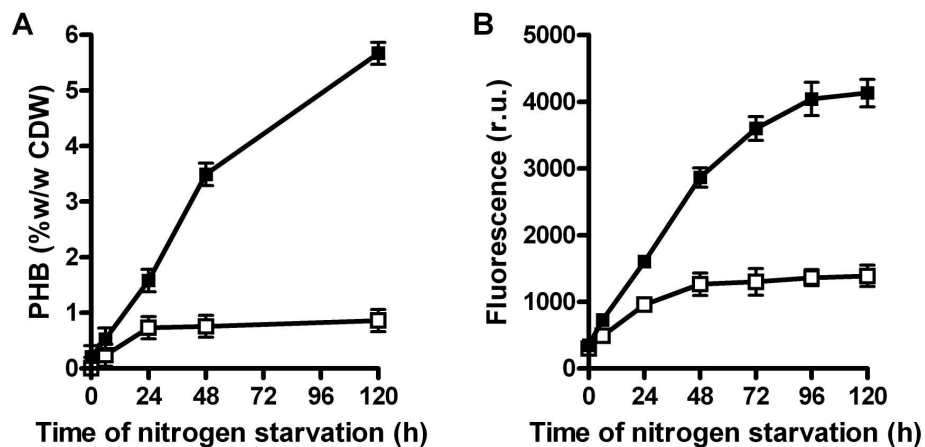


**Figure 3.11: Quantification of PHB accumulation.** - (A) HPLC analysis of the PHB content of *Synechocystis* PCC 6803 wild type (filled squares) and the Sll0783 mutant (open squares). (B) Spectroscopic quantification of Nile red fluorescence in wild type (filled squares) and the Sll0783 mutant (open squares). Standard deviations from triplicate experiments are indicated by error bars. (Schlebusch & Forchhammer, 2010). (CDW = cell dry weight)

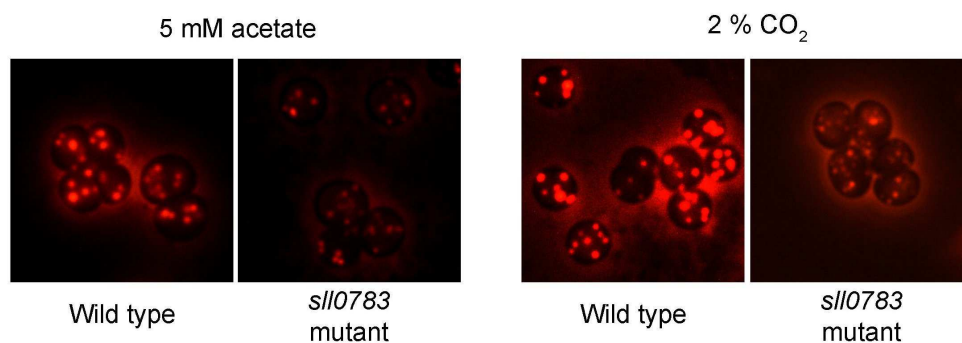


**Figure 3.12: Influence of different carbon sources on PHB accumulation** - *Synechocystis* PCC 6803 wild type and Sll0783 mutant were cultivated under nitrogen starvation conditions supplemented with 5 mM Na-acetate or bubbling with 2% CO<sub>2</sub> as indicated. Cells were cultivated for 72 h and stained with Nile red.

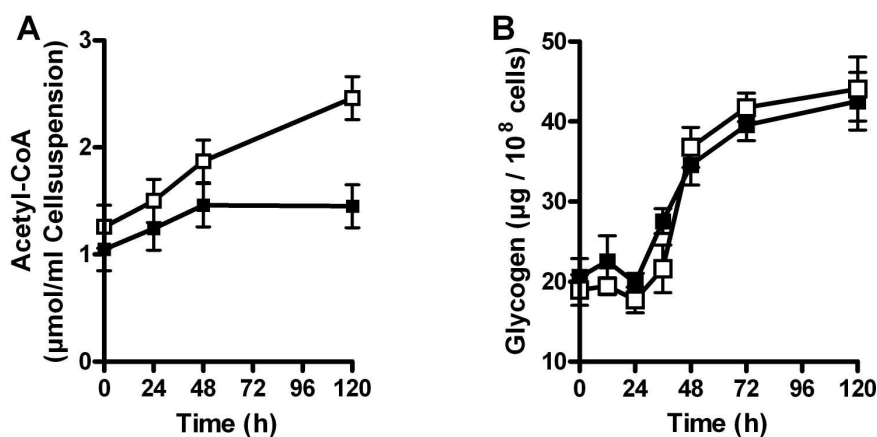


**Figure 3.13: Quantification of the acetyl-CoA and glycogen during nitrogen starvation.** - (A) Acetyl-CoA Content of wild type (filled squares) and the Sll0783 mutant (open squares). (B) Glycogen content of wild type (filled squares) and the Sll0783 mutant (open squares). Standard deviations from triplicate experiments are indicated by error bars.

### 3.3.3 Influence of potassium and phosphate starvation on PHB accumulation

In *Synechocystis* PCC 6803, PHB was described to accumulate under conditions of nitrogen and phosphate deprivation. However, the molecular signal for PHB accumulation is not known, neither if different types of nutrient limitation trigger PHB accumulation by separate signals. To test whether the Sll0783 mutant was generally impaired in PHB accumulation or only under specific conditions, various conditions PHB-inducing treatments were performed. Phosphate starvation induced PHB accumulation in the wild type. By contrast, the Sll0783 mutant was impaired in PHB accumulation like upon nitrogen starvation. In contrast to that, potassium starvation resulted in PHB accumulation in wild type and Sll0783 mutant in the same manner. PHB accumulation was also induced in both strains by combined starvation for potassium and phosphate (Figure 3.14). However, deficiency of potassium in combination with starvation for nitrogen did not cause PHB accumulation in the Sll0783 mutant, indicating that the failure to accumulate PHB during nitrogen starvation is dominant over the induction of PHB synthesis by potassium starvation.

## 3.4 Expression of PHB synthesis genes

To evaluate transcript abundance of the four PHB synthesis genes, qRT-PCR with gene-specific primers was performed (Figure 3.15). In the wild type, all four genes involved in PHB synthesis were expressed at low levels under nitrogen-replete conditions. After 6 h of nitrogen depletion, transcript amount of all four genes was elevated. The highest induction



### 3. RESULTS

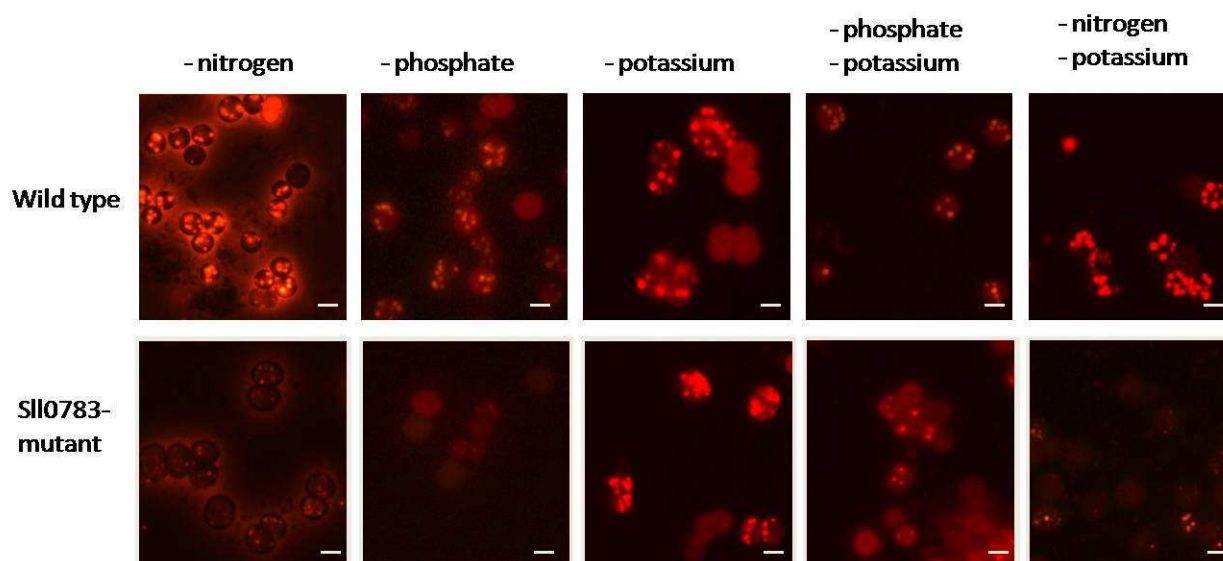


**Figure 3.14: Fluorescence microscopy of wild type and Sll0783 mutant under different nutrient starvation conditions.** - Cells were cultivated for 72 h, stained with Nile red and detected with the Cy3 channel. Starvation conditions are indicated. White bar: 1  $\mu\text{m}$ .

was measured for the acetoacetyl-CoA reductase with a 60-fold induction, whereas the genes for PHB synthase showed a 10-fold induction. In the course of time, transcript abundance of these four genes decreased but remained above the initial value. In the Sll0783 mutant, expression of these genes was slightly different to the wild type. The mutant showed higher transcript abundance for all four PHB synthesis genes under nitrogen-replete conditions. Following induction of nitrogen starvation, transcript levels of all four genes were transiently lower compared to the wild type strain but during prolonged starvation, transcript levels of acetoacetyl-CoA reductase gene (*slr1994*) increased and surpassed the level of the wild type (Figure 3.15B) (Schlebusch & Forchhammer, 2010).

## 3.5 Biochemical analysis of PHB synthase activity

### 3.5.1 PHB synthase activity in different fractions

To elucidate the reason for the impaired PHB accumulation in the Sll0783 mutant revealed by fluorescence microscopy, the activity of the PHB synthase was tested. PHB synthase is the last enzyme in PHB synthesis and catalyses the polymerisation of hydroxybutyryl-CoA. For other organisms it was shown that PHB synthase is associated to the PHB granule (Liebergesell *et al.*, 1992). To avoid preparation artefacts by separation of PHB granules from cell extracts, low speed centrifugation supernatants of crude extracts were used for PHB synthase activity assays. Wild type cells grown in nitrate sufficient medium showed only a very weak PHB synthase activity. After shifting the cells to nitrogen-depleted medium, PHB synthase activity raised and reached a maximum after 36 h. Over the course of time,

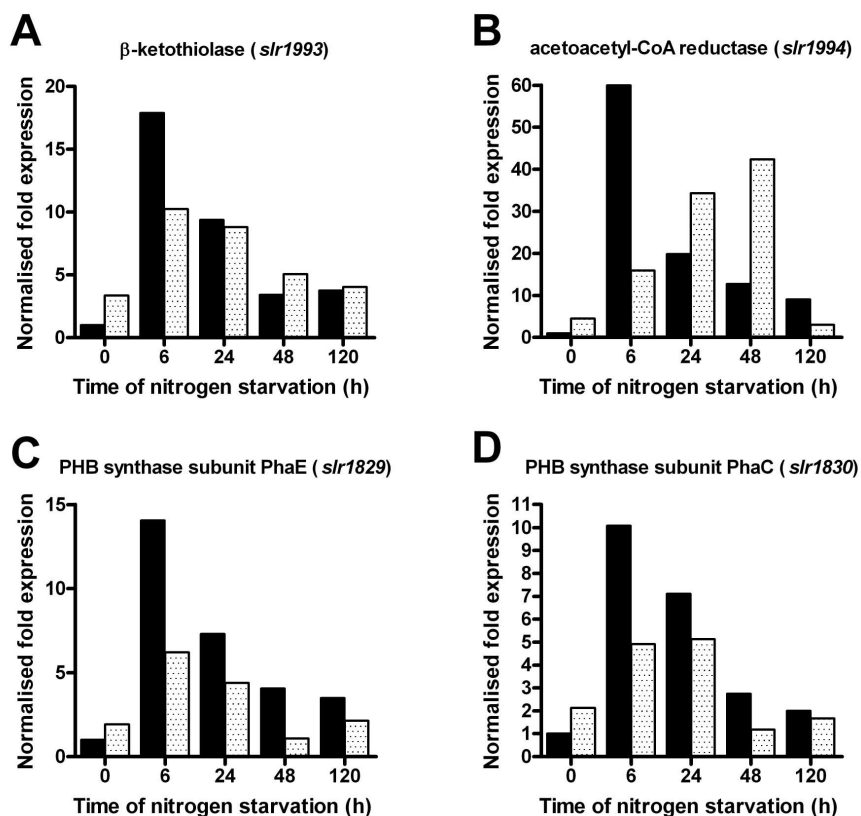


**Figure 3.15:** Transcript abundance of PHB synthesis genes in wild type (black bars) and the SII0783 mutant (spotted bars). - Transcript levels were determined by qRT-PCR with gene-specific primers. Transcript levels of the wild type at time point zero were set to 1. All values were normalised to the level of the reference gene *rnpB*. The four genes of the PHB synthesis pathway were examined (A)  $\beta$ -ketothiolase (*slr1993*), (B) acetoacetyl-CoA reductase (*slr1994*), (C) PHB synthase subunit PhaE (*slr1829*) and (D) PHB synthase subunit PhaC (*slr1830*) (Schlebusch & Forchhammer, 2010).

### 3. RESULTS

the activity decreased to 50 % of the maximal activity. Under nitrogen sufficient conditions, the Sll0783 mutant showed, like the wild type, very low PHB synthase activity. After shifting the cells to nitrogen-depleted conditions, the activity transiently increased after 24 h, but already after 48 h of nitrogen starvation, the activity ceased and was further on no more detectable (Figure 3.16). This failure to maintain PHB synthase activity matches the PHB deficient phenotype of the Sll0783 mutant.

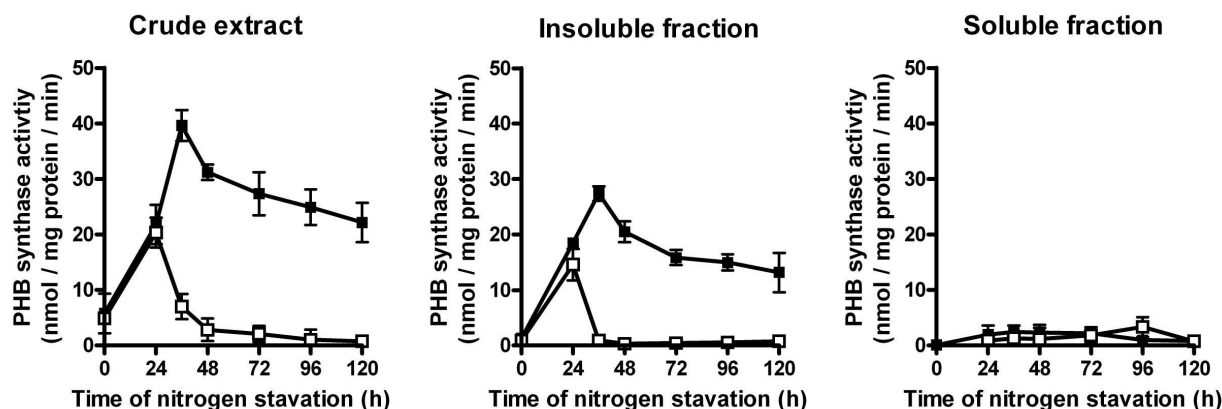


**Figure 3.16: PHB synthase activity assays from *Synechocystis* PCC 6803 wild type (filled squares) and Sll0783 mutant (open squares) upon nitrogen starvation.** - PHB synthase activity assay was performed with (A) crude extracts (supernatant from cell extracts after 1 min centrifugation at 1.000 *g*), (B) the insoluble fraction, obtained after high speed centrifugation ( 15 min, 25.000 *g*) and (C) the resulting soluble fraction of cell extracts. Standard deviations from triplicate experiments are indicated by error bars.

Since it was shown that in other organisms PHB synthase is associated to the PHB granules (Liebergesell *et al.*, 1992), we tested whether PHB synthase in *Synechocystis* PCC 6803 is also associated to the PHB granules. A rough separation of soluble proteins and membranes and other inclusions were performed by a 15 minute centrifugation step, whereupon the majority of PHB granules were found in the insoluble fraction (Figure 3.16). Performing PHB synthase assay with the different fractions revealed that the activity was associated with the PHB granule-containing insoluble fraction. In the wild type, PHB synthase activity increased only in the membrane fraction. The soluble fraction showed only a weak activity after 24 h, which vanished after 36 h. In the Sll0783 mutant, PHB synthase activity was also mostly present in the membrane fraction. After 48 h, PHB synthase activity decreased in a similar manner as shown in the PHB synthase assay with crude extracts (Figure 3.16). In both, wild type and Sll0783 mutant PHB synthase activity was exclusively detected in the insoluble fraction.

#### 3.5.2 Reactivation of the Sll0783 mutant PHB synthase

In order to reveal, if in the Sll0783 mutant an activator for PHB synthase is missing or an inhibitory compound accumulates, the insoluble fractions were incubated with the soluble

**Table 3.1:** Reactivation of PHB synthase by swapping different fractions. Standard deviations were calculated from triplicate experiments.

Strain and fraction	PHB synthase activity (U) $\pm$ SD
Wild type insoluble fraction	23.87 $\pm$ 1.04
+ wild type soluble fraction	37.87 $\pm$ 2.02
+ Sll0783 mutant soluble fraction	35.46 $\pm$ 2.12
Sll0783 mutant insoluble fraction	3.62 $\pm$ 1.06
+ wild type soluble fraction	8.26 $\pm$ 1.33
+ Sll0783 mutant soluble fraction	7.02 $\pm$ 1.36

fractions of the wild type. If an activator is missing in the mutant, incubation of the Sll0783 mutant insoluble fraction with the soluble fraction of the wild type should restore PHB synthase activity to wild type level. If in the Sll0783 mutant a substance accumulates which inhibits the PHB synthase, incubating the membrane fraction of the wild type with the soluble fraction of the Sll0783 mutant should result in decreased PHB synthase activity of the wild type. Therefore, the different fractions were swapped. In the experiment, the ratio insoluble to soluble fraction was chosen 1:10 (see Materials and methods 5.5.4 (p. 74)). Neither the wild type nor the Sll0783 mutant fraction was able to activate or inactivate the counterpart (Table 3.1).

#### 3.5.3 Influence of acetyl phosphate and other metabolites

Eleven putative activators were tested for *in vitro* activation of PHB synthase in crude extracts from *Synechocystis* PCC 6803 wild type and the Sll0783 mutant. Two different time points of nitrogen starvation were chosen, 24 h (Table 3.2) and 96 h (Table 3.3). After 24 h of nitrogen starvation the Sll0783 mutant showed PHB synthase activity whereas after 96 hours the activity vanished. As activators the intermediates of PHB synthesis, acetyl-CoA and acetoacetyl-CoA; the intermediates of glycolysis, phosphoenolpyruvate (PEP), 3-Phosphoglyceric acid (3-PGA), and pyruvate; intermediates of TCA cycle, citrate, isocitrate and 2-oxoglutarate (2-OG); and the substrates of phosphorylation, ATP and acetyl phosphate were used. Furthermore, NADPH as reduction equivalent was tested. The results show, that addition of acetyl phosphate increased the PHB synthase activity. In the wild type, the relative activation was between 35 % (after 24 h) (Table 3.2) and 55 % (after 96 h)(Table 3.3). In the Sll0783 mutant, the relative activation was similar to the wild type, but the absolute activation was significantly lower compared to the wild type. Particularly, in the later time point the activation in the Sll0783 mutant was insufficient to restore the PHB synthase activity to wild type level. The other metabolites caused only slight variations in the PHB synthase activity without any significance.

### 3. RESULTS

**Table 3.2:** Influence of different metabolites on PHB synthase activity

	After 24 h of nitrogen starvation			
	wild type		Sll0783 mutant	
	Activity (U)	Activation (%)	Activity (U)	Activation (%)
Control with H <sub>2</sub> O	26.70	0.00 %	22.16	0.00 %
Acetate (10 mM)	27.07	1.39 %	25.10	13.26 %
Acetyl-CoA (10 mM)	25.23	-5.50 %	24.56	10.85 %
Acetoacetyl-CoA (10 mM)	25.23	-5.50 %	23.26	4.95 %
PEP (30 mM)	26.72	0.10 %	24.98	12.71 %
3-PGA (30 mM)	24.18	-9.44 %	24.17	9.06 %
Pyruvate (30 mM)	22.92	-14.14 %	23.29	5.12 %
Citrate (10 mM)	26.31	-1.44 %	22.09	-0.30 %
Isocitrate (10 mM)	27.06	1.37 %	22.36	0.92 %
2-OG (10 mM)	28.85	8.06 %	18.13	-18.20 %
NADPH (1 mM)	27.13	1.61 %	23.47	5.77 %
ATP (30 mM)	21.77	-18.46 %	19.86	-10.37 %
Acetyl phosphate (30 mM)	35.90	34.48 %	29.24	31.95 %

**Table 3.3:** Influence of different metabolites on PHB synthase activity after 96h of nitrogen starvation

	After 96 h of nitrogen starvation			
	wild type		Sll0783 mutant	
	Activity (U)	Activation (%)	Activity (U)	Activation (%)
Control with H <sub>2</sub> O	16.70	0.00 %	2.16	0.00 %
Acetate (10 mM)	17.07	2.23 %	2.10	-2.87 %
Acetyl-CoA (10 mM)	15.23	-8.80 %	1.56	-27.59 %
Acetoacetyl-CoA (10 mM)	15.23	-8.80 %	1.26	-41.76 %
PEP (30 mM)	16.72	0.15 %	0.98	-54.81 %
3-PGA (30 mM)	14.18	-15.09 %	2.17	0.32 %
Pyruvate (30 mM)	13.92	-16.61 %	2.29	6.20 %
Citrate (10 mM)	16.31	-2.30 %	2.09	-3.10 %
Isocitrate (10 mM)	17.06	2.19 %	2.36	9.44 %
2-OG (10 mM)	18.85	12.89 %	1.13	-47.87 %
NADPH (1 mM)	17.89	7.12 %	2.68	24.07 %
ATP (30 mM)	14.77	-11.55 %	1.86	-13.84 %
Acetyl phosphate (30 mM)	25.90	55.13 %	4.03	86.57 %

### 3.5.4 The role of Sll0783 in the Nit1C cluster

Sll0783 is the first gene of a cluster with seven genes. The Sll0783 mutant was constructed by an insertion of a terminator-free, promoter-carrying kanamycin resistance cartridge in *sll0783*, driving transcription in direction of the downstream genes (*sll0784*) (Sauer *et al.*, 2001). As a consequence, *sll0784* is constitutively expressed (Schlebusch and Forchhammer 2010). Considering the genetic context of *sll0783* the question arose whether the other genes of the cluster may also cause impaired PHB accumulation. To resolve this issue, a knockout mutant of the second gene, *sll0784*, and a knockout of the complete Nit1C cluster were constructed. Fluorescence microscopy of a *sll0784* knockout mutant and a knockout of the whole Nit1C cluster revealed, that both mutant were able to accumulate PHB under nitrogen limiting conditions (Figure 3.17). Only the knockout of *sll0783* caused the impaired PHB accumulation.

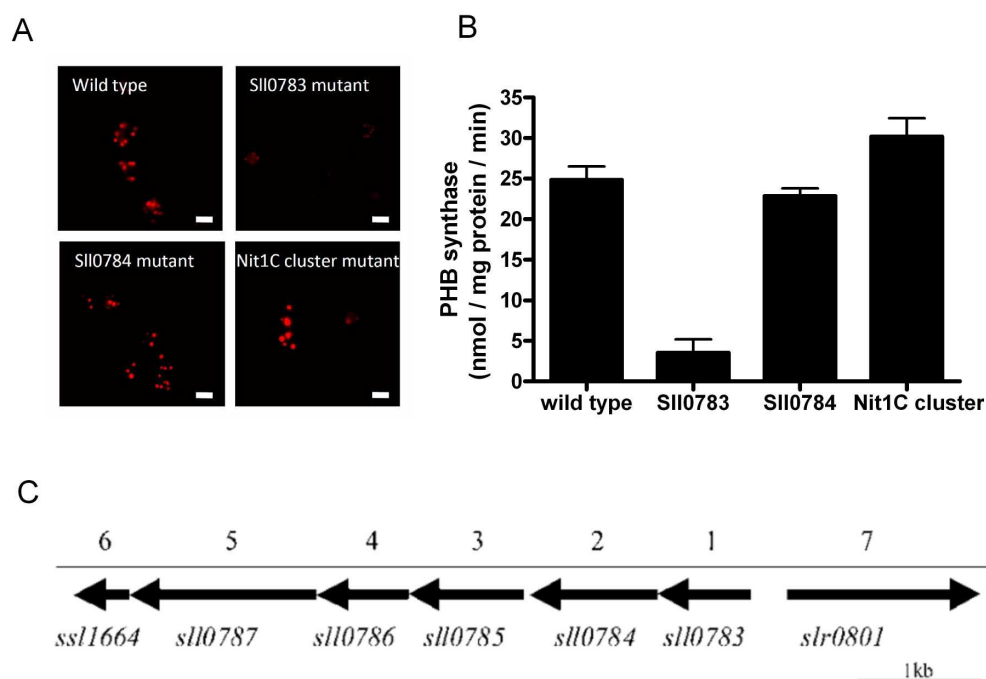


**Figure 3.17: The role of Sll0783 in the Nit1C cluster** - (A) Fluorescence microscopy of nitrogen starved cells (96 h). (B) PHB synthase activity. Standard deviations from triplicate experiments are indicated by error bars. (C) Schematic representation of the Nit1C cluster.

### 3.5.5 Phenotype of a PII mutant concerning PHB accumulation

PII plays a central role for the acclimation to changing carbon-nitrogen ratios. In *Synechocystis* PCC 6803, PII regulates the activity of N-acetyl-L-glutamate kinase (NAGK), which catalyses the rate limiting step in arginine biosynthesis. Arginine is a component of the storage polymer cyanophycin (multi L-arginyl-poly-L-aspartic acid), which accumulates during conditions of nitrogen excess (Maheswaran *et al.*, 2006). Since PHB accumulation

### 3. RESULTS

also depends on the carbon-nitrogen ratio (Miyake *et al.*, 1997), PII could have a regulatory effect on the PHB synthesis.

With this intention, a *Synechocystis* PCC 6803 PII mutant was examined towards its PHB accumulation potential. Fluorescence microscopy revealed an impaired PHB accumulation (Figure 3.18A) which was similar to the phenotype of the Sll0783 mutant. In contrast that, PHB synthase activity in the PII mutant was like in the wild type. PHB synthase remained active during nitrogen starvation. (Figure 3.18B).

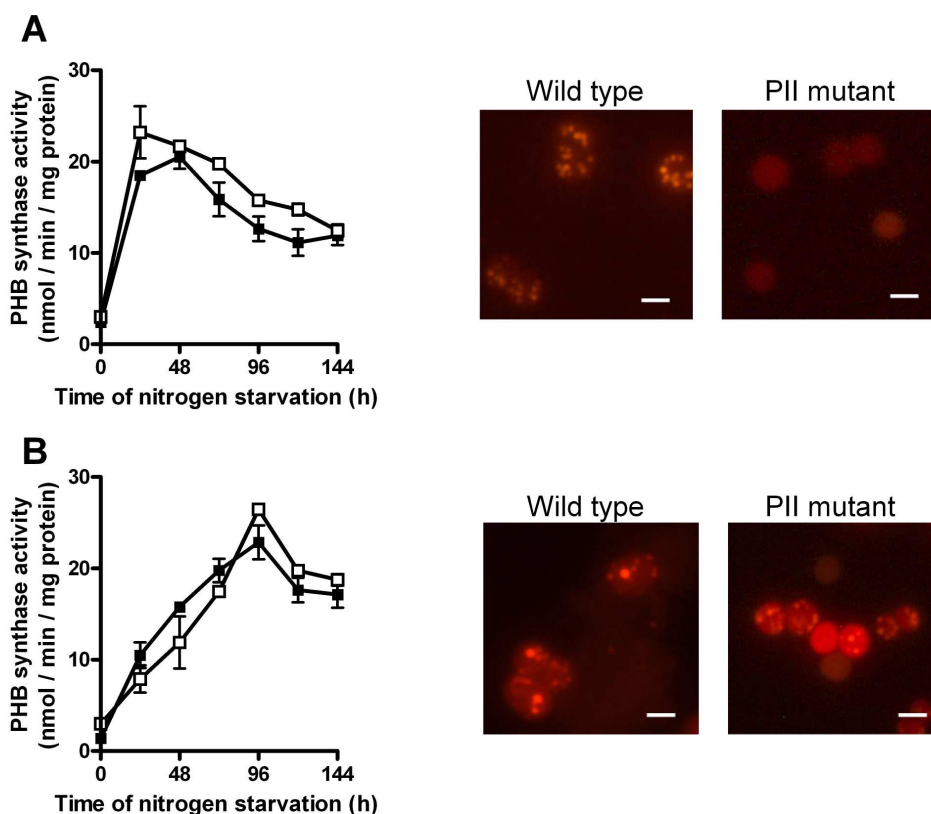


**Figure 3.18: Phenotype of a PII mutant regarding PHB accumulation upon nitrogen and phosphate starvation.** - (A) Nitrogen starvation and (B) combined starvation of potassium and phosphate analysed by PHB synthase activity of *Synechocystis* PCC 6803 wild type (filled squares) and PII mutant (opened squares) over course of nitrogen starvation. Activity was measured in crude extracts. Standard deviations from triplicate experiments are indicated by error bars. Fluorescence microscopy of *Synechocystis* PCC 6803 wild type and PII mutant cells after 96 h nutrient starvation. Cells were stained with Nile red and fluorescence was detected in the Cy3 channel.

### 3.6 Purification of PHB granules in Percoll gradients

In *Ralstonia eutropha* H16 and other PHB accumulating bacteria, PHB synthesis is accompanied with the synthesis of granule associated proteins (GAP). GAPs are known to influence

### 3.6 Purification of PHB granules in Percoll gradients

the size and amount of the PHB granules in the cell (Pötter *et al.*, 2005). The failure to maintain PHB synthase activity in the Sll0783 mutant might be caused by differences in the expression and composition of GAPs. For that reason, PHB granules from *Synechocystis* PCC 6803 wild type and the Sll0783 mutant were isolated and the associated proteome was analysed.

The PHB granules were purified from nitrogen starved cells in Percoll gradients. The separation resulted in two bands, which were used (Figure 3.19A): an upper band, containing intact cells, cell fragments and membranes; and a lower band, mostly containing PHB granules. In order to prove the quality of the preparation, different parameters were analysed. The PHB synthase activity assay detected the majority of the activity in the lower fraction (Figure 3.19B). Also, fluorescence microscopy verified the separation of the PHB granules (Figure 3.19C). SDS-PAGE analysis of the upper and lower fraction exposed several proteins in the lower fraction in contrast to the upper fraction, where only a minor amount of protein was detected (Figure 3.19D). The low amount of protein in the upper fraction was due to a washing-step after purification with Percoll, which leads to a 10-fold dilution. This step is necessary, because Percoll disables direct analysis of samples on the SDS-PAGE (see material and methods 5.5.6 (p. 74)).

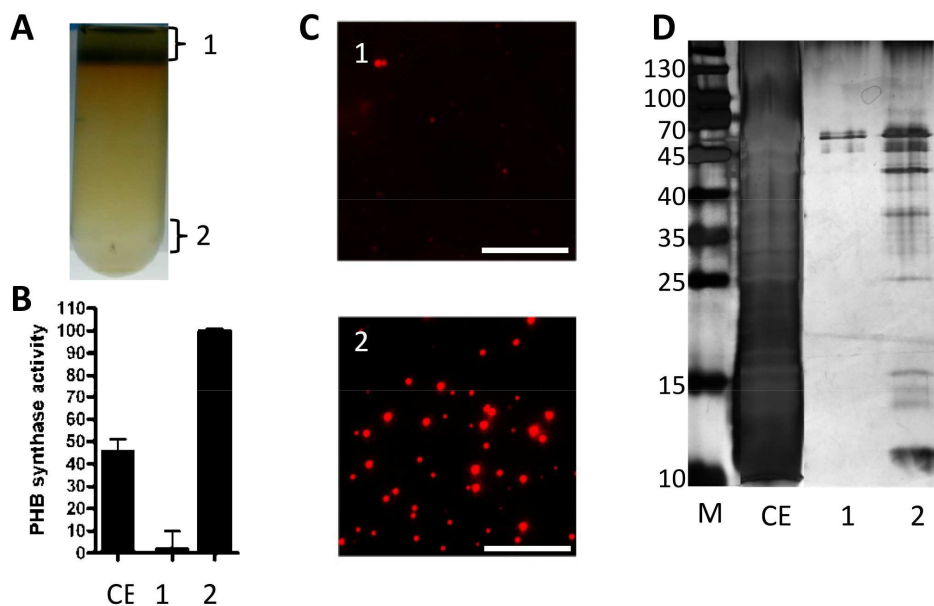


**Figure 3.19: PHB granule purification by Percoll gradient.** - Crude extract of nitrogen starved *Synechocystis* PCC 6803 wild type cells was loaded on top of 90 % Percoll and centrifuged. (A) After fractionation of crude extract (CE) in Percoll gradient a upper band (1) and a lower band (2) were visible. (B) PHB synthase activity assay of crude extract (CE), the upper (1) and the lower (2) fraction. Standard deviations from triplicate experiments are indicated by error bars. (C) Fluorescence microscopy of Nile red stained fractions. White bars: 10  $\mu$ m. (D) Silverstained 12 % SDS-PAGE with crude extract (CE), the upper (1) and the lower (2) fraction (each 20  $\mu$ g)



### 3. RESULTS

#### 3.6.1 Identification of PHB granule associated proteins

The PHB granule associated proteins were analysed by applying the suspensions of purified PHB granules to SDS-PAGE. As shown in Figure 3.20, separation of proteins associated with PHB granules indicated the presence of three bands representing proteins of 68, 58 and 48 kDa with various minor additional bands. There were no major differences in the protein pattern between the *Synechocystis* PCC 6803 wild type and the Sll0783 mutant visible.

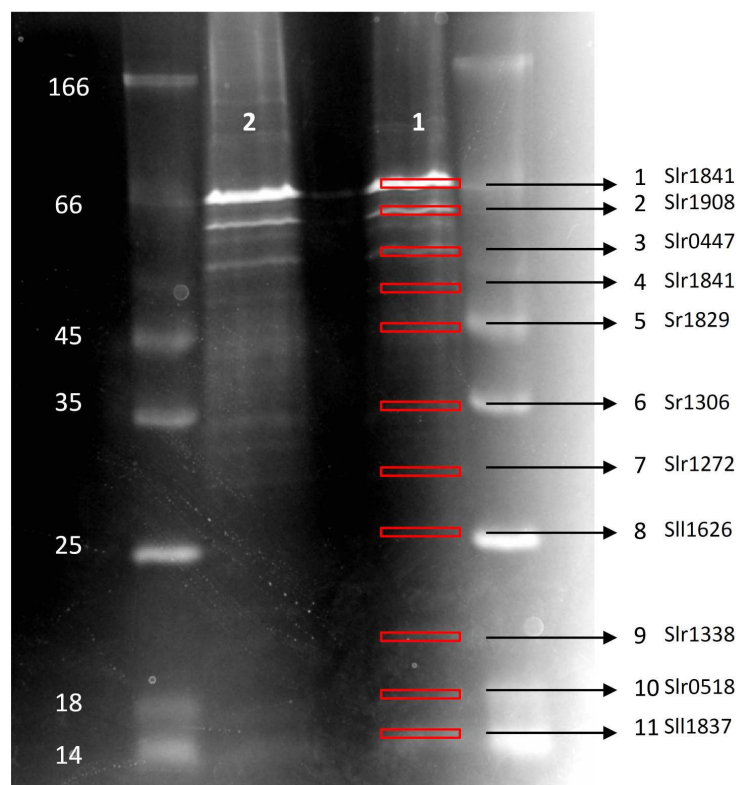


**Figure 3.20: SDS-PAGE analysis of native PHB granule** - PHB granules were isolated from *Synechocystis* wild type (2) and the Sll0783 mutant (1) cells after 168 h nitrogen starvation with Percoll gradients.

Eleven visible bands of the colloidal Coomassie blue stained SDS-PAGE were analysed by MALDI-TOF of tryptic digests. Since *Synechocystis* PCC 6803 wild type and the Sll0783 mutant showed no significant differences in the protein pattern, we analysed only the PHB granule associated proteins from the wild type in order to identify new granule associated proteins. Protein bands were excised, trypsinised and subsequent identified by MALDI-TOF (Table 3.4). The 68 kDa band was identified as Slr1841, which is annotated as probable porin. The 63 kDa band was identified as Slr1908, which is also annotated as probable porin. The 3. major band was identified as Slr0442, which is annotated as substrate binding protein of a urea transporter. As band 5, the PHB synthase subunit PhaE was identified, which verify the method. PhaC was also detected but in smaller amounts. The relatively low amount PHB synthase protein could be caused by the covalent linkage of the growing PHB molecule

### 3.6 Purification of PHB granules in Percoll gradients

**Table 3.4:** Assignment of single bands to ORFs of the *Synechocystis* PCC 6803 genome. Band Nr. indicated the place in the SDS-PAGE (Figure 3.20) and the calculated mass (cal. Mw) was calculated from the  $R_f$  values determined from the SDS-PAGE. Source of the protein description was cyanobase (<http://genome.kazusa.or.jp/cyanobase/Synechocystis>). Matched peptides and intensity indicate abundance of the proteins.

Band Nr.	cal. Mw	ORF	Protein Descriptions	Mw [kDa]	Intensity
1	68.17	<i>slr1841</i>	Probable proin; major outer membrane protein	67.6	552400000
2	63.60	<i>slr1908</i>	Probable proin; major outer membrane protein	64.51	2275100000
3	57.26	<i>slr0447</i>	Periplasmic protein	48.359	2460700000
4	56.86	<i>slr1841</i>	Probable proin; major outer membrane protein	67.6	969720000
5	42.73	<i>slr1829</i>	PhaE	38.047	653240000
6	36.73	<i>sll1306</i>	periplasmic protein	38.27	876220000
7	32.92	<i>sll1626</i>	LexA	22.744	435400000
8	25.84	<i>sll1626</i>	LexA	22.744	3720700
9	23.39	<i>sll1338</i>	unknown protein	20.183	279610000
10	18.94	<i>slr0518</i>	arabinofuranosidase	20.485	522070000
11	16.27	<i>sll1837</i>	periplasmic protein	15.467	24862000

### 3. RESULTS

---

**Table 3.5:** Table contains reciprocal best hit pairs by BLAST2 between different proteins and different cyanobacterial species. Table was sorted according to the blast score of *slr1829* from *Synechocystis* PCC 6803. *Acaryochloris marina* MBIC11017 represents cyanobacterial genomes without PHB synthase genes.

Strain	Slr1829	Slr1830	Slr0060	Ssl2501
<i>Synechocystis</i> sp. PCC 6803	675	772	762	180
<i>Cyanothece</i> sp. PCC 7822	556	577	579	88
<i>Cyanothece</i> sp. PCC 7425	285	552	458	97
<i>Cyanothece</i> sp. PCC 7424	275	565	571	81
<i>Microcystis aeruginosa</i> NIES-843	267	575	575	81
<i>Arthrospira platensis</i> NIES-39	260	572	258	89
<i>Acaryochloris marina</i> MBIC11017	30	36	30	29

with the subunits. This inhibits the formation of distinct bands in the SDS-PAGE. In band 4 and 5 the protein Slr0060 was identified in minor amounts. This protein is a predicted esterase of the alpha-beta hydrolase superfamily and is only present in cyanobacteria with a PHB synthase (Table 3.5). This protein could be the PHB depolymerase. Band 6 was identified as Sll1306 which is annotated as periplasmic protein with unknown function. Furthermore, LexA was identified in band 7 and 8 whereas the quantity in band 8 was very low. In *Synechocystis* PCC 6803, LexA regulates genes involved in carbon assimilation or controlled by the carbon source and the bidirectional hydrogenase. Band 9 was identified as Sll1338 which is annotated as unknown protein. Previously, Sll1338 was detected in the outer membrane (Huang *et al.*, 2004). Band 10 was identified as Slr0518 which is annotated as arabinofuranosidase. Band 11 was identified as Sll1837 which is annotated as protein of unknown function. Also detected in band 11 was the protein Ssl2501, but in minor amounts. This protein was characterised as thylakoid associated protein (Wang *et al.*, 2000). Homologues of Ssl2501 are only present in PHB accumulating cyanobacteria (Table 3.5).

In the proteome analysis of the PHB granules most identified proteins are located in the outer membrane or periplasma. However, the fact that the PHB synthase component PhaE was also identified shows that the method of PHB granule purification was reliable.

#### 3.6.2 Identification of outer membrane particles as contamination of PHB granule purification process

The appearance of a variety of outer membrane proteins was possibly due to contamination of the PHB granules by membranes or unspecific binding of proteins to the PHB granules. Labelling the outer membrane proteins with a fluorescence dye, Oregon green can be used to quantify the amount of outer membrane in the PHB granule fraction, visualised in the fluorescence microscope. Oregon green binds covalently free amino groups. This linkage should

### 3.6 Purification of PHB granules in Percoll gradients

sustain the purification process. Labelling with Oregon green 488-X was done with intact cells, so that only the outer membrane proteins were stained (Priyadarshini *et al.*, 2007). After cell lysis, labelled outer membrane and Nile red stained PHB granules were uniform by distribution (Figure 3.211A-D). After separation of PHB granules with Percoll, only minor amounts of PHB granules remain in the upper fraction (Figure 3.212A-D), whereas most of them appeared in the PHB granule fraction (Figure 3.213A-D). By contrast, the Oregon green labelled outer membrane behaved conversely and remained mainly in the upper fraction (Figure 3.212A-D). Nevertheless, fluorescence microscopy of the purified PHB granule fraction revealed contaminations of small spherical outer membrane particles, which were not stained with Nile red (Figure 3.213A-D). In the overlay picture, red and green but no orange dots were visible. Even though the quantity of these contaminations was significantly smaller than the amount of PHB granules. This could be a source of the identified outer membrane proteins in the proteome analysis.

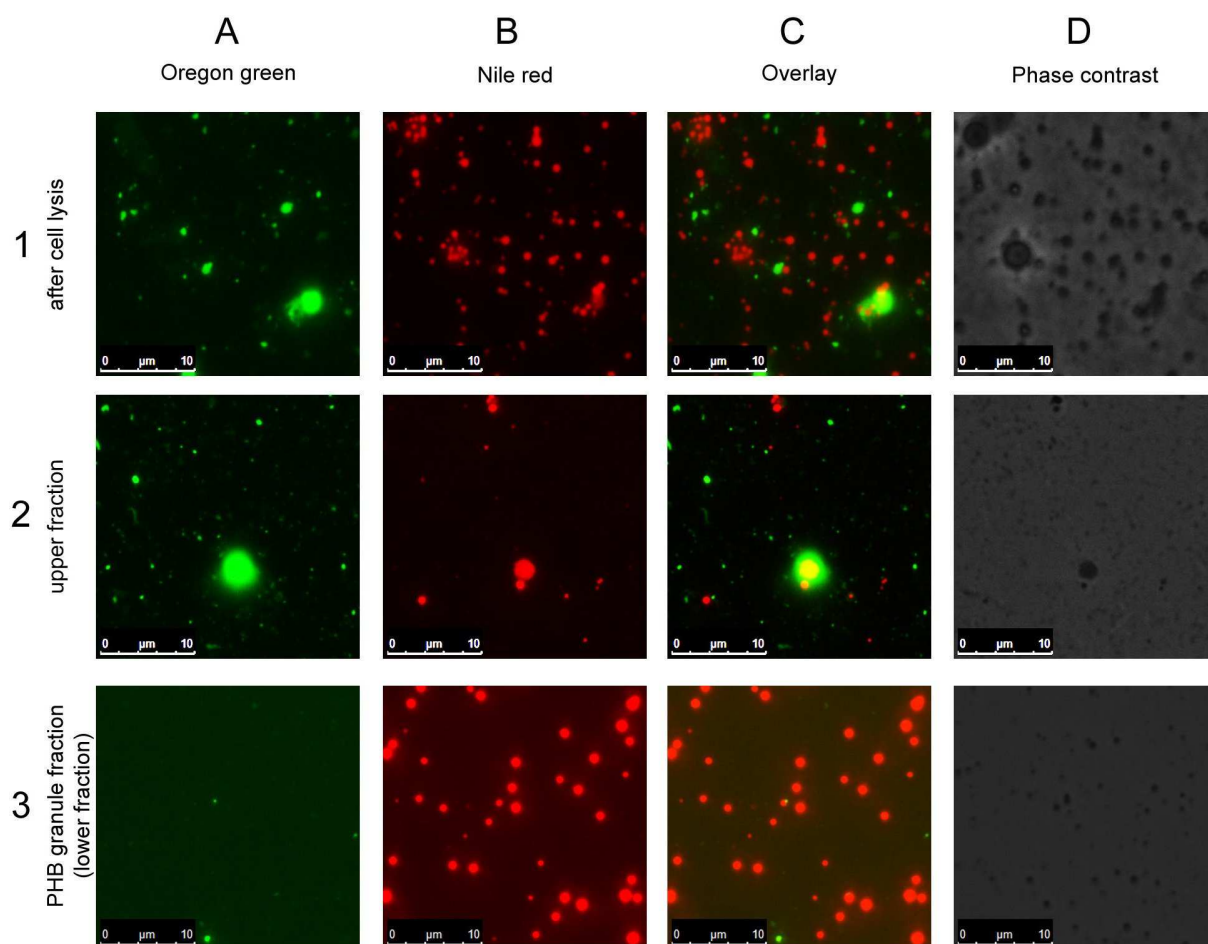


**Figure 3.21: Fluorescence microscopy of PHB granules and labelled outer membranes during the Percoll purification procedure.** - (1A-D) cell extract, (2A-D) upper fraction and (3A-D) PHB granule fraction where analysed by fluorescence microscopy. Application of filter is indicated above the panels.

## 3.7 Subcellular localisation of the PHB synthase

Since the identified proteins from PHB granule preparation were mostly outer membrane contamination, it was not possible to determine, whether the PHB synthase is attached to the granules. This is important because the impaired PHB accumulation in the Sll0783 mutant could be due to a deficient localisation process. For the subcellular localisation of the PHB synthase, C-terminal Gfp-fusion proteins of the PHB synthase subunits were created. Fusion of *phaE* (*slr1829*) and *phaC* (*slr1830*) genes with their native promoter region (Figure 3.23), to the eGfp fragment was obtained by long flanking homologue PCR. Subsequently, the fragments were cloned in the vector pVZ322 and transferred into *Synechocystis* PCC 6803 wild type and the Sll0783 mutant by conjugation (see Material and methods 5.4.6 (p. 72)).

Applying nitrogen starvation to the cells, the eGfp fluorescence forms spherical foci, mostly located in the periphery of the cells (Figure 3.22). After 96 h of nitrogen starvation, fluorescence of eGFP (Gfp channel) and the fluorescence of Nile red (Cy3 channel) co-localised. This was indicated by the yellow colour in the overlay picture. There were no differences in the PHB synthase localisation between the wild type and the Sll0783 mutant. This experiment clearly indicates, that both subunits of the PHB synthase were located to the PHB granules at a time point where the PHB synthase activity is vanished in the Sll0783 mutant.

## 3.8 Metabolomic profiling

The analysis of glycogen and acetyl-CoA level revealed no hint of a major metabolic limitation. Since these two metabolites reflect only a small part of the metabolism, we analysed 39 non-steady state metabolites by a non-targeted GC-MS-based metabolic profiling of *Synechocystis* PCC 6803 wild type and the Sll0783 mutant under nitrogen limiting conditions. The metabolic profiling covered the central C and N metabolism, which is dominated by the Calvin cycle and the associated 2-phosphoglycolate metabolism as well as glycolysis, OPP, and an incomplete TCA cycle. The N-metabolism is connected to the C-metabolism via the incomplete TCA cycle, which is thought to produce C-skeletons for amino acid biosynthesis (Zhang *et al.*, 2006). As expected, after shifting the cells to nitrogen-free medium, the TCA cycle intermediates citric acid, 2-OG, fumaric acid and malic acid increased (Figure 3.24). Succinic acid and oxalic acid level showed a slight decrease. In the Sll0783 mutant, metabolites of the TCA cycle citrate, fumarate, malate and 2-OG were reduced compared to the wild type, whereas, fumaric acid and malic acid showed higher levels.

In the wild type, the amino acid concentrations showed a short term increase (after 6 h) followed by a significant reduction after 168 h of nitrogen starvation (Figure 3.25). In the Sll0783 mutant, change in the amino acid pools is deregulated. The mutant showed no increase after 6 h nitrogen starvation and the decrease in the long term starvation was less

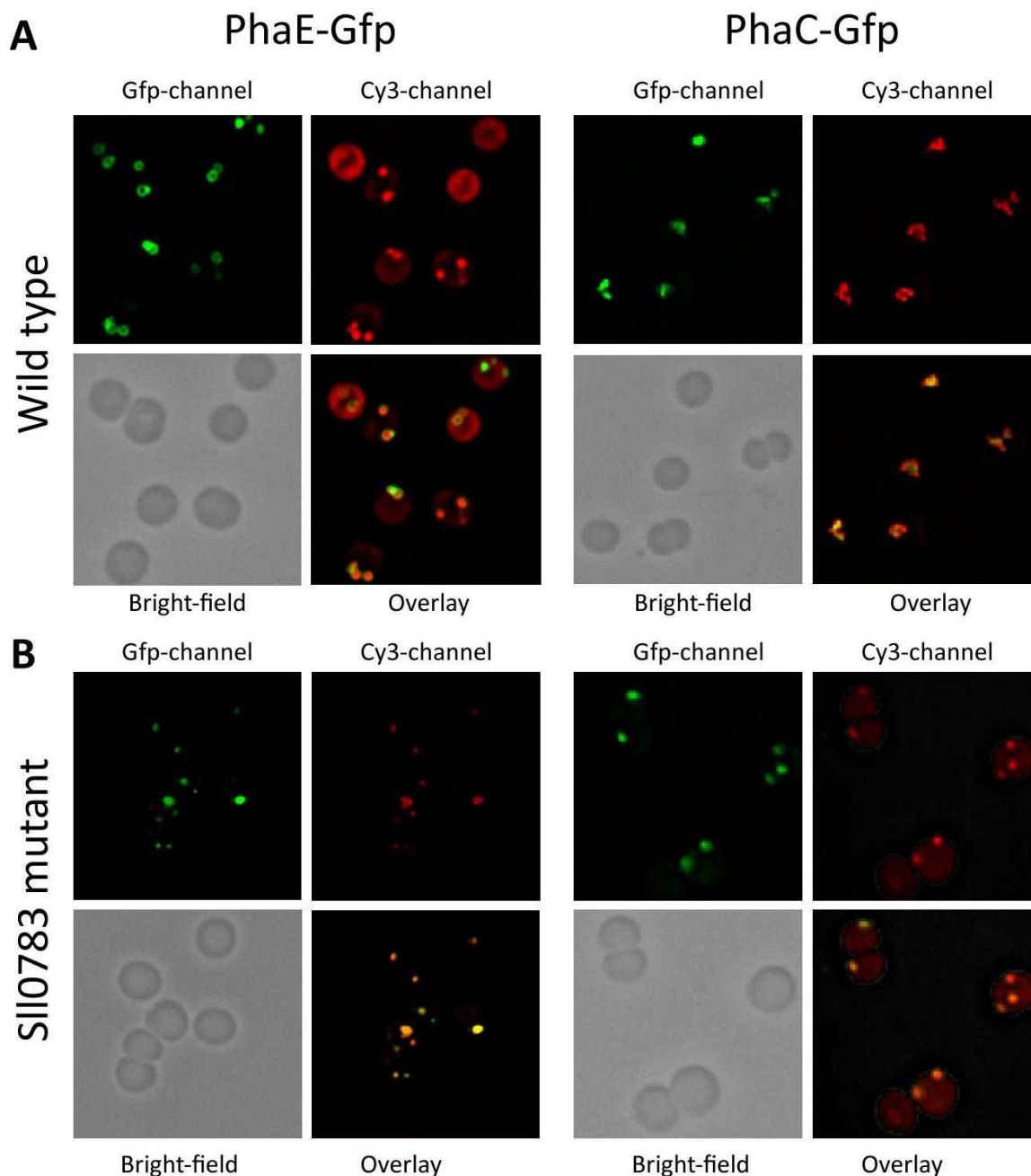


**Figure 3.22: Subcellular localisation of PHB synthase fusion proteins (PhaE-Gfp and PhaC-Gfp) under nitrogen starvation** - *Synechocystis* PCC 6803 wild type and the Sll0783 mutant with PhaE-Gfp and PhaC-Gfp fusion proteins were grown in BG11<sub>-N</sub> media and visualised under bright field, the gfp-channel for the gfp-fluorescence and the Cy3-channel for the Nile red fluorescence. Overlay was done without the bright field.

### 3. RESULTS

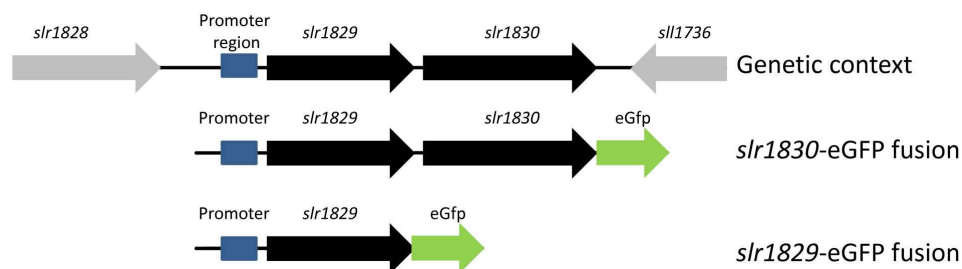


**Figure 3.23: Schematic model of the C-terminal Gfp fusion proteins (PhaE-Gfp and PhaC-Gfp)** - Fusion with gfp was done by LFH-PCR. Subsequently the fragments were cloned in the pVZ322 vector. (For details see Material and methods 5.4.6 (p. 72))

marked as in the wild type.

Metabolites of glycolysis like fructose-6-phosphate, glucose-6-phosphate and phosphoenolpyruvate (PEP) showed an initial increase in the wild type followed by a decrease in long term starvation (160 h) (Figure 3.26). Levels of sugars and polyols were increased under nitrogen starvation. The level of glycolysis intermediates glucose-6-phosphate and fructose-phosphate were higher than in the wild type whereas phosphoenolpyruvate level was significantly reduced (Figure 3.26). Major changes were observed in the level of sorbitol. In the wild type, sorbitol is 35-fold increased after 24 h. After 168 h the value is 11-fold higher than at time point 0 h. In the Sll0783 mutant, the sorbitol pool was only 4-fold increased after 6 h, followed by a decrease at 168 h. Sorbitol is synthesised by the sorbitol-6-phosphate dehydrogenase, which uses NADPH as reduction equivalents and glucose-6-phosphate as substrate.

### 3.9 The role of the NADPH pool

PHB synthesis is stimulated by excess of reduction equivalents (Madison & Huisman, 1999). Upon phosphate starvation ATP synthesis is decreased, while reduction of  $\text{NADP}^+$  through photosynthetic electron flow is not inhibited (Bottomley & Stewart, 1976; Konopka & Schnur, 1981). The impaired PHB accumulation under phosphate starvation in the Sll0783 mutant as well as the impaired sorbitol synthesis suggested that the Sll0783 mutant has a deficiency in providing reduction equivalents. In order to check these hypothesis, artificial inhibitors were used to manipulate the cellular NADPH/ATP ratio. DCMU inhibits PS II by blocking the  $Q_B$  binding site (Metz *et al.*, 1986). This reduces the NADPH synthesis by linear photosynthetic electron transport while ATP synthesis is unaffected. The uncoupler CCCP abolishes ADP phosphorylation by uncoupling the membrane potential. DCCD inhibits specifically the ATP synthase without inhibiting photosynthetic electron transport (Izawa & Good, 1972). Under such condition a rise in reducing power is expected.

In the experiment cells were shifted to nitrogen-free medium and the inhibitors DCMU, CCCP and DCCP were added at indicated concentrations (Figure 3.27). To ensure that the PHB accumulation is not affected by a reduced  $\text{CO}_2$  fixation, 10 mM acetate which directly

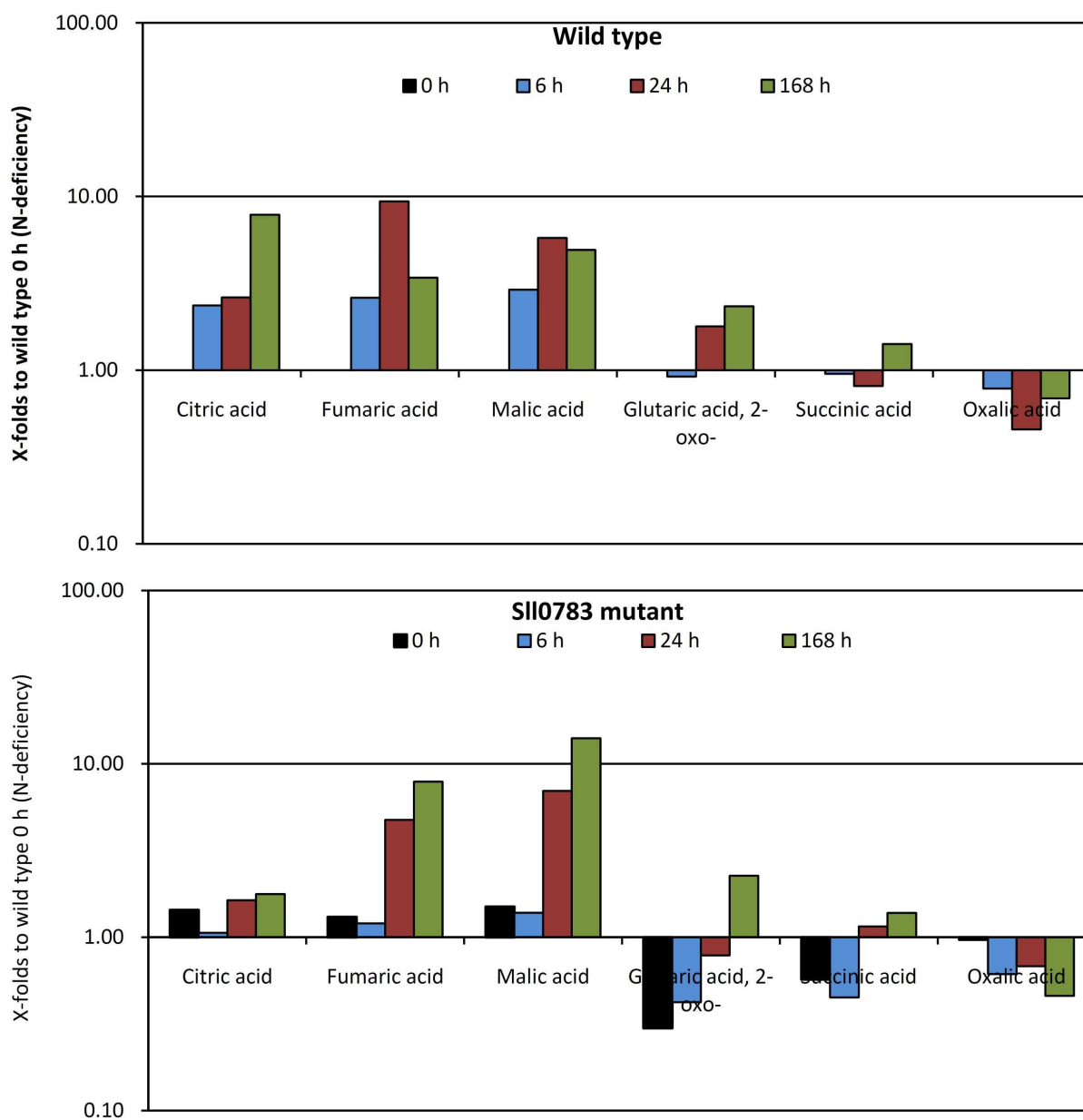


**Figure 3.24: Relative contents of TCA cycle metabolites.** - *Synechocystis* PCC 6803 wild type and Sll0783 mutant cells upon nitrogen starvation were compared to nitrogen sufficient conditions. Values are x-folds compared to wild type 0 h value. Values are means from duplicate experiments.



### 3. RESULTS

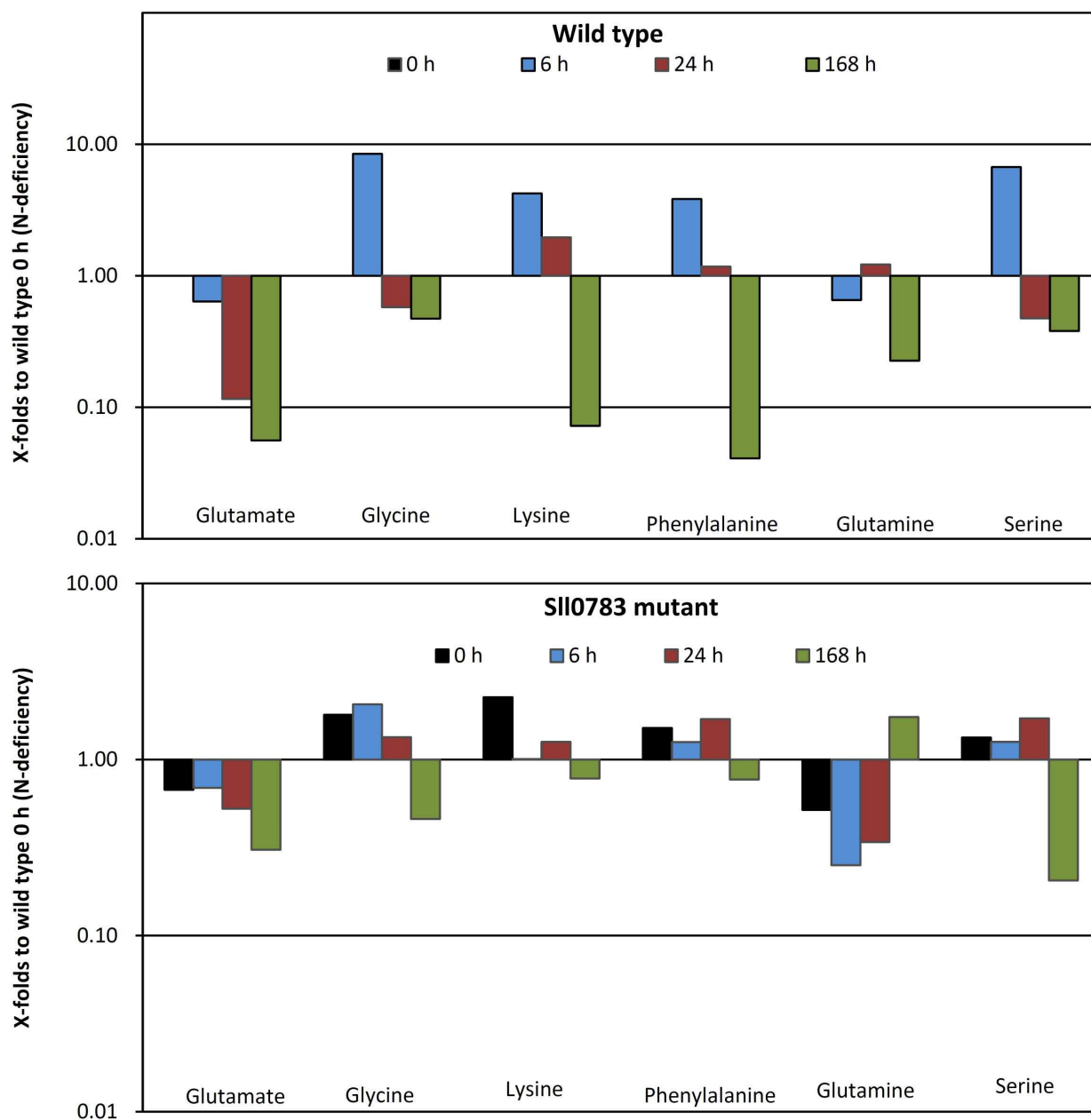


**Figure 3.25: Relative contents of selected amino acids.** - *Synechocystis* PCC 6803 wild type and Sll0783 mutant cells upon nitrogen starvation were compared to nitrogen sufficient conditions. Values are x-folds compared to wild type 0 h value. Values are means from duplicate experiments.

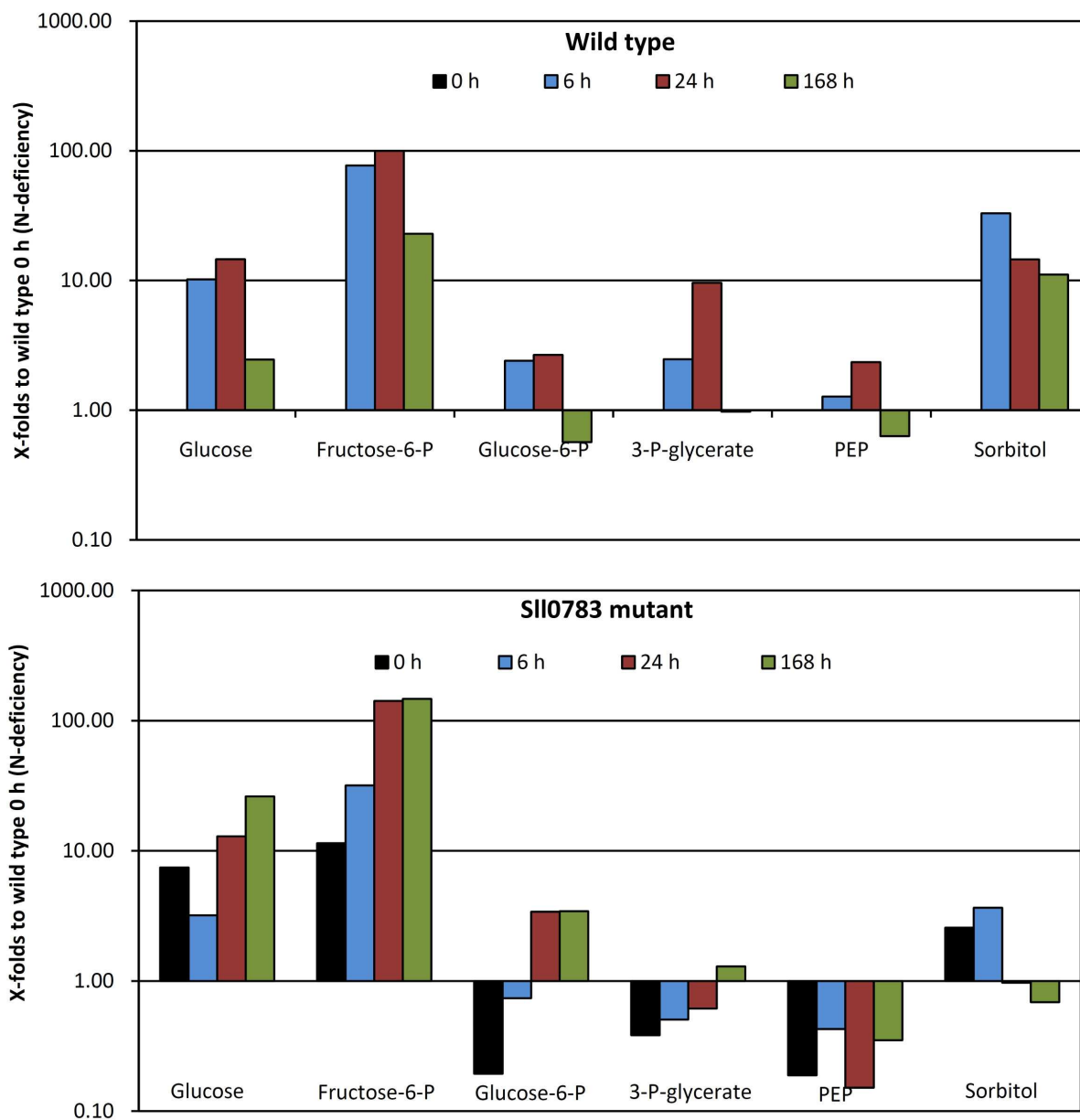


**Figure 3.26: Relative contents of glycolysis metabolites and sorbitol.** - *Synechocystis* PCC 6803 wild type and Sll0783 mutant cells upon nitrogen starvation were compared to nitrogen sufficient conditions. Values are x-folds compared to wild type 0 h value. Values are means from duplicate experiments. (PEP = phosphoenolpyruvate)

### 3. RESULTS

fuels PHB synthesis, was added to the cells. After 96 h of nitrogen starvation PHB synthase activity was measured. In this study DCMU decreased the PHB synthase activity in the *Synechocystis* PCC 6803 wild type and in the Sll0783 mutant, whereas the decrease in the mutant is significantly higher as in the wild type. In contrast to the influence of DCMU, both CCCP and DCCD caused an increased PHB synthase activity. CCCP stimulated the PHB synthase activity of the Sll0783 mutant nearly to wild type level.

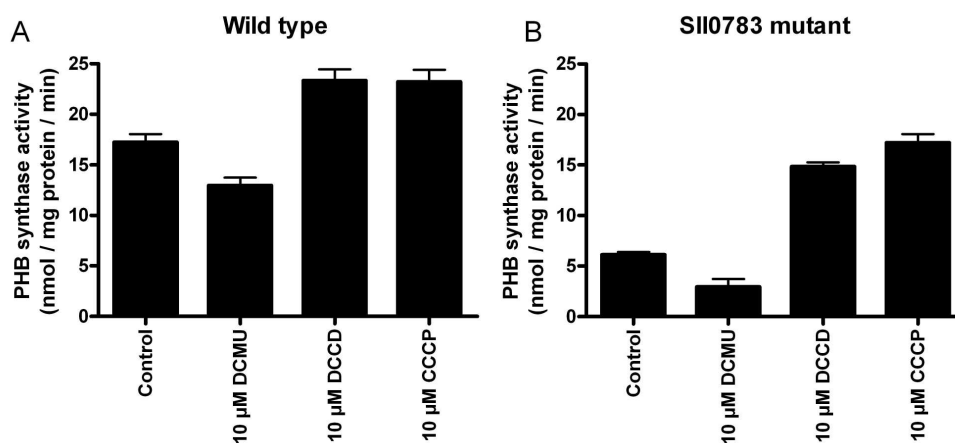


**Figure 3.27: Influence of specific inhibitors on the PHB synthase activity.** - (A) *Synechocystis* PCC 6803 wild type and (B) Sll0783 mutant were shifted to nitrogen free media and inhibitors were added at indicated concentrations. After 72 h of nitrogen starvation PHB synthase activity was measured. Standard deviations from triplicate experiments are indicated by error bars.

#### 3.9.1 Quantification of NADPH and NADP<sup>+</sup> upon nitrogen starvation

The previous results suggest that NADPH/ATP ratio is crucial for the PHB synthase activity. Consequently, the impaired PHB accumulation in the Sll0783 mutant could be a result of an imbalanced energy/redox balance. Therefore, the ratio of NADPH/NADP<sup>+</sup> in nitrogen-starved cells was analysed. These experiments were carried out with the *Synechocystis* PCC 6803 wild type, the Sll0783 mutant as well as the Nit1C cluster mutant and with the *S. elongatus* PCC 7942 wild type and the Nsi5 mutant, a knockout of the *sll0783* homologue in *S. elongatus* PCC 7942. As shown in section 3.5.4 (p.37) deletion of the Nit1C cluster resulted in a wild type like PHB accumulation.

Figure 3.28A shows the NADPH/NADP<sup>+</sup> ratio of *Synechocystis* PCC 6803 wild type, the Sll0783 mutant and the Nit1C cluster mutant after 72 h of nitrogen starvation. At this point of nitrogen starvation, PHB activity in the Sll0783 mutant is reduced to the detection level (see section 3.5.1 (p.32)). Compared to the wild type, NADPH/NADP<sup>+</sup> ratio was significantly reduced in the Sll0783 mutant, whereas the NADPH/NADP<sup>+</sup> ratio of the Nit1C cluster mutant was increased. In addition, this experiment was carried out with

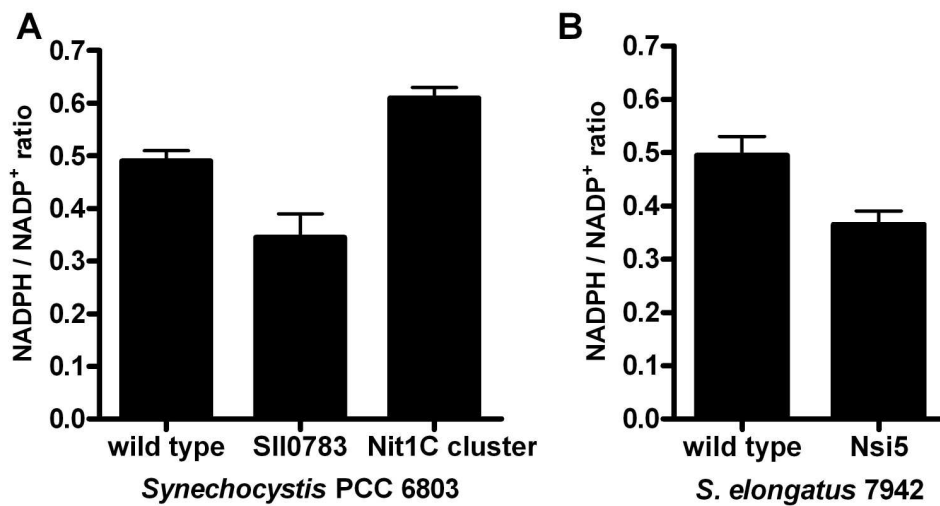


**Figure 3.28: NADPH/NADP<sup>+</sup> ratio of different strains under nitrogen starvation.** - NADPH and NADP<sup>+</sup> were quantified after 72 h of nitrogen starvation in different strains with a NADPH/NADP<sup>+</sup> quantification kit. Standard deviations from triplicate experiments are indicated by error bars.

the *S. elongatus* PCC 7942 wild type and Nsi5 mutant 3.28B. The *S. elongatus* PCC 7942 strains showed the same pattern as the corresponding *Synechocystis* PCC 6803 strains.

### 3. RESULTS

---

# 4

## Discussion

This study aimed to reveal the function of the Sll0783 protein during N-starvation in the cyanobacterium *Synechocystis* PCC 6803 to gain deeper insights in the physiological response to N-starvation and to shed light on the Nit1C gene cluster, which can be found dispersed in the bacterial kingdom. Since cyanobacteria are key players in the global carbon and nitrogen cycle, the cellular responses imposed by nutrient starvation have been deeply investigated. Nonetheless, there remain many unanswered questions. In a previous work, a gene cluster of seven genes, the Nit1C cluster, was found to be highly induced upon nitrogen starvation. The function of the Nit1C cluster was completely unclear. Initial investigations of a Sll0783 mutant, where the first gene of the Nit1C cluster was knocked out, indicated that PHB accumulation might be impaired, but confirmation was missing. However, there was no link between the Sll0783 product and PHB synthesis. In general, limited knowledge on cyanobacterial PHB accumulation complicated interpretation of the Sll0783 mutant phenotype. Therefore, a detailed characterisation of the Sll0783 mutant and the PHB accumulation was necessary.

### 4.1 Analysis of the gene *sll0783*

The gene *sll0783* is part of a gene cluster of seven genes (Figure 4.1), which is broadly but sparsely distributed among the bacteria. It has been termed Nit1C due to sequence homology of the second gene to the aliphatic nitrilase (Podar *et al.*, 2005). It occurs in a variety of  $\alpha$ -,  $\beta$ - and  $\gamma$ -proteobacteria as well as in some Gram-positives. Slight variations of the cluster architecture resemble the major taxonomical groups. This gene cluster is highly conserved on the level of amino acid sequence of the individual genes as well as on the level of gene arrangements, suggesting a conserved function. Almost all heterotrophic strains containing this gene cluster are able to produce PHB and many of them are able to fix nitrogen. The Nit1C cluster is present in some unicellular, non-diazotrophic cyanobacteria, which are adapted to mostly nutrient-poor environments. The similarity of cyanobacterial *sll0783* homologues to the corresponding phylogenetic relationships of the 16S rRNA genes

## 4. DISCUSSION

suggests that this gene cluster was probably acquired early in cyanobacterial evolution but was maintained only in those species that could take advantage of its functions. This is supported by the presence of the Nit1C cluster in the strain *Prochlorococcus marinus* PCC 9301, which harbours one of the smallest cyanobacterial genomes. This strain is adapted to an extremely nutrient-poor environment and is known for a reductive evolution (Dufresne *et al.*, 2003). Another strain containing the Nit1C cluster in its genome is *Acarlychloris marinus* MBI 11017. This strain can live in a symbiotic relationship with an ascidie, suggesting a high niche adaptation.

Previously, it was shown that in *S. elongatus* 7942 the Nit1C cluster is under control of

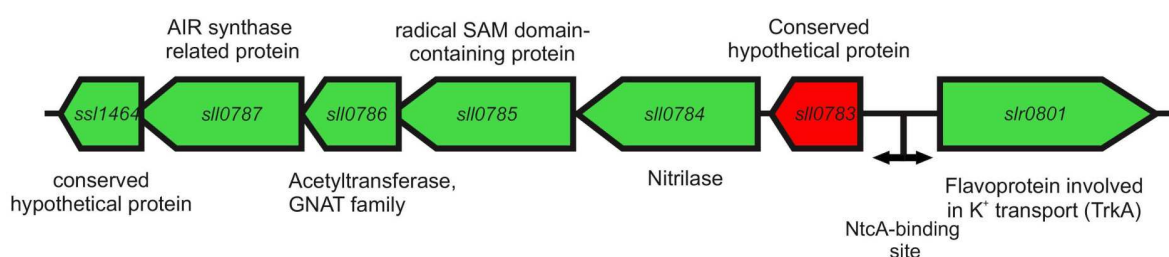


**Figure 4.1: Schematic representation of the Nit1C cluster of *Synechocystis* PCC 6803.** - Indicated function predictions were obtained by PSI-blast searches (<http://blast.ncbi.nlm.nih.gov/Blast.cgi>).

the NtcA promoter (Rasch, 2009). Here, we could show that the NtcA-binding site is also conserved in other cyanobacterial Nit1C homologous. In *Synechocystis* PCC 6803 we could identify a putative non-canonical class I promoter with a  $-35$  site and a putative NtcA binding site 107 bp upstream of the transcription start point. Analysing microarray experiments of *Synechocystis* PCC 6803, which were previously performed in the context of CO<sub>2</sub> utilisation and photorespiration, revealed that under CO<sub>2</sub>-limiting conditions the genes of this cluster are coherently repressed (Eisenhut *et al.*, 2007) as is the case for other NtcA activated genes. Under CO<sub>2</sub>-limiting conditions, the low 2-OG level inhibits the NtcA activity.

### 4.2 Physiological analysis of the Sll0783 mutant

Since the Sll0783 mutant was only superficially investigated before, a more detailed analysis of the physiology of this mutant was performed in this study. Upon nitrogen starvation the Sll0783 mutant was unimpaired in the process of chlorosis as revealed by changes in cell density, photosynthetic activity and pigment content compared to the *Synechocystis* PCC 6803 wild type. This is accord with previous investigations on a *S. elongatus* 7942 mutant strain of the *slI0783* homologue, where no phenotype was observed (Rasch, 2009). In addition to the nitrogen starvation response, the ability to recover from nitrogen starvation was investigated. Therefore, a nitrogen source was added to nitrogen-starved cells. This experiment

revealed that the Sll0783 mutant was significantly impaired in the recovery process. Cell density, pigment content and photosynthetic activity were clearly reduced compared to the wild type. Microscopic analysis of the nitrogen starved cells revealed that the Sll0783 mutant was lacking intracellular PHB granules. The wild type stores under nutrient starvation the excess of fixed carbon in PHB granules. In contrast to PHB metabolism, it was shown that glycogen metabolism was not affected in the Sll0783 mutant.

The impaired recovery process was strikingly depending on the nitrogen source used in the experiment. The major differences is the requirement for reductive equivalents for the assimilation of ammonium and nitrate: whereas only two electrons are used for  $\text{NH}_4^+$  assimilation via the GS-GOGAT, eight additional electrons are required for the reduction of nitrate to  $\text{NH}_4^+$  via NR and NiR. Whereas the recovery with ammonium caused only slight differences between the Sll0783 mutant and the wild type, the mutant was highly impaired to recover with nitrate as N-source. This suggests that the impaired recovery is due to an reduced availability of reduction equivalents and not caused by the lack of C-skeletons generated by PHB degradation. Since PHB degradation yields not only acetyl-CoA but also reduction equivalents, the reduced PHB level could cause an reduced level of reduction equivalents during the recovery in the Sll0783 mutant. In agreement with the lack of reduction equivalents, the recovery with nitrate was less severe under high light conditions ( $100 \mu\text{M}$  photons  $\text{m}^{-2}\text{s}^{-1}$ ) than under lower light conditions ( $20\text{-}30 \mu\text{M}$  photons  $\text{m}^{-2}\text{s}^{-1}$ ). The excess of light could enable the mutant cells to compensate the lack of reduction equivalents by increased photosynthesis. To finally clarify the cause of this phenotype, investigations about the recovery of a PHB deficient mutant are necessary.

A striking and unexpected phenotype was observed at the recovery of bleached cells in the darkness. Whereas no pigmentation occurred in the wild type, the mutant cells started to synthesise pigments. Currently, there is no explanation for this phenotype. Pigment recovery in the dark may be fuelled by glycogen mobilisation, indicating that the glycogen metabolism in the dark might be de-regulated in the mutant.

### 4.3 PHB accumulation in the Sll0783 mutant

PHB accumulation was initially analysed by fluorescence microscopy with the PHB specific dye Nile red. This analysis showed that the *Synechocystis* PCC 6803 wild type and the Sll0783 mutant start with the formation of PHB granules. Over the course of nitrogen starvation, the amount and size of wild type PHB granules increased. The Sll0783 mutant ceased PHB accumulation after 36 h. The impaired PHB accumulation was confirmed and quantified by HPLC analysis as well as by spectroscopic analysis (Figure 4.2). Additionally, it was shown that the stop in PHB accumulation is not accompanied with a reduction of glycogen or acetyl-CoA, implying that a precursor limitation is not the cause of impaired



## 4. DISCUSSION

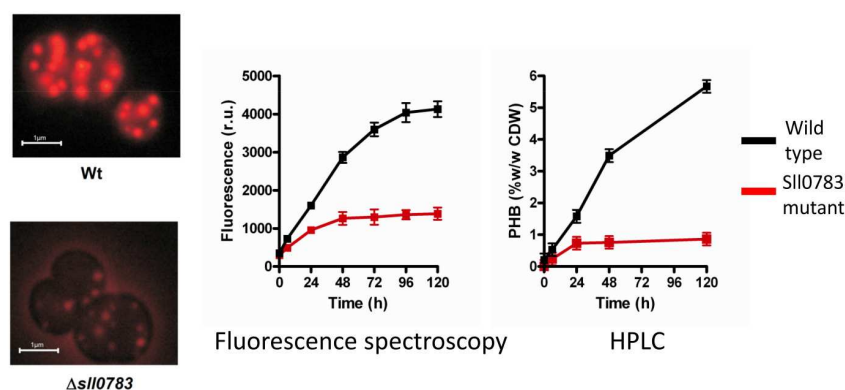


**Figure 4.2: Analysis of the impaired PHB accumulation of the Sll0783 mutant** - Impaired PHB accumulation demonstrated by fluorescence microscopy (left) and spectroscopy (centre) as well as by HPLC analysis (right). Standard deviations from triplicate experiments are indicated by error bars.

PHB accumulation in the Sll0783 mutant. Instead of a reduction, the acetyl-CoA pool increased in the Sll0783 mutant compared to the wild type suggesting a metabolic blockage of PHB synthesis. Furthermore, it can be excluded that the Sll0783 mutant has a general deficiency in carbon acquisition. This is supported by the fact that the impaired PHB accumulation could not be restored by addition of acetate or 2% CO<sub>2</sub>.

On the level of gene expression of the PHB synthesis genes two differences in the transcript abundance were detected: (i) the early induction of the genes after six hours of nitrogen starvation was lower than in the wild type (ii) the expression of the acetoacetyl-CoA reductase (*slr1994*) was significantly increased after 24 and 48 h. This is interesting, since the acetoacetyl-CoA reductase catalyses the NADPH consuming step of PHB synthesis and the time point of induced expression matches the arrest of PHB accumulation observed between 24 h and 48 h via microscopy. This could correlate with the reduced NADPH level in the Sll0783 mutant: the mutant may compensate the reduced NADPH level by increasing the transcription rate of the acetoacetyl-CoA reductase. The present finding that *slr1993* and *slr1994* were differentially expressed is in contrast to previous assumptions that these genes constitute a single operon (Taroncher-Oldenburg *et al.*, 2000). A more recent study detected two antisense RNAs in the genetic region of this gene cluster (Georg *et al.*, 2009), which may explain the contradictory results. The antisense RNAs could be part of an regulatory feedback loop, which recognises the product of the reaction, hydroxybutyryl-CoA. Overall, the differences between wild type and Sll0783 mutant in gene expression of PHB synthesis genes is subtle and can not explain the impaired PHB accumulation in the Sll0783 mutant. In addition to nitrogen starvation, the effect of potassium and phosphate starvation was investigated. Nitrogen, phosphate and potassium starvation trigger PHB accumulation in different ways. While PHB accumulation upon nitrogen starvation is due to an imbalance in the C/N ratio (Miyake *et al.*, 1997), the PHB accumulation upon phosphate starvation

is induced by an excess of reduction equivalents (Panda *et al.*, 2006). Under phosphate starvation increasing phosphatase activity causes a reduction in the ATP level, while linear photosynthetic electron flow continue in NADPH production (Bottomley & Stewart, 1976; Konopka & Schnur, 1981). The potassium starvation is a more pleiotropic stress: maintenance of turgor, intracellular pH and enzyme activation are discussed in the literature (Booth & Higgins, 1990). In a heterocystous, nitrogen-fixing cyanobacterium, *Anabaena torulosa*, it was shown that deprivation of  $K^+$  caused an impairment of the vital metabolic processes of photosynthesis and nitrogen fixation in addition to the expected loss of turgor (Alahari & Apte, 2004). Therefore, it can be assumed that  $K^+$ -starvation causes a general decrease of anabolic metabolism with a concomitant accumulation of metabolic precursors, which can be used for the synthesis of PHB. Here, it was shown that phosphate starvation did not induce PHB accumulation in the Sll0783 mutant (Table 4.1). Since the Sll0783 mutant is unable to maintain the NADPH/NADP<sup>+</sup> ratio under nitrogen starvation, one can suggest that the failure to accumulate PHB of the Sll0783 mutant under phosphate starvation is also due to a reduced amount of reduction equivalents. However, the pleiotropic stress of potassium starvation was able to induce PHB accumulation in the Sll0783 mutant, even in combination with phosphate starvation. The stimulatory effect of potassium starvation on PHB accumulation in the Sll0783 mutant was vanished under nitrogen starvation, which could be explained by the unbalanced expression of the Nit1C cluster. This could be the cause of the disturbed NADPH/NADP<sup>+</sup> ratio (see section 4.6.1 (p.60)). Detailed analysis on expression of the Nit1C cluster under the various nutrient-stress conditions are necessary to confirm this hypothesis.

**Table 4.1:** PHB accumulation upon different nutrient starvation conditions

	-P	-K	-P-K	-N-K
Wild type	+	+	+	+
Sll0783 mutant	-	+	+	-

## 4.4 Purification of PHB granules

Since PHB granules are complex organised subcellular structures where structural, biosynthetic, catabolic and regulatory proteins are associated (Jendrossek, 2009), we investigated the PHB granule associated proteins of *Synechocystis* PCC 6803. One reason of the impaired PHB accumulation could be a deficiency in the assemble process. Therefore, we purified the PHB granules from nitrogen starved cells and analysed the attached proteins. Commonly, PHB granules are purified by glycerol or sucrose density centrifugation. Isolation of PHB granules from *Synechocystis* PCC 6803 cells by this method was not suitable because no PHB specific layer was identified. However, purification of PHB granules with a Percoll

## 4. DISCUSSION

---

gradient resulted in a pure PHB granule fraction, which was further used for proteome identification. The major proteins of the purified granules were outer membrane or periplasmic proteins. Outer membrane proteins are often identified in purified PHB preparations (Jendrossek, personal communication, Matsumoto *et al.* (2002)). The proteins Slr1841 and Slr1908 are annotated as probable porins. Since there is no plausible explanation for the occurrence of outer membrane proteins in the cytosol, these findings were interpreted as artefacts. However, other characteristic outer membrane proteins like TOC75 and PilQ as well as the lipoproteins Sll0180 and Sll1638 were not identified, which argues against an unspecific contamination by the outer membrane or cell wall.

Contamination during the purification process can never be excluded and the method of purification has also an effect on the PHB granules structure (Jendrossek, 2007). In order to validate the Percoll purification method, especially in the context of outer membrane contaminations, the free amino groups of the outer membrane proteins were covalently labelled with the fluorescence dye Oregon green. This was done before cell lysis to prevent unspecific staining. This experiment revealed that the stained outer membrane particles were predominantly present in the upper fraction of the gradient enriched with membranes, but in minor amount also in the PHB specific lower fraction. It is questionable if this small amount of visible outer membrane particle is an explanation for the occurrence of the outer membrane proteins in the PHB granule preparation, considering that abundant proteins like TOC75 or lipoproteins, which are characteristic for the outer membrane, were absent in the preparation.

Barnard & Sanders (1989) postulated that PHB granules are not homogeneously. They suggest that the PHB granules are subdivided in an inner solid core and a mobile shell where water acts as plasticiser. In this model, porin-like structures are needed to provide sufficient exchange between the PHB granule and the cytosol. In a more recent study such porin-like structures were indeed identified by using AFM analysis of PHB granules from *R. eutropha* (Dennis *et al.*, 2008). In this study 15-nm-diameter pores were detected on the surface of the PHB granules. These pores could form the connections between the mobile shell, where synthesis and depolymerisation of the amorphous polymer core takes place, and the cytoplasm. These pores are about three times larger than normal outer membrane pores and therefore, it is unclear whether these porin-like structures are composed of porins. Information about the surface structure of cyanobacterial PHB granules is lacking, but Slr1841 and Slr1908 are likely candidates if porin structures exist on the surface of the PHB granules (Figure 4.3). Proteome analysis of the outer membrane and the cytoplasmic membrane of *Synechocystis* PCC 6803 revealed that both proteins, Slr1841 and Slr1908, are present in the outer membrane as well as in the cytoplasmic membrane (Huang *et al.*, 2004). Taken the budding model as basis, integration of porins from the cytoplasmic membrane into the surface of growing PHB granules is possible.

In addition to the outer membrane proteins, both subunits of the PHB synthase (Slr1829

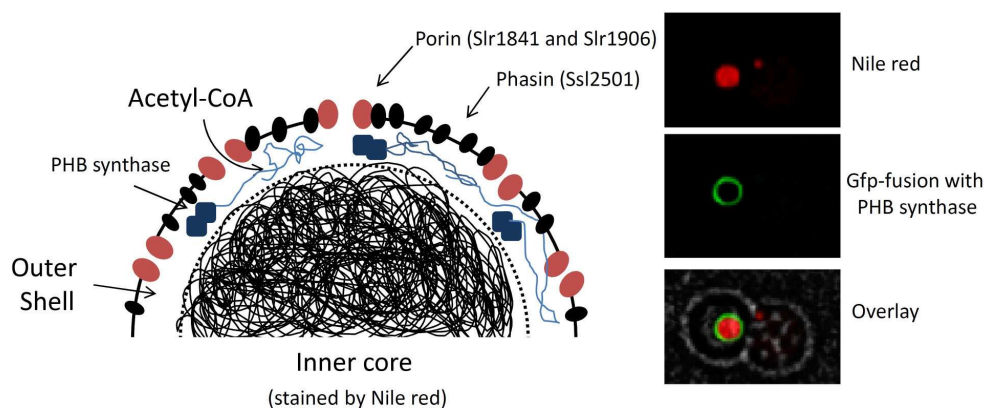


**Figure 4.3: Proposed model of PHB granules considering function of porins -** Fluorescence microscopy of PHB granules in *Synechocystis* PCC 6803 wild type with slr1829-gfp fusion protein. The fluorescence of the gfp-fusion of the PHB synthase forms a distinct ring around the Nile red stained core of the PHB granules. (right )

and Slr1830) were identified in the PHB granules preparation, but only in minor amounts. Furthermore, two proteins (Ssl2501 and Slr0060), which were identified in minor amounts, showed exactly the same distribution among cyanobacteria like the PHB synthase subunits. This may be a hint that they are relevant for the PHB accumulation. The protein Ssl2501 shows similarity to a phasin. Slr0060 is a predicted esterase of the alpha-beta hydrolase superfamily. This protein could be a potential intracellular PHB depolymerase.

#### 4.4.1 Subcellular localisation of the PHB granules

The PHB granule preparation was not suitable to detect differences in the composition of PHB granule-associated proteins. Therefore, Gfp-fusion proteins of the PHB synthase and the putative phasin Ssl2501 respectively, were constructed. In a current diploma thesis it was shown that the PHB synthase and the putative phasin binds to the PHB granules (Hauf, W: diploma thesis; Lehrstuhl für Mikrobiologie/Organismische Interaktionen Tübingen). Furthermore, there was no difference observed between the localisation process in the wild type and the Sll0783 mutant. Taken together, the investigations of the PHB granules did not provide a link to the PHB deficient phenotype in the Sll0783 mutant: The Sll0783 mutant initialise PHB granules formation in the same way than the wild type and PHB synthase remains PHB associated in the mutant. The decay of PHB synthase activity in the Sll0783 mutant occurs on intact granules.

## 4.5 Evaluation of the metabolic profiling

Metabolic profiling of the wild type and the Sll0783 mutant under nitrogen starvation by non-targeted GC-TOF-MS analysis enables an overview of the central C and N metabolism

## 4. DISCUSSION

---

as well as different pool sizes in the wild type and the Sll0783 mutant. The data showed that most TCA metabolites increase during nitrogen starvation. Interestingly to see, that 2-OG has no superior role in the metabolic pool sizes, while it is essential for C/N balance sensing. The amino acid pools increased transiently during the short time starvation period (6 h) and decreased only during the long term starvation. This may be due to increased protein degradation, while protein synthesis is blocked. In the Sll0783 mutant, the amino acid pools did not show this strong increase after 6 h and the reduction after 168 h was less marked than in the wild type. One point of interest is the metabolite sorbitol. Sorbitol is an important osmoprotectant in algae and plants (Yancey *et al.*, 1982), which is synthesised by the sorbitol-6-phosphate dehydrogenase with glucose-6-phosphate and NADPH as substrates. In the wild type, sorbitol increased dramatically upon the deprivation of combined nitrogen. Maybe, the NADPH accumulation triggers the sorbitol synthesis in the wild type. In the Sll0783 mutant, the sorbitol pools size is significantly lower than in the wild type, while the glucose-6-phosphate pool increased during the long time nitrogen starvation. Since the sorbitol synthesis needs reduction equivalents, the observation is consistent with the reduced NADPH level of the Sll0783 mutant.

### 4.6 PHB synthase activity is influenced by NADPH

Fractionation of cell extracts revealed that PHB synthase activity was exclusively found in the insoluble fraction, which contains almost all PHB granules. This is accord with the subcellular localisation of the PHB synthase by Gfp-fusion proteins. In the Sll0783 mutant PHB synthase was only transiently active upon nitrogen starvation. The activity ceased during long term starvation, which explains the observed phenotype of the mutant and is consistent with the data obtained by fluorescence microscopy and HPLC analysis.

The drop in activity showed that the PHB synthase is target of an activity regulation. Since the NADPH pool is reduced in the mutant, one can assume that NADPH has a regulatory influence on the PHB synthase. The way, how NADPH influences the PHB synthase activity, remains unclear. In *in vitro* reconstitution experiments, NADPH as well as eleven additional metabolites were unable to restore the PHB synthase activity in the Sll0783 mutant. Only acetyl phosphate showed activating properties in the enzyme assay, but activation was not sufficient to increase the activity to wild type level. Furthermore, an approach by swapping supernatants of the wild type and the Sll0783 mutant did also not lead to an activation of the PHB synthase in the Sll0783 mutant.

#### 4.6.1 NADPH/NADP<sup>+</sup> ratio is crucial for PHB accumulation

Another approach to analyse the influence of NADPH on PHB accumulation was the manipulation of the cellular NADPH/ATP ratio using artificial inhibitors. The NADPH/ATP

ratio resembles the energy status of the cell and is essential for PHB accumulation (Philipis *et al.*, 1992). The inhibitor DCMU reduces the NADPH level, expecting a decreased PHB accumulation. DCCP and CCCP should decrease the ATP level without affecting the NADPH level, which should induce PHB accumulation. The obtained data fully supported our suggestion. PHB synthase activity was measured to quantify the influence of the inhibitors. In the wild type, DCMU reduced PHB synthase activity while CCCP and DCCP had stimulatory effects. In the Sll0783 mutant, the inhibitors CCCP and DCCP were able to restore PHB synthase activity completely to wild type level. These data were supported by colorimetric NADPH quantification, which showed that the NADPH pool is significantly reduced in the Sll0783 mutant. This explains the impaired PHB accumulation in the mutant, because, in addition to an excess of carbon, sufficient reductive equivalents are necessary for PHB accumulation. The influence of the NADPH pool was previously reported by Lee *et al.* (1995). In this study, they showed that in *R. eutropha* NADPH/NADP<sup>+</sup> level increased under nitrogen-limiting conditions. Furthermore, they showed that high NADPH level inhibited citrate synthase in the TCA cycle implying that NADPH level regulates whether acetyl-CoA is metabolised in the TCA cycle or stored as PHB. The authors suggested, that NADPH is the limiting factor of PHB accumulation. Our data confirm the crucial role of the NADPH level. In addition, we suppose that NADPH level has a regulatory influence on PHB synthase activity. Further work is required to elucidate how the NADPH pool affects the PHB synthase activity.

The identification of the NADPH pool as a crucial factor, which determines PHB synthase activity was an important step towards elucidation of the function of the Sll0783 protein. Since the *sll0783* gene is the first gene of a cluster with seven genes, the question arises how the other genes affect the NADPH pool and the PHB accumulation. Therefore, a knockout of *sll0784* and a knockout of the entire Nit1C cluster were constructed. A knockout of the second gene of the Nit1C cluster (*sll0784*), which is a nitrilase, showed a wild type-like PHB accumulation, PHB synthase activity and NADPH/NADP<sup>+</sup> ratio. In this mutant transcription of the genes in front of the nitrilase gene, the genes *slr0801* and *sll0783* should be unaffected. Moreover, a knockout of the complete Nit1C cluster resulted in a slightly increased PHB synthase activity and NADPH/NADP<sup>+</sup> ratio. This was unexpected since the knockout of the entire Nit1C cluster contains the *sll0783* gene and a PHB accumulation like in the Sll0783 mutant was expected.

Together, these data imply that the absence of the *sll0783* product with a concomitant high expression of *slr0801* leads to the PHB-negative phenotype. The expression of *slr0801* in the absence of *sll0783* would thus be the cause of reduced NADPH/NADP<sup>+</sup> levels. The following arguments are in favour of a functional interaction of Slr0801 and Sll0783. Slr0801 shares divergent promoter with *sll0783*, which is frequently found in the transcription of functional pairs. Figure 4.4 shows a predicted model of Slr0801, which is a predicted monooxygenase, compared with the structure of the closely related phenylacetone monooxygenase

## 4. DISCUSSION

---

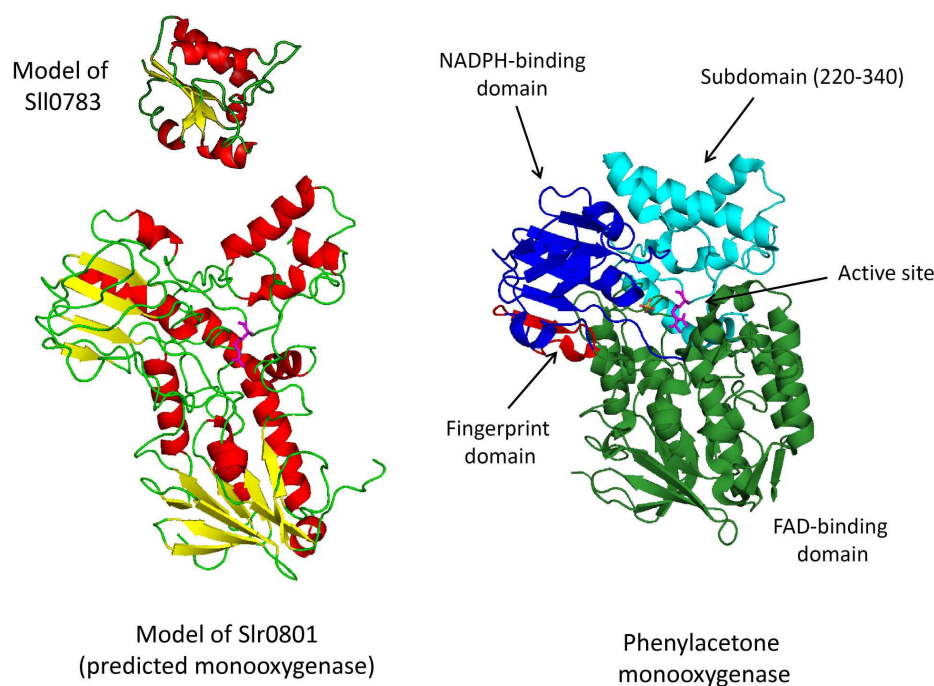


**Figure 4.4: Comparison of predicted models of the monooxygenase Slr0801 and the Sll0783 protein with the structure of phenylacetone monooxygenase (PdB:1w4x) (Malito *et al.*, 2004) - Prediction was carried out by Phyre Server (<http://www.sbg.bio.ic.ac.uk/phyre>)**

(Malito *et al.*, 2004). The Slr0801 structure was modelled on the basis highest homologies with known structures. Therefore, it resemble mostly of the phenylacetone monooxygenase (PHMO) structure except of the subdomain with the residues 220–340 (cyan), which is required for proper NADPH binding. The predicted structure of Sll0783 resemble the structure of the PHMO subdomain (220–340), which is highly suggestive for the interaction of Sll0783 with the monooxygenase. One can speculate that in the absence of the Sll0783 protein, the monooxygenase consumes excessive NADPH, which decreases the NADPH/NADP<sup>+</sup> level significantly and in consequence impairs the accumulation of PHB in the Sll0783 mutant. Summarising the results from this study, a model of the impaired PHB accumulation in the Sll0783 mutant is presented (Figure 4.5). In the wild type, PHB accumulation is induced upon nitrogen starvation by an increasing acetyl-CoA level in combination with a sufficient amount of reduction equivalents (NADPH). Nitrogen starvation also induces the expression of the Nit1C cluster from which the function is still unknown. In the presence of the Sll0783 protein, the monooxygenase operates correctly. In the Sll0783 mutant, nitrogen starvation also results in an increased acetyl-CoA level. After a transient phase of PHB accumulation the PHB synthase activity vanishes, which is due to a reduction of the NADPH level. This study indicates that the sole monooxygenase Slr0801 in absence of Sll0783, reduces the NADPH level, which subsequently inhibits the PHB synthase and results in a stop of PHB accumulation.

## 4.6 PHB synthase activity is influenced by NADPH

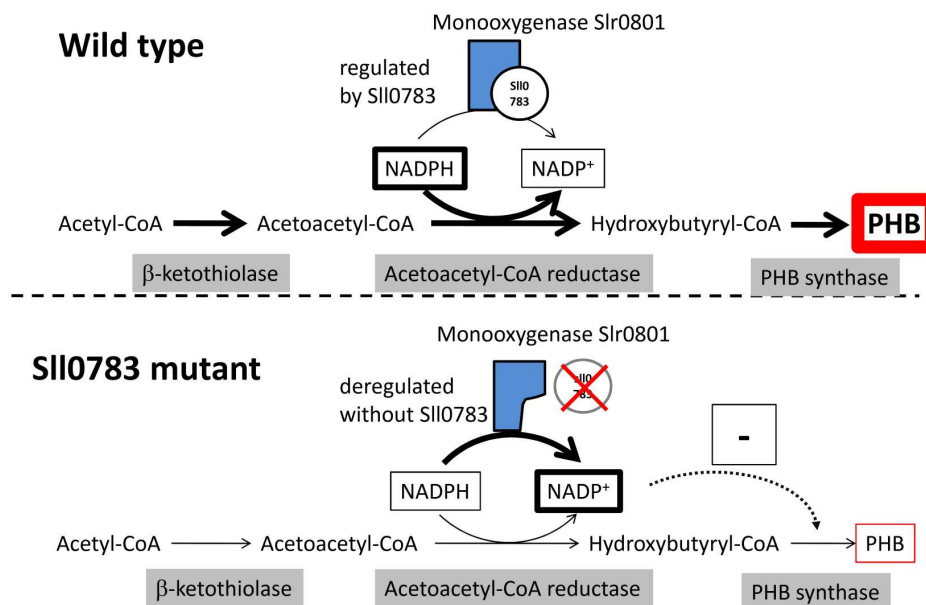


**Figure 4.5: Model of the impaired PHB accumulation in the SII0783 mutant** - Bold arrows indicate metabolic activity, dotted arrow indicate the inhibitory effect of the reduced NADPH level onto the PHB synthase. Grey boxes indicate the enzymes for PHB synthesis



## 4. DISCUSSION

---

# 5

## Materials & methods

### 5.1 Organisms and culture conditions

#### 5.1.1 Strains and organisms used in this work

Table 5.1 contains the relevant bacterial strains of *Escherichia coli* and *Synechocystis PCC 6803* with genotype and references. Plasmids which were used for cloning and proteinexpression are listed in Table 5.2.

**Table 5.1:** Strains and organisms relevant for this work.

Strain	Genotype	Reference
<i>Escherichia coli</i> XL1–Blue	<i>endA1, recA1, gyrA96, thi1, hsdR17, relA1, supE44, lac</i>	(Bullock <i>et al.</i> , 1987)
<i>Escherichia coli</i> BL21 DE3	<i>F–, opmT, hsdSB, λDE3</i>	(Grodberg & Dunn, 1988)
<i>Synechocystis PCC 6803</i>	Wild type	(Grigorieva & Sheshtakov, 1982)
<i>Synechocystis PCC 6803</i> MPII	<i>glnB::strep<sup>r</sup></i>	(Hisbergues <i>et al.</i> , 1999)
<i>Synechocystis PCC 6803</i> MS110783	<i>sll0783::kan<sup>r</sup></i>	(Sauer, 2001)
<i>Synechocystis PCC 6803</i> S110784	<i>sll0784::kan<sup>r</sup></i>	This work
<i>Synechocystis PCC 6803</i> Nit1C	<i>(slr0801–ssl1464)::kan<sup>r</sup></i>	This work
<i>Synechococcus elongatus PCC 7942</i>	Wild type	(Kuhlemeier <i>et al.</i> , 1983)
<i>Synechococcus elongatus PCC 7942</i> Nsi5	<i>nsi5::kan<sup>r</sup></i>	(Rasch, 2009)

## 5. MATERIALS & METHODS

---

**Table 5.2:** Plasmids used in this study

Plasmid	Genotype	Refernece
pJET1.2/blunt	Cloning vector with <i>amp<sup>r</sup></i> , Eco47IR	Fermentas
pGEM-T-Easy	TA-Cloning vector with <i>amp<sup>r</sup></i>	Promega
pVZ322	Vector for <i>Synechocystis</i> PCC 6803	(Zinchenko <i>et al.</i> , 1999)
pCESL19	Vector with <i>gfp</i>	(Muro-Pastor <i>et al.</i> , 2006)
pASK-IBA3	Expression vector with C-terminal Strep-tag	IBA
pMSsll0784ko	pJET + <i>sll0784</i> :kan <sup>r</sup>	This work
pMSnsi5ko	pJET + ( <i>slr0801-sll1464</i> ):kan <sup>r</sup>	This work
pMSsll0783ox	pASK-IBA3 + <i>sll0783</i>	This work
pMSslr1829ox	pASK-IBA3 + <i>slr1829</i>	This work
pMSslr1829-gfp	pVZ322 + <i>slr1829</i> + <i>gfp</i>	This work
pMSslr1930-gfp	pVZ322 + <i>slr1830</i> + <i>gfp</i>	This work
pMSssl2501-gfp	pVZ322 + <i>ssl2501</i> + <i>gfp</i>	This work

### 5.1.2 Culture conditions for cyanobacteria

The wild type strain of *Synechocystis* PCC 6803 and the corresponding mutants were grown photoautotrophically in BG11 medium (Rippka, 1988) supplemented with 5 mM NaHCO<sub>3</sub> in flasks shaken at 150 rpm with a continuous photon flux density of 50  $\mu\text{mol photons m}^{-2} \text{s}^{-1}$  at 28 °C. For initiation of nitrogen deprivation, 50 ml of exponentially growing cells were harvested by centrifugation (8 min, 4,000 *g*), the pellet was resuspended in NaNO<sub>3</sub>-free BG11 medium (BG11<sub>-N</sub>) and centrifuged again. Finally, the washed cells were resuspended again in BG11<sub>-N</sub> to an optical density (OD<sub>750nm</sub>) of 0.4 and incubated as described above. To examine the recovery of cells after 72 h of nitrogen deprivation, the starved cells were diluted in BG11<sub>-N</sub> to an optical density (OD<sub>750nm</sub>) of 0.4 and NaNO<sub>3</sub> was added to a final concentration of 5 mM.

### 5.1.3 Culture conditions of *E. coli*

*Escherichia coli* cells were grown in lysogeny-broth (LB) medium (Miller, 1972) at 37 °C. Supplements and antibiotics were used according to standard techniques (Sambrook, 1982).

## 5.2 Bioinformatic data analyses

The predicted *sll0783* amino acid sequence was used to perform a PSI-Blast search (Altschul *et al.*, 1997) against the non-redundant protein sequences database of the NCBI homepage (<http://blast.ncbi.nlm.nih.gov/Blast.cgi>). Conserved domains were automatically detected by CD-search (Marchler-Bauer & Bryant, 2004) and protein parameters were obtained from the ExpASY platform (Gasteiger *et al.*, 2003). The phylogenetic relationships

were calculated using the neighbour-joining method (Saitou & Nei, 1987), which is integrated in the ClustalX v2.0.11 software package (Thompson *et al.*, 1997). The results were visualised as a rectangular tree with the phylogenetic tree plotting program TreeView (Page, 1996).

## 5.3 Analytical methods and fluorescence microscopy

### 5.3.1 Growth and pigmentation

Growth of the cells was followed by measuring the optical density of the culture at 750 nm with a LKB Ultrospec III spectrophotometer (Pharmacia). Differences in pigmentation were analysed by difference spectra as follows. From each sample, a spectrum in the range from 350 nm to 750 nm was recorded with a Specord 205 (Analytic Jena, Germany). Thereafter, the WinAspect 2.2.1.0 (Analytic Jena, Germany) software was used to correct the wavelength-dependent light-scattering by baseline correction using 750 nm and 400 nm as reference points. Then, the corrected spectrum at time point zero was subtracted from the corrected spectra at subsequent time points. From the difference spectra the peaks at 630 nm and 680 nm were determined to the baseline at 750 nm. These values quantify the change in amount of phycobilisomes and chlorophyll *a*.

### 5.3.2 Modulated chlorophyll fluorescence

Modulated chlorophyll fluorescence was measured according to Sauer *et al.* (2001). A WATER-PAM chlorophyll fluorometer (Heinz Walz GmbH, Effeltrich, Germany) consisting of the WATER-ED emitter-detector unit, the PAM-CONTROL unit, and the WinControl Data Acquisition software was used to estimate the effective quantum yield from cyanobacterial cells. The sample (3 mL), which was in a 15-mm diameter quartz cuvette, was illuminated by a circular array of 14 red light emitting diodes peaking at 655 nm, three of which served for pulse modulated measuring light, whereas the rest provided actinic light and saturation pulses. A miniature photomultiplier module (type H-677901, Hamamatsu, Hamamatsu City, Japan) served as fluorescence detector at wavelengths above 700 nm. The experiments were carried out at room temperature (24 °C). The effective quantum yield of PSII photochemistry was determined by the saturation pulse method (Genty *et al.*, 1989; Schreiber, 1994).

### 5.3.3 Fluorescence microscopy of PHB granules

PHB granules in *Synechocystis* PCC 6803 cells were visualised by staining with the fluorescent dye Nile red. To 20 µl of cell culture, 6.6 µl Nile red solution (1 µg ml<sup>-1</sup> in ethanol) was added. Of this mixture, 10 µl were dropped on glass slides, which had been covered

## 5. MATERIALS & METHODS

---

with 1 ml 2% agarose in H<sub>2</sub>O and dried. The cells were analysed by fluorescence microscopy using a Leica DM5500B microscope with a 100x/1.3 oil objective lens (Leica Microsystems, Germany) and a filter cube with 535/50 nm excitation and 610/75 suppression. Pictures were taken with a Leica DFC360FX camera. Fluorescence of eGfp fusion proteins were analysed with a 63x/1.3 glycerin lens (Leica Microsystems, Germany) and a filter cube with 470/40 excitation and 525/50 suppression. In some cases autofluorescence was detected with the Cy5 channel (620/60 excitation and 700/75 suppression). Z-Stacks of 0.1–0.2 µm were recorded and processed with the deconvolution software Leica LAS AF. Standard deconvolution procedure was done by using blind method and 20 iterations.

### 5.3.4 Outer membrane stain

In order to label the outer membrane of intact cells with Oregon Green 488-X (2.5 mg ml<sup>-1</sup> in H<sub>2</sub>O) (Invitrogen, Molecular Probes), 10 ml of a cell culture was washed three times with phosphate buffer (0.1 M, pH 7.8) and incubated for 30 min with Oregon Green 488-X stain (2.5 mg ml<sup>-1</sup> in H<sub>2</sub>O). Thereafter, the cell suspension was washed three times with phosphate buffer (0.1 M, pH 7.8). Oregon green fluorescence was detected with the gfp channel.

### 5.3.5 Fluorescence quantification

For quantification of the Nile red fluorescence, 180 µl cells were stained with 20 µl Nile red solution (1 µg ml<sup>-1</sup> in ethanol). The fluorescence was measured in a fluorescence microplate reader (Infinite 200, Tecan) with an excitation wavelength of 530 nm and emission of 570 nm. Growth medium containing Nile red without cells was used as blank.

### 5.3.6 Acetyl-CoA determination

Acetyl-CoA was determined by a coupled assay in which the formation of oxaloacetate and NADH from malate and NAD was coupled to the formation of citrate from oxaloacetate and acetyl-CoA (Decker, 1974). To perform the assay, 50 ml cell culture were harvested by centrifugation (4,000 *g*, 10 min, 4°C) and resuspended in 5 ml 4 M perchloric acid. After 5 min incubation on ice, the sample was neutralised with KOH and adjusted to a pH value between 6.3 and 6.7 with KHCO<sub>3</sub>. After centrifugation (4,000 *g*, 5 min, 4°C), the supernatant was freeze-dried and the residue was used for acetyl-CoA determination. The samples were dissolved in 0.5 ml H<sub>2</sub>O and mixed with TrisHCl, pH 8.1 (final concentration 200 mM), L-malate (final concentration 2.5 mM) and NAD (final concentration 1.5 mM) to give a final volume of 1 ml. Then 5 µl malate dehydrogenase was added (final concentration 0.9 U/ml). When A 339 nm was constant, the value was recorded (A1). After that, citrate synthase was added (final concentration of 75 mU/ml) and A 339 nm (A2) was determined when the absorbance was constant. The acetyl-CoA concentration was calculated according

to following equation:

$$c = 0.325x(A2A1)/v,$$

where  $c$  is the concentration of acetyl-CoA and  $v$  the sample volume in the assay mixture.

### 5.3.7 Glycogen determination

2 ml of a bacterial culture with an optical density ( $OD_{750nm}$ ) of 0.5 was harvested by centrifugation (2 min, 13,000  $g$ ) and resuspended in 0.5 ml of BG11<sub>-N</sub>. 10  $\mu$ l 54 %  $H_2SO_4$  was added to 200  $\mu$ l of this suspension and incubated for 20 min at 100 °C. The reaction was stopped by neutralisation with 20  $\mu$ l 5 M NaOH. For the determination of glucose (derived from acid hydrolysis of glycogen), 1 ml *o*-toluidine reagent (Sigma-Aldrich) (Hultman, 1959) was added. After 3 min incubation on ice, absorbance at 635 nm was measured and glucose was quantified with a glucose standard curve.

### 5.3.8 NADP<sup>+</sup>/NADPH assay

Colorimetric assays were performed using commercial kit NADP<sup>+</sup>/NADPH Quantification Kit (Biovision, USA). Cell pellets from 25 ml cell culture were resuspended in 200  $\mu$ l NADP<sup>+</sup>/NADPH extraction buffer and disrupted in a Fast-Prep24 apparatus (MP Biomedicals, USA) for 3 x 20 sec with an intensity setting of 6.5 M/s. Cell debris was removed by centrifugation at 1,000  $g$  for 1 min. The supernatant was centrifuged again at 25,000  $g$  for 30 min. Afterwards, the supernatants were normalised to protein level before they were passed through a Microcon YM-10 filter (Millipore, USA) to remove NADPH consuming enzymes. The flow-through was used for the detection of both, NADPH and total NADP<sup>+</sup>/NADPH level according to the manual. All samples were processed in a single multiwell experiment run to aid quantification and comparability. Colorimetric measurements were made at 25 °C using optical density measurements at 450nm ( $OD_{450}$ ) in a microplate reader EL808 (BioTek, USA).  $OD_{450}$  measurements were converted to ng/mg protein using a standard curve for NADPH.

### 5.3.9 GC-EI-TOF-MS compound identification and data processing

Samples of 5 to 10 ml cells, equivalent to about  $10^9$  cells/ml, were separated from the medium by filtration (0.45-mm nitrocellulose filters, Schleicher and Schuell), were subsequently placed in 2-ml Eppendorf tubes and immediately frozen in liquid nitrogen. The GC-EI-TOF-MS profiling analysis, compound identification and data processing were done by Dr. Joachim Kopka (Max-Planck-Institut für Molekulare Pflanzenphysiologie, 14476 Golm, Germany) according to the method of Eisenhut et al. (2008).

### 5.4 Molecular genetic methods

#### 5.4.1 Standard methods

Standard procedures like DNA fragment separation, DNA precipitation, 5-dephosphorylation of DNA fragments were carried out according to standard protocols (Sambrook, 1982). Restriction and ligation of DNA procedures were used according to the manufacturers instructions.

#### 5.4.2 Long flanking homology polymerase chain reaction (LFH-PCR)

To construct a *sll0784* and Nit1C cluster mutant strain, the long flanking homology PCR (LFH-PCR) technique was used (Wach, 1996). Briefly, the upstream and downstream sequences flanking the target gene were amplified in two separate reactions. The reverse primer of the upstream flanking sequence and the forward primer of the downstream flanking sequence possess a 20 bp sequence with homologies to the kanamycin resistance cartridge. In addition, the kanamycin resistance cartridge (aminoglycoside 3-phosphotransferase of the plasmid pVZ322) was amplified with gene specific primers. 30 ng of gel-purified flanking sequences were mixed with 120 ng DNA of the kanamycin resistance cartridge and used as template for the LFH-PCR. As primers the forward primer of the upstream flank and the reverse primer of the downstream flank were used. All PCR reactions were carried out with the Phusion Flash Master Mix (NEB) according to the product manual. The final blunt-end LFH-PCR product was purified and cloned in the pJET vector (Fermentas). The *Synechocystis* PCC 6803 wild type was transformed with the resulting plasmid according to the method of Golden (Golden *et al.*, 1987) and selected on BG11 agar plates with 5 mM NaHCO<sub>3</sub> and 50 µg ml<sup>-1</sup> kanamycin. Segregation was confirmed by colony PCR.

#### 5.4.3 Analysis of 5' end of *sll0783* transcript

For determination of the 5' end of the *sll0783* transcript, the 5'RACE Kit, 2nd generation (Roche Applied Science, Mannheim, Germany) was used according to the manufacturers instruction. *Synechocystis* PCC 6803 wild type cells in the mid-exponential phase of growth were shifted to nitrogen-free medium and after 6 hours of starvation 50 ml of culture (OD<sub>750nm</sub> of 0.8) were harvested on ice by centrifugation (4,000 *g*, 10 min, 4 °C) and used for RNA extraction. For the cDNA synthesis of the first strand, 0.5 µg RNA and an antisense gene specific primer sll0783-SP1 (Table 5.4) located 205 bp downstream of ATG and for the nested PCR the PCR anchor primer (Roche) and an antisense gene specific primer sll0783-SP2 (Table 5.4) located 115 bps downstream of ATG were used. Amplification products were checked by agarose gel electrophoresis. The final amplification products were purified with Gel Purification Kit (Qiagen, Germany) and subcloned into the pGMT-EASY vector

**Table 5.3:** List of oligonucleotides for LFH-PCR. Boldface indicates homology to kanamycin resistance cartridge.

Primer	DNA target	Sequence (5' → 3')
sll0784upfor	<i>sll0784</i>	CTA AGC CAG CTC ACC AAA C
Sll0784uprev	<i>sll0784</i>	<b>GTC AGC AAC ACC TTC TTC ACG AGG</b> GAT TTT TCC CAG CAC AAC GA
Sll0784downfor	<i>sll0784</i>	<b>TAA TCA GAA TTG GTT AAT TGG TTG</b> CGG CAG TAA GTG ATC CAG AG
Sll0784downrev	<i>sll0784</i>	ATA TTG ACC CGC GCT TTA ATG
Nsi5upfor	<i>slr0801</i>	GCA AGG CTG TTA TCT CAG AC
Nsi5uprev	<i>slr0801</i>	<b>GTC AGC AAC ACC TTC TTC ACG AGG</b> CCG TGA TGC GGA ATA TTT AG
Nsi5downfor	<i>ssl1464</i>	<b>TAA TCA GAA TTG GTT AAT TGG TTG</b> GGC AGA CCC TGC TCG ATG GC
Nsi5downrev	<i>ssl1464</i>	TGA CCG AAG CAA ATG CAA GTG

using the pGMT-EASY cloning kit (Fermentas, Germany). Following transformation of *E. coli*, insert containing plasmids were selected and analysed by sequencing. The sequences were aligned against the upstream region of *sll0783* (sequence available in Cyanobase <http://bacteria.kazusa.or.jp/cyano/>).

**Table 5.4:** List of oligonucleotides used for 5' RACE

Primer	Sequence (5' → 3')
sll0783-SP1	GTAACACCGGGACCATAGAG
sll0783-Sp2	CCTTCAAACGCCACTGTA

#### 5.4.4 RNA isolation and cDNA synthesis

35 ml of cell cultures from different growth conditions were rapidly cooled by addition of ice and harvested by centrifugation (4,000 *g*, 10 min, 4°C) and RNA was isolated by an hot acid phenol-chloroform extraction and ethanol precipitation combined with the High Pure RNA Isolation Kit (Roche) according to the manufacturers instruction (Eisenhut *et al.*, 2007). cDNA synthesis was performed by using the iscript<sup>TM</sup> Select cDNA Synthesis Kit (Bio-Rad) according to manufacturers instruction with 1 µg total RNA.

#### 5.4.5 quantitative RT-PCR

Transcript levels were quantified by qRT-PCR using the iQ5 qRT-PCR detection system (Bio-Rad). Amplifications were performed using the IQ SYBR green supermix (Bio-Rad)



## 5. MATERIALS & METHODS

and gene specific primers (Table 5.5). Two-step cycling was performed by amplification with an initial preheating step of 10 min at 95 °C, 30 cycles at 95 °C for 15 s and 60 °C for 30 s and a final 10 min elongation step at 72 °C. The level of *rnpB* was used as loading control (Paz-Yepes *et al.*, 2003). Relative (normalised to *rnpB*-level) mRNA levels of each specific transcript were determined with the Bio-Rad software according to the  $2^{-\Delta\Delta CT}$  method (Livak & Schmittgen, 2001). The transcript level of wild type cells at time point zero was set as one. For the correct calculation of transcript abundance, the PCR efficiency was determined by dilution series with genomic DNA. Analyses were performed using triplicate technical replicates from duplicate biological cultures. To determine melting temperatures for the amplification products of the specific primers, the temperature was raised after qRT-PCR from 65 °C to 95 °C, and fluorescence was detected continuously.

**Table 5.5:** List of oligonucleotides used for qPCR

Primer	Gene	Sequence (5' → 3')
rnpB-F	<i>rnpB</i>	AAAGGGTAAGGGTGCAAAGG
rnpB-R	<i>rnpB</i>	AATTCCTCAAGCGGTTCCAC
sll0783-F	<i>sll0783</i>	GCTCTATGGTCCCGGTGTTA
sll0783-R	<i>sll0783</i>	GTGCAAAGCGACAAGCATAA
slr0801-F	<i>slr0801</i>	GGTACGCCACAAAACAAACC
slr0801-R	<i>slr0801</i>	TAGAGATGCATGCCCTCAAG
slr1829-F	<i>slr1829</i>	GGACATGGATGGTTTATGGC
slr1829-R	<i>slr1829</i>	AAGGCGATCGCATAAACTG
slr1830-F	<i>slr1830</i>	GGGCACATTTAGCCTGTGTT
slr1820-R	<i>slr1830</i>	TGGCATCCACCATTAAGTCA
slr1993-F	<i>slr1993</i>	TTTCAGCCGGATAGAATTGG
slr1993-R	<i>slr1993</i>	AGACTTTCCACGGTGGTGTC
slr1994-F	<i>slr1994</i>	TTTTCCCAAATTAACCCCC
slr1994-R	<i>slr1994</i>	ACTAATGGCCACAATGGAGC

### 5.4.6 Construction of C-terminal eGfp fusion proteins

The target gene fragments for subsequent construction of eGfp fusion were first PCR amplified with genomic *Synechocystis* PCC 6803 DNA using specific primers (Table 5.6). The amplified fragments include the upstream promoter region of the gene. If the gene was part of an operon, the upstream gene with the native promoter was included. The eGfp gene was amplified with specific primer from the plasmid pCSEL19 (Muro-Pastor *et al.*, 2006). Fusion of target gene fragment and eGfp fragment were obtained by long flanking homologue PCR (Wach, 1996). For that purpose, the reverse primer for the target gene includes a 20 bp sequence corresponding to the N-terminus of eGfp. After the PCR amplification of the target

gene the gene specific forward primer and eGfp specific reverse primer were provided with the restriction sites *SalI* and *PstI*, respectively. After LFH-PCR, the joined PCR fragment was restricted with *SalI* and *PstI* and afterwards ligated in the conjugative, self-replicating plasmid pVZ322. The resulting plasmid was transferred to *Synechocystis* PCC 6803 wild type and Sll0783 mutant strain by conjugation (Wolk *et al.*, 1984), whereupon exconjugants were selected on BG11 agar plates with 5 mM NaHCO<sub>3</sub> containing up to 5 µg gentamycin ml<sup>-1</sup> and 50 µg kanamycin ml<sup>-1</sup>; the latter one due to the insertion in the *sll0783* mutant background. Segregation was confirmed by colony PCR.

**Table 5.6:** List of oligonucleotides for the construction C-terminal eGfp fusion proteins. Bold indicates homology to the eGfp gene for the LFH-PCR; Terminal restriction sites for the ligation in pVZ322 are underlined.

Primer	DNA target	Sequence (5' → 3')
ssl2501for	ssl2501 + promoter	GATC <u>GTCGACT</u> AATGGAGACGTGCGATACC
ssl2501rev	ssl2501	<b>AGTTCTTCTCCTTTACTCAT-</b> GTTAGCCGATACGGGCTCTT
ssl2502rev	ssl2502	<b>AGTTCTTCTCCTTTACTCAT-</b> TCGTTGGCGGTAGTTCCTTG
slr1829for	slr1829 + promoter	GATC <u>GTCGACGCGGCCA</u> AGGTTAGATTC
slr1829rev	slr1829	<b>AGTTCTTCTCCTTTACTCAT-</b> GCCTGGGTTTGCTTCTGTTT
slr1830rev	slr1830	<b>AGTTCTTCTCCTTTACTCAT-</b> CTGTCGTTCCGATAGCCAAT
gfpfor	eGfp	ATGAGTAAAGGAGAAGAACT
gfprev	eGfp	GATC <u>CCTGCAGT</u> TATTTGTATAGTTCATCCA

## 5.5 Protein techniques

### 5.5.1 Protein quantification

Protein concentration was quantified according to Bradford (1976).

### 5.5.2 Preparation of cell extracts

All steps for preparing cell extracts were performed at 4 °C or on ice. Cells of *Synechocystis* PCC 6803 and corresponding mutants were harvested from nitrogen-limited or nitrogen-sufficient cultures by centrifugation for 8 min at 4,000 *g*. Then, they were resuspended in lysis buffer (25 mM Tris/HCl, pH 7.4, 50 mM KCl, 5 mM MgCl<sub>2</sub> and 0.5 mM EDTA) and disrupted in a Fast-Prep24 apparatus (MP Biotechnology, Germany) for 3 x 20 sec with an

## 5. MATERIALS & METHODS

---

intensity setting of 6.5 M/s. Cell debris was removed by centrifugation at 1,000 *g* for 1 min to obtain the crude extract. For further analysis, crude extract was separated into a soluble and insoluble fraction by centrifugation at 20,000 *g* for 15 min. The insoluble fraction was resuspended in 0.5 ml Tris/HCl, pH 7.4.

### 5.5.3 PHB synthase assay

Assay of PHB synthase activity was carried out as described (Valentin & Steinbüchel, 1994). The assay mixtures (200  $\mu$ l) contained 50  $\mu$ l cell extracts with 20  $\mu$ g of protein, 100  $\mu$ M DL-3-hydroxybutyryl-CoA and 1 mM 5,5-dithiobis(2-nitrobenzoic acid) (DTNB) in 25 mM Tris/HCl, pH 7.4 buffer with 20 mM MgCl<sub>2</sub>. The reaction mixtures were transferred to microplate wells and the reaction was started by the addition of the substrate DL-3-hydroxybutyryl-CoA. The reaction was recorded in a microplate reader EL808 (BioTek, USA) at a temperature setting of 30 °C and the time course of absorbance change at 409 nm (due to reaction of released CoA with DTNB) was followed for 5 min.

### 5.5.4 Reactivation of PHB synthase by swapping supernatants

In order to reveal if in the Sll0783 mutant an activator is missing or an inhibitory compound accumulates, insoluble fractions were incubated with the soluble fractions of the wild type. After preparation of cell extracts, 5  $\mu$ g of the insoluble fraction were incubated with 45  $\mu$ g of the soluble fraction for 10 min and subsequently used for the PHB synthase assay. As control extracts were incubated with reaction buffer.

### 5.5.5 *In vitro* activation of PHB synthase

For the *in vitro* activation of the PHB synthase, 150  $\mu$ l 25 mM Tris/HCl, pH 7.4 containing 40  $\mu$ g of protein and the putative activators were incubated for 10 min at 30 °C. Subsequently, 50  $\mu$ l of the mixtures were used for assay of the PHB synthase activity.

### 5.5.6 Granula preparation

Cells (1.5 l) were harvested by centrifugation (4,000 *g*, 10 min, 4 °C), washed with PBS, and resuspended in 5 ml 25 mM Tris/HCl, pH 7.5 buffer. Cells were disrupted in a Fast-Prep24 apparatus (3 x 20 sec, intensity setting of 6.5 M/s). After cell debris was removed (1000 *g*, 1 min, 4 °C), an additional sonication step (20 kHz, 70 W, 5 min, 4 °C) was necessary to release the PHB granules. The resulting homogenate was diluted with buffer and centrifuged (6000 *g*, 60 min, 4 °C). The resuspended pellet (5 ml) was directly applied onto 90% Percoll in 0.15 M NaCl (20 ml) in centrifuge tubes and centrifuged (13,000 *g*, 55 min, 4 °C) in a fixed-angle rotor. After centrifugation, fractions were collected and analysed for PHB granules. PHB granules were analysed by fluorescence microscopy and PHB synthase enzyme assay. To

liberate the granules from the residual Percoll, the fractions containing PHB granules were diluted 10 fold with 25 mM Tris/HCl, pH 7.4 buffer and further concentrated by centrifugation (10,000 *g*, 20 min, 4 °C).

Purified PHB granules were analysed by SDS-PAGE and stained by blue silver stain (Candiano *et al.*, 2004). Subsequently, the visible bands were excised, trypsinised and analysed by MALDI-TOF by the Proteom Center Tübingen.

### 5.5.7 Overexpression and purification of Slr1829

The *slr1829* gene from *Synechocystis* PCC 6803 was PCR amplified from *Synechocystis* PCC 6803 genomic DNA using primer slr1829Strep-for and slr1829Strep-rev (Table 5.7). After restriction with *BsaI*, the PCR product was ligated into *BsaI*-restricted pASK-IBA3. The resulting plasmid, pMSslr1829ox, was used for overproduction of Slr1829 Strep-tag fusion protein in *E. coli* BL21 (DE3) cells. Slr1829 was predominantly found in inclusion bodies, which were washed according to standard procedures. SDS-PAGE analysis with Coomassie staining confirmed that purified recombinant Slr1829 was almost homogeneous (ca. 85% purity).

**Table 5.7:** List of oligonucleotides for Slr1829 overexpression.

Primer	Sequence (5' → 3')
slr1829Strep-for	TGCGCGAGGTCTCGAATGGAATCGACAAATAAAAC
slr1829Strep-rev	GCTGCAGGTCTCAGCGCTGCCTGGGTTTGCTTCTGTTT

### 5.5.8 Overexpression and purification of Sll0783

The *sll0783* gene from *Synechocystis* PCC 6803 was PCR amplified from *Synechocystis* PCC 6803 genomic DNA using primer combination sll0783Strep-for and sll0783Strep-rev (Table 5.8). After restriction with *BsaI*, the PCR product was ligated into *BsaI*-restricted pASK-IBA3. The resulting plasmid, pMSsll0783ox, was used for overproduction of Sll0783 Strep-tag fusion protein in *E. coli* BL21 (DE3) cells. Sll0783 was purified with Strep-Tactin Superflow columns (IBA, Göttingen, Germany) according to the manufacturers instructions. SDS-PAGE analysis with Coomassie staining confirmed that purified recombinant Sll0783 was almost homogeneous (ca. 95% purity).

**Table 5.8:** List of oligonucleotides for Sll0783 overexpression.

Primer	Sequence (5' → 3')
sll0783Strep-for	TGACTGGGTCTCTCGAATGCCAGAGGTAAGCC
sll0783Strep-rev	AGTCGCGGTCTCCGCGCTCATTGTCCAAGTATCAAGAA

### 5.5.9 Generation of antiserum

For the generation of a specific antiserum, 2 mg of purified protein was sent to Pineda Antikörper-Service (Berlin, Germany) for a four month immunisation procedure in rabbits.

### 5.5.10 Immunoblot analysis

For immunoblot analysis, the samples were separated on 12% SDS-PAGE gels. After electrophoresis, the proteins were transferred to a nitrocellulose membrane (PALL cooperation, USA) by semi-dry electroblotting. Primary antibodies were used overnight (4 °C) at a dilution of 1:10.000. Subsequently, the primary antibodies were visualised with secondary antibodies (anti-rabbit IgGPOD) (Sigma-Aldrich, Germany) and the LumiLight detection system (Roche Diagnostics, Mannheim, Germany).

# References

- ALAHARI, A. & APTE, S. (2004). A novel potassium deficiency-induced stimulon in *Anabaena torulosa*. *Journal of Biosciences*, **29**, 153–161. 57
- ALDEHNI, F., SAUER, J., SPIELHAUPTER, C., SCHMID, R. & FORCHHAMMER, K. (2003). Signal transduction protein pii is required for ntca-regulated gene expression during nitrogen deprivation in the cyanobacterium *Synechococcus elongatus* strain pcc 7942. *Journal of Bacteriology*, **185**, 2582–2591. 14
- ALDEHNI, M.F. & FORCHHAMMER, K. (2006). Analysis of a non-canonical NtcA-dependent promoter in *Synechococcus elongatus* and its regulation by NtcA and PII. *Arch Microbiol*, **184**, 378–86. 20
- ALTSCHUL, S.F., MADDEN, T.L., SCHAFFER, A.A., ZHANG, J., ZHANG, Z., MILLER, W. & LIPMAN, D.J. (1997). Gapped blast and psi-blast: a new generation of protein database search programs. *Nucleic Acids Res*, **25**, 3389–402. 66
- BANERJEE, A., KAUL, P. & BANERJEE, U.C. (2006). Purification and characterization of an enantioselective arylacetone nitrilase from *Pseudomonas putida*. *Arch Microbiol*, **184**, 407–18. 15
- BARNARD, G.N. & SANDERS, J.K. (1989). The poly-beta-hydroxybutyrate granule in vivo. a new insight based on nmr spectroscopy of whole cells. *J Biol Chem*, **264**, 3286–91. 6, 58
- BOOTH, I. & HIGGINS, C. (1990). Enteric bacteria and osmotic stress: Intracellular potassium glutamate as a secondary signal of osmotic stress? *FEMS Microbiology Letters*, **75**, 239–246. 57
- BOSSEMEYER, D., BORCHARD, A., DOSCH, D.C., HELMER, G.C., EPSTEIN, W., BOOTH, I.R. & BAKKER, E.P. (1989). K<sup>+</sup>-transport protein trkA of *Escherichia coli* is a peripheral membrane protein that requires other trk gene products for attachment to the cytoplasmic membrane. *J Biol Chem*, **264**, 16403–10. 16
- BOTTOMLEY, P. & STEWART, W. (1976). Atp pools and transientss in the blue-green alga, *Anabaena cylindrica*. *Arch Microbiol*, **108**, 249–58. 12, 46, 57
- BRADFORD, M.M. (1976). A rapid and sensitive method for the quantitation of microgram quantities of protein utilizing the principle of protein-dye binding. *Anal Biochem*, **72**, 248–54. 73
- BULLOCK, W.O., FERNANDEZ, J.M. & SHORT, J.M. (1987). X11-blue - a high-efficiency plasmid transforming *Escherichia coli* strain with beta-galactosidase selection. *Biotechniques*, **5**, 376–381. 65

## REFERENCES

---

- CANDIANO, G., BRUSCHI, M., MUSANTE, L., SANTUCCI, L., GHIGGERI, G.M., CARNEMOLLA, B., ORECCHIA, P., ZARDI, L. & RIGHETTI, P.G. (2004). Blue silver: A very sensitive colloidal coomassie g-250 staining for proteome analysis. *ELECTROPHORESIS*, **25**, 1327–1333. 75
- CARR, N.G. & WHITTON, B.A. (1982). *The Biology of cyanobacteria*. Botanical monographs v. 19, University of California Press, Berkeley, 82001906 edited by N.G. Carr and B.A. Whitton. ill. ; 24 cm. Bibliography: p. 565-670. Includes index. 1
- CHINENOV, Y. (2002). A second catalytic domain in the elp3 histone acetyltransferases: a candidate for histone demethylase activity? *Trends Biochem Sci*, **27**, 115–7. 16
- COOLEY, J.W. & VERMAAS, W.F. (2001). Succinate dehydrogenase and other respiratory pathways in thylakoid membranes of synechocystis sp. strain pcc 6803: capacity comparisons and physiological function. *J Bacteriol*, **183**, 4251–8. 3
- COOLEY, J.W., HOWITT, C.A. & VERMAAS, W.F. (2000). Succinate:quinol oxidoreductases in the cyanobacterium synechocystis sp. strain pcc 6803: presence and function in metabolism and electron transport. *J Bacteriol*, **182**, 714–22. 3, 5
- DAHL, C., SCHULTE, A., STOCKDREHER, Y., HONG, C., GRIMM, F., SANDER, J., KIM, R., KIM, S.H. & SHIN, D.H. (2008). Structural and molecular genetic insight into a widespread sulfur oxidation pathway. *J Mol Biol*, **384**, 1287–300. 15
- DAWES, E.A. & SENIOR, P.J. (1973). The role and regulation of energy reserve polymers in micro-organisms. *Adv Microb Physiol*, **10**, 135–266. 29
- DECKER, K. (1974). *Acetyl Coenzyme A*. Methods of enzymatic analysis, Verlag Chemie; Academic Press, Weinheim, New York, 3rd edn., 73075657 GFR\*\*\* Methoden der enzymatischen Analyse. English edited by Hans Ulrich Bergmeyer, in collaboration with Karlfried Gawehn. translated from the third German ed. [by Dermot H. Williamson ; with the editorial assistance of Patricia Lund]. ill. ; 24 cm. Translation of Methoden der enzymatischen Analyse. Includes bibliographical references and index. 68
- DENNIS, D., SEIN, V., MARTINEZ, E. & AUGUSTINE, B. (2008). Phap is involved in the formation of a network on the surface of polyhydroxyalkanoate inclusions in cupriavidus necator h16. *J Bacteriol*, **190**, 555–63. 7, 9, 58
- DOI, Y., SEGAWA, A., KAWAGUCHI, Y. & KUNIOKA, M. (1990). Cyclic nature of poly(3-hydroxyalkanoate) metabolism in alcaligenes eutrophus. *FEMS Microbiol Lett*, **55**, 165–9. 9
- DUFRESNE, A., SALANOUBAT, M., PARTENSKY, F., ARTIGUENAVE, F., AXMANN, I.M., BARBE, V., DUPRAT, S., GALPERIN, M.Y., KOONIN, E.V., LE GALL, F., MAKAROVA, K.S., OSTROWSKI, M., OZTAS, S., ROBERT, C., ROGOZIN, I.B., SCANLAN, D.J., DE MARSAC, N.T., WEISSENBAACH, J., WINCKER, P., WOLF, Y.I. & HESS, W.R. (2003). Genome sequence of the cyanobacterium *Prochlorococcus marinus* ss120, a nearly minimal oxyphototrophic genome. *Proceedings of the National Academy of Sciences*, **100**, 10020–10025. 54

- DUNLOP, W.F. & ROBARDS, A.W. (1973). Ultrastructural study of poly- $\beta$ -hydroxybutyrate granules from *Bacillus cereus*. *Journal of Bacteriology*, **114**, 1271–1280. 6
- EISENHUT, M., BAUWE, H. & HAGEMANN, M. (2007). Glycine accumulation is toxic for the cyanobacterium *synechocystis* sp. strain pcc 6803, but can be compensated by supplementation with magnesium ions. *FEMS Microbiol Lett*, **277**, 232–7. 54, 71
- ESPINOSA, J., FORCHHAMMER, K., BURILLO, S. & CONTRERAS, A. (2006). Interaction network in cyanobacterial nitrogen regulation: Pipx, a protein that interacts in a 2-oxoglutarate dependent manner with pii and ntca. *Mol Microbiol*, **61**, 457–69. 13
- FAY, P., STEWART, W.D., WALSBY, A.E. & FOGG, G.E. (1968). Is the heterocyst the site of nitrogen fixation in blue-green algae? *Nature*, **220**, 810–2. 1
- FLORES, E. & HERRERO, A. (2005). Nitrogen assimilation and nitrogen control in cyanobacteria. *Biochem Soc Trans*, **33**, 164–7. 13
- FORCHHAMMER, K. (2004). Global carbon/nitrogen control by pii signal transduction in cyanobacteria: from signals to targets. *FEMS Microbiol Rev*, **28**, 319–33. 13
- FORCHHAMMER, K. (2008). P(ii) signal transducers: novel functional and structural insights. *Trends Microbiol*, **16**, 65–72. 13
- FORCHHAMMER, K. & TANDEAU DE MARSAC, N. (1994). The pii protein in the cyanobacterium *synechococcus* sp. strain pcc 7942 is modified by serine phosphorylation and signals the cellular n-status. *J Bacteriol*, **176**, 84–91. 13
- FRASCH, W.D. (1994). The f-type atpase in cyanobacteria: Pivotal point in the evolution of a universal enzyme. In D.A. Bryant, ed., *The Molecular Biology of Cyanobacteria*, 361–380, Kluwer Academic Publishers, Dordrecht, Boston & London. 2
- GALLON, J.R. (2001). N<sub>2</sub> fixation in phototrophs: adaptation to a specialized way of life. *Plant and Soil*, **230**, 39–48. 12
- GASTEIGER, E., GATTIKER, A., HOOGLAND, C., IVANYI, I., APPEL, R.D. & BAIROCH, A. (2003). Expasy: The proteomics server for in-depth protein knowledge and analysis. *Nucleic Acids Res*, **31**, 3784–8. 66
- GENTY, B., BRIANTAIS, J. & BAKER, N. (1989). The relationship between the quantum yield of photosynthetic electron transport and quenching of chlorophyll fluorescence. *Biochim Biophys Acta*, **990**, 8792. 67
- GEORG, J., VOSZ, B., SCHOLZ, I., MITSCHKE, J., WILDE, A. & HESS, W.R. (2009). Evidence for a major role of antisense rnas in cyanobacterial gene regulation. *Mol Syst Biol*, **5**, 309. 56
- GOLDEN, S.S., BRUSSLAN, J. & HASELKORN, R. (1987). Genetic engineering of the cyanobacterial chromosome. *Methods Enzymol*, **153**, 215–31. 70



## REFERENCES

---

- GRIEBEL, R., SMITH, Z. & MERRICK, J.M. (1968). Metabolism of poly-beta-hydroxybutyrate. i. purification, composition, and properties of native poly-beta-hydroxybutyrate granules from bacillus megaterium. *Biochemistry*, **7**, 3676–81. 6
- GRIGORIEVA, G. & SHESTAKOV, S. (1982). Transformation in the cyanobacterium synechocystis sp. 6803. *FEMS Microbiology Letters*, **13**, 367–370. 65
- GRODBERG, J. & DUNN, J.J. (1988). Ompt encodes the escherichia-coli outer-membrane protease that cleaves t7-rna polymerase during purification. *Journal of Bacteriology*, **170**, 1245–1253. 65
- HAI, T., HEIN, S. & STEINBUCHER, A. (2001). Multiple evidence for widespread and general occurrence of type-iii pha synthases in cyanobacteria and molecular characterization of the pha synthases from two thermophilic cyanobacteria: Chlorogloeopsis fritschii pcc 6912 and synechococcus sp. strain ma19. *Microbiology*, **147**, 3047–60. 10
- HANDRICK, R., REINHARDT, S. & JENDROSSEK, D. (2000). Mobilization of poly(3-hydroxybutyrate) in ralstonia eutropha. *J Bacteriol*, **182**, 5916–8. 9
- HEIN, S., TRAN, H. & STEINBUCHER, A. (1998). Synechocystis sp. pcc6803 possesses a two-component polyhydroxyalkanoic acid synthase similar to that of anoxygenic purple sulfur bacteria. *Arch Microbiol*, **170**, 162–70. 12
- HEINEKE, D. (2001). *Photosynthesis: Dark reaction*. Encyclopedia of Life Sciences, Nature Publishing Group, London. 2
- HEINEMANN, U., ENGELS, D., BURGER, S., KIZIAK, C., MATTES, R. & STOLZ, A. (2003). Cloning of a nitrilase gene from the cyanobacterium synechocystis sp. strain pcc6803 and heterologous expression and characterization of the encoded protein. *Appl Environ Microbiol*, **69**, 4359–66. 15
- HERRERO, A., MURO-PASTOR, A.M. & FLORES, E. (2001). Nitrogen control in cyanobacteria. *J Bacteriol*, **183**, 411–25. 14, 20
- HERRERO, A., MURO-PASTOR, A.M., VALLADARES, A. & FLORES, E. (2004). Cellular differentiation and the ntca transcription factor in filamentous cyanobacteria. *FEMS Microbiol Rev*, **28**, 469–87. 20
- HILL, S.A. (2001). Plant respiration. In *Encyclopedia of Plant Sciences*, 1–8, Nature Publishing Group, London. 3
- HISBERGUES, M., JEANJEAN, R., JOSET, F., TANDEAU DE MARSAC, N. & BDU, S. (1999). Protein pii regulates both inorganic carbon and nitrate uptake and is modified by a redox signal in synechocystis pcc 6803. *FEBS Letters*, **463**, 216–220. 65
- HOWDEN, A.J., HARRISON, C.J. & PRESTON, G.M. (2009). A conserved mechanism for nitrile metabolism in bacteria and plants. *Plant J*, **57**, 243–53. 15

- HUANG, F., HEDMAN, E., FUNK, C., KIESELBACH, T., SCHRODER, W.P. & NORLING, B. (2004). Isolation of outer membrane of *synechocystis* sp. pcc 6803 and its proteomic characterization. *Mol Cell Proteomics*, **3**, 586–95. 42, 58
- HUIJBERTS, G.N., EGGINK, G., DE WAARD, P., HUISMAN, G.W. & WITHOLT, B. (1992). *Pseudomonas putida* kt2442 cultivated on glucose accumulates poly(3-hydroxyalkanoates) consisting of saturated and unsaturated monomers. *Appl Environ Microbiol*, **58**, 536–44. 10
- HULTMAN, E. (1959). Rapid specific method for determination of aldosesaccharides in body fluids. *Nature*, **183**, 108–9. 69
- IZAWA, S. & GOOD, N. (1972). Inhibition of photosynthetic electron transport and photophosphorylation. In A.S. Pietro, ed., *Photosynthesis and Nitrogen Fixation Part B*, vol. 24 of *Methods in Enzymology*, 355 – 377, Academic Press. 46
- JENDROSSEK, D. (2005). Fluorescence microscopical investigation of poly(3-hydroxybutyrate) granule formation in bacteria. *Biomacromolecules*, **6**, 598–603. 8
- JENDROSSEK, D. (2007). Peculiarities of pha granules preparation and pha depolymerase activity determination. *Appl Microbiol Biotechnol*, **74**, 1186–96. 8, 58
- JENDROSSEK, D. (2009). Polyhydroxyalkanoate granules are complex subcellular organelles (carbonosomes). *J Bacteriol*, **191**, 3195–3202. 57
- JENDROSSEK, D. & HANDRICK, R. (2002). Microbial degradation of polyhydroxyalkanoates\*. *Annual Review of Microbiology*, **56**, 403–432. 9
- JUNTARAJUMNONG, W., EATON-RYE, J.J. & INCHAROENSAKDI, A. (2007). Two-component signal transduction in *synechocystis* sp. pcc 6803 under phosphate limitation: role of acetyl phosphate. *J Biochem Mol Biol*, **40**, 708–14. 11
- JURASEK, L. & MARCHESSAULT, R.H. (2004). Polyhydroxyalkanoate (pha) granule formation in *ralestonia eutropha* cells: a computer simulation. *Appl Microbiol Biotechnol*, **64**, 611–7. 9
- KE, B. (2001). *Photosynthesis: photobiochemistry and photobiophysics*. Kluwer Academic Publishers. 1
- KHATIPOV, E., MIYAKE, M., MIYAKE, J. & ASADA, Y. (1998). Accumulation of poly-beta-hydroxybutyrate by *rhodobacter sphaeroides* on various carbon and nitrogen substrates. *Fems Microbiology Letters*, **162**, 39–45. 12
- KLOFT, N. & FORCHHAMMER, K. (2005). Signal transduction protein pii phosphatase ppha is required for light-dependent control of nitrate utilization in *synechocystis* sp. strain pcc 6803. *J Bacteriol*, **187**, 6683–90. 14
- KLUGHAMMER, B., SULTEMEYER, D., BADGER, M.R. & PRICE, G.D. (1999). The involvement of nad(p)h dehydrogenase subunits, ndhd3 and ndhf3, in high-affinity co2 uptake in *synechococcus* sp. pcc7002 gives evidence for multiple ndh-1 complexes with specific roles in cyanobacteria. *Mol Microbiol*, **32**, 1305–15. 4

## REFERENCES

---

- KONOPKA, A. & SCHNUR, M. (1981). Biochemical composition and photosynthetic carbon metabolism of nutrient limited cultures of *Merismopedia tenuissima* (cyanophyceae)1. *Journal of Phycology*, **17**, 118–122. 12, 46, 57
- KROMKAMP, J.C. (1987). Formation and functional significance of storage products in cyanobacteria. *New Zealand Journal of Marine and Freshwater Research*, **21**, 457–465. 5
- KUHLEMEIER, C., THOMAS, A., VAN DER ENDE, A., VAN LEEN, R., BORRIAS, W., VAN DEN HONDEL, C. & VAN ARKEL, G. (1983). A host-vector system for gene cloning in the cyanobacterium *Anacystis nidulans* r2. *Plasmid*, **10**, 156 – 163. 65
- LEE, S.Y., LEE, K.M., CHAN, H.N. & STEINBUCHER, A. (1994). Comparison of recombinant *Escherichia coli* strains for synthesis and accumulation of poly-(3-hydroxybutyric acid) and morphological changes. *Biotechnol Bioeng*, **44**, 1337–47. 10
- LIEBERGESELL, M., SCHMIDT, B. & STEINBUCHER, A. (1992). Isolation and identification of granule-associated proteins relevant for poly(3-hydroxyalkanoic acid) biosynthesis in *Chromatium vinosum* d. *FEMS Microbiol Lett*, **78**, 227–32. 32, 34
- LIVAK, K.J. & SCHMITTGEN, T.D. (2001). Analysis of relative gene expression data using real-time quantitative pcr and the  $2^{-(\Delta\Delta C_t)}$  method. *Methods*, **25**, 402–8. 72
- LUQUE, I. & FORCHHAMMER, K. (2007). Nitrogen assimilation and c/n balance sensing. In A. Herrero & E. Flores, eds., *The Cyanobacteria: Molecular Biology, Genomics and Evolution*, 335–382, Caister Academic Press. 12
- LUQUE, I., FLORES, E. & HERRERO, A. (1994). Nitrate and nitrite transport in the cyanobacterium *Synechococcus* sp pcc-7942 are mediated by the same permease. *Biochimica Et Biophysica Acta-Bioenergetics*, **1184**, 296–298. 13, 14
- MADISON, L.L. & HUISMAN, G.W. (1999). Metabolic engineering of poly(3-hydroxyalkanoates): From dna to plastic. *Microbiology and Molecular Biology Reviews*, **63**, 21–53. 46
- MAEDA, S., BADGER, M.R. & PRICE, G.D. (2002). Novel gene products associated with ndh3/d4-containing ndh-1 complexes are involved in photosynthetic CO<sub>2</sub> hydration in the cyanobacterium, *Synechococcus* sp. pcc7942. *Mol Microbiol*, **43**, 425–35. 4
- MAHESWARAN, M., URBANKE, C. & FORCHHAMMER, K. (2004). Complex formation and catalytic activation by the p<sub>ii</sub> signaling protein of n-acetyl-l-glutamate kinase from *Synechococcus elongatus* strain pcc 7942. *J Biol Chem*, **279**, 55202–10. 13
- MAHESWARAN, M., ZIEGLER, K., LOCKAU, W., HAGEMANN, M. & FORCHHAMMER, K. (2006). P<sub>ii</sub>-regulated arginine synthesis controls accumulation of cyanophycin in *Synechocystis* sp. strain pcc 6803. *J Bacteriol*, **188**, 2730–4. 37
- MALITO, E., ALFIERI, A., FRAAIJE, M.W. & MATTEVI, A. (2004). Crystal structure of a baeyer-villiger monooxygenase. *Proceedings of the National Academy of Sciences of the United States of America*, **101**, 13157–13162. viii, 62

- MARCHLER-BAUER, A. & BRYANT, S.H. (2004). Cd-search: protein domain annotations on the fly. *Nucleic Acids Res*, **32**, W327–31. 66
- MATSUMOTO, K., MATSUSAKI, H., TAGUCHI, K., SEKI, M. & DOI, Y. (2002). Isolation and characterization of polyhydroxyalkanoates inclusions and their associated proteins in pseudomonas sp. 61-3. *Biomacromolecules*, **3**, 787–792. 58
- MEEKS, J.C. & ELHAI, J. (2002). Regulation of cellular differentiation in filamentous cyanobacteria in free-living and plant-associated symbiotic growth states. *Microbiol Mol Biol Rev*, **66**, 94–121; table of contents. 1
- MERRICK, M.J. & EDWARDS, R.A. (1995). Nitrogen control in bacteria. *Microbiol Rev*, **59**, 604–22. 12
- METZ, J.G., PAKRASI, H.B., SEIBERT, M. & ARNTZER, C.J. (1986). Evidence for a dual function of the herbicide-binding d1 protein in photosystem ii. *FEBS Letters*, **205**, 269 – 274. 46
- MILLER, J.H. (1972). *Experiments in molecular genetics*. Cold Spring Harbor Laboratory, Cold Spring Harbor, N.Y. 66
- MITSUI, A., KUMAZAWA, S., TAKAHASHI, A., IKEMOTO, H., CAO, S. & ARAI, T. (1986). Strategy by which nitrogen-fixing unicellular cyanobacteria grow photoautotrophically. *Nature*, **323**, 720–722. 1
- MIYAKE, M., KATAOKA, K., SHIRAI, M. & ASADA, Y. (1997). Control of poly-beta-hydroxybutyrate synthase mediated by acetyl phosphate in cyanobacteria. *J Bacteriol*, **179**, 5009–13. 11, 38, 56
- MIYAKE, M., MIYAMOTO, C., SCHNACKENBERG, J., KURANE, R. & ASADA, Y. (2000). Phosphotransacetylase as a key factor in biological production of polyhydroxybutyrate. *Appl Biochem Biotechnol*, **84-86**, 1039–44. 10
- MIYAMOTO, C.M., SUN, W. & MEIGHEN, E.A. (1998). The luxr regulator protein controls synthesis of polyhydroxybutyrate in vibrio harveyi. *Biochim Biophys Acta*, **1384**, 356–64, miyamoto, C M Sun, W Meighen, E A Research Support, Non-U.S. Gov't Netherlands Biochimica et biophysica acta Biochim Biophys Acta. 1998 May 19;1384(2):356-64. 10
- MONTESINOS, M.L., MURO-PASTOR, A.M., HERRERO, A. & FLORES, E. (1998). Ammonium/methylammonium permeases of a cyanobacterium. identification and analysis of three nitrogen-regulated amt genes in synechocystis sp. pcc 6803. *J Biol Chem*, **273**, 31463–70. 13
- MORRISON, S.S., MULLINEAUX, C.W. & ASHBY, M.K. (2005). The influence of acetyl phosphate on dspa signalling in the cyanobacterium synechocystis sp. pcc6803. *BMC Microbiol*, **5**, 47. 11
- MURO-PASTOR, A.M., OLMEDO-VERD, E. & FLORES, E. (2006). All4312, an ntca-regulated two-component response regulator in anabaena sp strain pcc 7120. *Fems Microbiology Letters*, **256**, 171–177. 66, 72

## REFERENCES

---

- MURO-PASTOR, M.I., BARRERA, F.N., REYES, J.C., FLORENCIO, F.J. & NEIRA, J.L. (2003). The inactivating factor of glutamine synthetase, if7, is a "natively unfolded" protein. *Protein Sci*, **12**, 1443–54. 13
- OMATA, T., PRICE, G.D., BADGER, M.R., OKAMURA, M., GOHTA, S. & OGAWA, T. (1999). Identification of an atp-binding cassette transporter involved in bicarbonate uptake in the cyanobacterium *synechococcus* sp. strain pcc 7942. *Proc Natl Acad Sci U S A*, **96**, 13571–6. 4
- OSANAI, T., KANESAKI, Y., NAKANO, T., TAKAHASHI, H., ASAYAMA, M., SHIRAI, M., KANEHISA, M., SUZUKI, I., MURATA, N. & TANAKA, K. (2005). Positive regulation of sugar catabolic pathways in the cyanobacterium *synechocystis* sp. pcc 6803 by the group 2 sigma factor sigE. *J Biol Chem*, **280**, 30653–9. 14
- PAGE, R.D. (1996). Treeview: an application to display phylogenetic trees on personal computers. *Comput Appl Biosci*, **12**, 357–8. 67
- PANDA, B., SHARMA, L. & MALLICK, N. (2005). Poly-beta-hydroxybutyrate accumulation in *nostoc muscorum* and *spirulina platensis* under phosphate limitation. *J Plant Physiol*, **162**, 1376–9. 12
- PANDA, B., JAIN, P., SHARMA, L. & MALLICK, N. (2006). Optimization of cultural and nutritional conditions for accumulation of poly-beta-hydroxybutyrate in *synechocystis* sp. pcc 6803. *Bioresour Technol*, **97**, 1296–301. 12, 57
- PAZ-YEPES, J., FLORES, E. & HERRERO, A. (2003). Transcriptional effects of the signal transduction protein p(ii) (glnB gene product) on ntca-dependent genes in *synechococcus* sp. pcc 7942. *FEBS Lett*, **543**, 42–6. 72
- PEARL, H.W. (2000). Marine plankton. In P.M. Whitton B. A., ed., *The Ecology of Cyanobacteria: Their diversity in time and space*, 121–148, Kluwer Academic Publishers, The Netherlands. 1
- PETERS, V. & REHM, B.H. (2005). In vivo monitoring of pha granule formation using gfp-labeled pha synthases. *FEMS Microbiol Lett*, **248**, 93–100. 8
- PHILIPPIS, R.D., ENA, A., GUASTINI, M., SILI, C. & VINCENZINI, M. (1992). Factors affecting poly-r-hydroxybutyrate accumulation in cyanobacteria and in purple non-sulfur bacteria. *FEMS Microbiology Letters*, **103**, 187 – 194. 61
- PODAR, M., EADS, J.R. & RICHARDSON, T.H. (2005). Evolution of a microbial nitrilase gene family: a comparative and environmental genomics study. *BMC Evol Biol*, **5**, 42. 14, 53
- POTT, A.S. & DAHL, C. (1998). Sirohaem sulfite reductase and other proteins encoded by genes at the dsr locus of *chromatium vinosum* are involved in the oxidation of intracellular sulfur. *Microbiology*, **144** ( Pt 7), 1881–94. 15
- PÖTTER, M., MÜLLER, H. & STEINBÜCHEL, A. (2005). Influence of homologous phasins (phap) on pha accumulation and regulation of their expression by the transcriptional repressor phar in *Ralstonia eutropha* h16. *Microbiology*, **151**, 825–833. 39

- PRICE, G.D., WOODGER, F.J., BADGER, M.R., HOWITT, S.M. & TUCKER, L. (2004). Identification of a sulph-type bicarbonate transporter in marine cyanobacteria. *Proc Natl Acad Sci U S A*, **101**, 18228–33. 4
- PRIES, A., PRIEFERT, H., KRUGER, N. & STEINBUCHER, A. (1991). Identification and characterization of two *alcaligenes eutrophus* gene loci relevant to the poly(beta-hydroxybutyric acid)-leaky phenotype which exhibit homology to *ptsh* and *ptsI* of *Escherichia coli*. *J Bacteriol*, **173**, 5843–53. 10
- PRIYADARSHINI, R., DE PEDRO, M.A. & YOUNG, K.D. (2007). Role of peptidoglycan amidases in the development and morphology of the division septum in *Escherichia coli*. *J Bacteriol*, **189**, 5334–47. 43
- PROMMEENATE, P., LENNON, A.M., MARKERT, C., HIPPLER, M. & NIXON, P.J. (2004). Subunit composition of *ndh-1* complexes of *Synechocystis* sp. pcc 6803: identification of two new *ndh* gene products with nuclear-encoded homologues in the chloroplast *ndh* complex. *J Biol Chem*, **279**, 28165–73. 4
- RAI, A.N., BERGMAN, B. & RASMUSSEN, U. (2002). *Cyanobacteria in symbiosis*. Kluwer Academic Pub., Dordrecht ; Boston. 1
- RASCH, G. (2009). *Chlorose in Synechococcus elongatus PCC 7942 : Untersuchung des Response Regulators NblR und des Transkriptionsfaktors NtcA*. Ph.D. thesis, Universität Gießen. 14, 16, 19, 54, 65
- REHM, B. (2006). Genetics and biochemistry of polyhydroxyalkanoate granule self-assembly: The key role of polyester synthases. *Biotechnology Letters*, **28**, 207–213. 6, 7, 8
- RHOADS, D.B., WATERS, F.B. & EPSTEIN, W. (1976). Cation transport in *Escherichia coli*. viii. potassium transport mutants. *J Gen Physiol*, **67**, 325–41. 16
- RIPPKA, R. (1988). Isolation and purification of cyanobacteria. *Methods Enzymol.*, **167**, 3–27. 66
- SAITOU, N. & NEI, M. (1987). The neighbor-joining method: a new method for reconstructing phylogenetic trees. *Mol Biol Evol*, **4**, 406–25. 67
- SAMBROOK, J. (1982). *Molecular cloning : a laboratory manual*. Manual for genetic engineering, Cold Spring Harbor Laboratory, Cold Spring Harbor, N.Y. :. 66, 70
- SAUER, J. (2001). *Molekulare Grundlagen der Stickstoffmangelreaktion in Synechococcus PCC 7942 : Chlorose als Überlebensstrategie*. Ph.D. thesis, Universität Tübingen. 16, 65
- SAUER, J., SCHREIBER, U., SCHMID, R., VOLKER, U. & FORCHHAMMER, K. (2001). Nitrogen starvation-induced chlorosis in *Synechococcus* pcc 7942: Low-level photosynthesis as a mechanism of long-term survival. *Plant Physiol*, **126**, 233–43. 37, 67
- SCANLAN, D.J., OSTROWSKI, M., MAZARD, S., DUFRESNE, A., GARCZAREK, L., HESS, W.R., POST, A.F., HAGEMANN, M., PAULSEN, I. & PARTENSKY, F. (2009). Ecological genomics of marine picocyanobacteria. *Microbiol Mol Biol Rev*, **73**, 249–99. 19

## REFERENCES

---

- SCHEMBRI, M.A., WOODS, A.A., BAYLY, R.C. & DAVIES, J.K. (1995). Identification of a 13-kDa protein associated with the polyhydroxyalkanoic acid granules from acinetobacter spp. *Fems Microbiology Letters*, **133**, 277–283. 10
- SCHLEBUSCH, M. & FORCHHAMMER, K. (2010). Requirement of the nitrogen starvation-induced protein sll0783 for polyhydroxybutyrate accumulation in synechocystis sp. strain pcc 6803. *Appl Environ Microbiol*, **76**, 6101–7. 20, 21, 22, 23, 26, 30, 32, 33
- SCHMETTERER, G. (1994). Cyanobacteria respiration. In D.A. Bryant, ed., *The Molecular Biology of Cyanobacteria*, pp 409–435, Kluwer Academic Publishers, Dodrecht, Boston & London. 3
- SCHREIBER, U. (1994). New emitter-detector-cuvette assembly for measuring modulated chlorophyll fluorescence of highly diluted suspensions in conjunction with the standard pam fluorometer. *Zeitschrift Fur Naturforschung C-a Journal of Biosciences*, **49**, 646–656. 67
- SHARMA, L. & MALLICK, N. (2005). Accumulation of poly-beta-hydroxybutyrate in nostoc muscorum: regulation by ph, light-dark cycles, n and p status and carbon sources. *Bioresour Technol*, **96**, 1304–10. 11
- SHIBATA, M., OHKAWA, H., KANEKO, T., FUKUZAWA, H., TABATA, S., KAPLAN, A. & OGAWA, T. (2001). Distinct constitutive and low-co<sub>2</sub>-induced co<sub>2</sub> uptake systems in cyanobacteria: genes involved and their phylogenetic relationship with homologous genes in other organisms. *Proc Natl Acad Sci U S A*, **98**, 11789–94. 4
- SHIBATA, M., KATO, H., SONODA, M., OHKAWA, H., SHIMOYAMA, M., FUKUZAWA, H., KAPLAN, A. & OGAWA, T. (2002). Genes essential to sodium-dependent bicarbonate transport in cyanobacteria: function and phylogenetic analysis. *J Biol Chem*, **277**, 18658–64. 4
- SOFIA, H.J., CHEN, G., HETZLER, B.G., REYES-SPINDOLA, J.F. & MILLER, N.E. (2001). Radical sam, a novel protein superfamily linking unresolved steps in familiar biosynthetic pathways with radical mechanisms: functional characterization using new analysis and information visualization methods. *Nucleic Acids Res*, **29**, 1097–106. 15
- STAL, L.J. & MOEZELAAR, R. (1997). Fermentation in cyanobacteria. *Fems Microbiology Reviews*, **21**, 179–211. 5
- STERNER, D.E. & BERGER, S.L. (2000). Acetylation of histones and transcription-related factors. *Microbiol Mol Biol Rev*, **64**, 435–59. 15
- SU, Z., OLMAN, V., MAO, F. & XU, Y. (2005). Comparative genomics analysis of ntca regulons in cyanobacteria: regulation of nitrogen assimilation and its coupling to photosynthesis. *Nucleic Acids Research*, **33**, 5156–5171. 14
- SUZUKI, I., SUGIYAMA, T. & OMATA, T. (1993). Primary structure and transcriptional regulation of the gene for nitrite reductase from the cyanobacterium synechococcus pcc-7942. *Plant and Cell Physiology*, **34**, 1311–1320. 13

- TABITA, F.R. (1994). The biochemistry and molecular regulation of carbon dioxide metabolism in cyanobacteria. In D.A. Bryant, ed., *The Molecular Biology of cyanobacteria*, 437–467, Kluwer Academic Publishers, Dordrecht, Boston & London. 2
- TAKATANI, N., KOBAYASHI, M., MAEDA, S. & OMATA, T. (2006). Regulation of nitrate reductase by non-modifiable derivatives of pii in the cells of *synechococcus elongatus* strain pcc 7942. *Plant and Cell Physiology*, **47**, 1182–6. 14
- TARONCHER-OLDENBURG, G., NISHINA, K. & STEPHANOPOULOS, G. (2000). Identification and analysis of the polyhydroxyalkanoate-specific beta-ketothiolase and acetoacetyl coenzyme a reductase genes in the cyanobacterium *synechocystis* sp. strain pcc6803. *Appl Environ Microbiol*, **66**, 4440–8. 12, 56
- THOMPSON, J.D., GIBSON, T.J., PLEWNIAK, F., JEANMOUGIN, F. & HIGGINS, D.G. (1997). The clustal<sub>x</sub> windows interface: flexible strategies for multiple sequence alignment aided by quality analysis tools. *Nucleic Acids Res*, **25**, 4876–82. 67
- TIAN, J., SINSKEY, A.J. & STUBBE, J. (2005). Kinetic studies of polyhydroxybutyrate granule formation in *wautersia eutropha* h16 by transmission electron microscopy. *J Bacteriol*, **187**, 3814–24. 7
- TIMM, A. & STEINBUCHEL, A. (1992). Cloning and molecular analysis of the poly(3-hydroxyalkanoic acid) gene locus of *pseudomonas aeruginosa* pao1. *Eur J Biochem*, **209**, 15–30. 10
- VALENTIN, H. & STEINBÜCHEL, A. (1994). Application of enzymatically synthesized short-chain-length hydroxy fatty acid coenzyme a thioesters for assay of polyhydroxyalkanoic acid synthases. *Appl Microbiol Biotechnol*, **40**, 699–709. 74
- VEGA-PALAS, M.A., FLORES, E. & HERRERO, A. (1992). Ntca, a global nitrogen regulator from the cyanobacterium *synechococcus* that belongs to the crp family of bacterial regulators. *Mol Microbiol*, **6**, 1853–9. 14
- VERMAAS, W.F.J. (2001). Photosynthesis and respiration in cyanobacteria. In *Encyclopedia of Life Sciences*, 1–7, Nature Publishing Group, London. 2, 3
- WACH, A. (1996). Pcr-synthesis of marker cassettes with long flanking homology regions for gene disruptions in *s. cerevisiae*. *Yeast*, **12**, 259–265. 70, 72
- WANG, Y., SUN, J. & CHITNIS, P.R. (2000). Proteomic study of the peripheral proteins from thylakoid membranes of the cyanobacterium *synechocystis* sp. pcc 6803. *Electrophoresis*, **21**, 1746–54. 42
- WHITTON, B.A. & POTTS, M. (2000). *The ecology of cyanobacteria : their diversity in time and space*. Kluwer Academic. 1
- WIECZOREK, R., PRIES, A., STEINBUCHEL, A. & MAYER, F. (1995). Analysis of a 24-kilodalton protein associated with the polyhydroxyalkanoic acid granules in *alcaligenes eutrophus*. *J Bacteriol*, **177**, 2425–35. 9



## REFERENCES

---

- WOLK, C.P., THOMAS, J., SHAFFER, P.W., AUSTIN, S.M. & GALONSKY, A. (1976). Pathway of nitrogen metabolism after fixation of  $^{13}\text{N}$ -labeled nitrogen gas by the cyanobacterium, *Anabaena cylindrica*. *J Biol Chem*, **251**, 5027–34. 13
- WOLK, C.P., VONSHAK, A., KEHOE, P. & ELHAI, J. (1984). Construction of shuttle vectors capable of conjugative transfer from *Escherichia coli* to nitrogen-fixing filamentous cyanobacteria. *Proc Natl Acad Sci U S A*, **81**, 1561–5. 73
- YANCEY, P.H., CLARK, M.E., HAND, S.C., BOWLUS, R.D. & SOMERO, G.N. (1982). Living with water stress: evolution of osmolyte systems. *Science*, **217**, 1214–22. 60
- YOSHIKAWA, K., ADACHI, K., NISHIJIMA, M., TAKADERA, T., TAMAKI, S., HARADA, K., MOCHIDA, K. & SANO, H. (2000). beta-cyanoalanine production by marine bacteria on cyanide-free medium and its specific inhibitory activity toward cyanobacteria. *Appl Environ Microbiol*, **66**, 718–22. 15
- ZHANG, C.C., LAURENT, S., SAKR, S., PENG, L. & BEDU, S. (2006). Heterocyst differentiation and pattern formation in cyanobacteria: a chorus of signals. *Mol Microbiol*, **59**, 367–75. 5, 44
- ZHANG, P., BATTCHIKOVA, N., JANSEN, T., APPEL, J., OGAWA, T. & ARO, E.M. (2004). Expression and functional roles of the two distinct *ndh-1* complexes and the carbon acquisition complex *ndhd3/ndhf3/cupa/sll1735* in *Synechocystis* sp pcc 6803. *Plant Cell*, **16**, 3326–40. 4
- ZINCHENKO, V.V., PIVEN, I.V., MELNIK, V.A. & SHESTAKOV, S.V. (1999). Vectors for the complementation analysis of cyanobacterial mutants. *Russian Journal of Genetics*, **35**, 228–232. 66

## Contributions

Waldemar Hauf performed the transformation of the *Synechocystis* PCC6803 wild type and the Sll0783 mutant with the pVZ322 vectors harbouring the phaC and phaE gfp-fusion constructs.

The GC-EI-TOF-MS and the compound identification were performed by Dr. Joachim Kopka (Max-Planck-Institute für Molekulare Pflanzenphysiologie, Golm, Germany).

The Proteome Center Tübingen excised, trypsinised and analysed the visible bands of the PHB granule preparation.